Downloaded from orbit.dtu.dk on: Mar 30, 2019

DTU Library

Comparative Study of Test Methods for Bituminized and other Low- and Medium-Level Solidified Waste Materials

Brodersen, Knud Erik; Forskningscenter Risø, Roskilde; Vinther, Arne

Publication date:
1983

Document Version
Publisher's PDF, also known as Version of record

Link back to DTU Orbit

Citation (APA):
Brodersen, K. E., Mose Pedersen, B., & Vinther, A. (1983). Comparative Study of Test Methods for Bituminized and other Low- and Medium-Level Solidified Waste Materials. Roskilde: Risø National Laboratory.

General rights
Copyright and moral rights for the publications made accessible in the public portal are retained by the authors and/or other copyright owners and it is a condition of accessing publications that users recognise and abide by the legal requirements associated with these rights.

- Users may download and print one copy of any publication from the public portal for the purpose of private study or research.
- You may not further distribute the material or use it for any profit-making activity or commercial gain
- You may freely distribute the URL identifying the publication in the public portal

If you believe that this document breaches copyright please contact us providing details, and we will remove access to the work immediately and investigate your claim.

RISØ-M-2415

COMPARATIVE STUDY OF TEST METHODS FOR BITUMINIZED AND OTHER LOW- AND MEDIUM-LEVEL SOLIDIFIED WASTE MATERIALS

Knud Brodersen, Bodil Mose Pedersen, and Arne Vinther
Chemistry Department, NRL Risø

Final report (1981-1982) for Contract WAS 235 DK(G) under The Indirect Action Program (1980-1984) of the European Atomic Energy Community: "Management and Storage of Radioactive Waste". (Characterization of Low- and Medium-Level Radioactive Waste Forms.)

Abstract. Various aspects of the behaviour of bituminized or cemented simulated low- or medium-level radioactive waste in contact with water have been investigated.

The solubility (~ 0.5%) and the diffusion coefficient (~ $5 \cdot 10^{-9}$ cm^2/sec) determining transport of water in pure bitumen have been measured for Mexphalte 40/50 at room temperature.

(Continued on next page)

December 1983
Risø National Laboratory, DK-4000 Roskilde, Denmark

A weighing method has been and used to study the behaviour of bituminized sodium nitrate, sodium sulphate or cation-exchange resin in contact with water or various salt solutions. This method permits the simultaneous measurement of water uptake; swelling and leaching. The particle size of the embedded waste material was found to be an important parameter. Development of solution-filled porosity in the samples was demonstrated in many cases. The swelling of samples in contact with water or weak salt solutions was in some cases very pronounced. In strong salt solutions the tendency to swell is much less.

Thermal pre-treatment of cation-exchange resin before bituminization was investigated; it does not seem to improve the quality of the final product.

The interaction between bituminized ion-exchange resin and concrete barrier materials has been studied.

Microbial degradation of bitumen and bituminized sodium nitrate under aerobic conditions has been investigated. The phenomenon seems to be of minor importance as far as leaching from the materials is concerned.

A method for measuring the leaching from a plane surface of cemented waste has been developed. The method avoids the problem of cracks between the sample and the container. It was demonstrated that such cracks can introduce considerable errors in the measured leach rates.

Leaching of cemented sodium nitrate or sodium sulphate was investigated. The absorption of CO_2 from the atmosphere was found to influence the chemistry of the leach solution. This had only a minor effect on Cs- and Na-leaching but gave a very pronounced decrease in Ca-leaching.

The use of silica-fume as an additive to cemented sodium nitrate decreased the leach rates by about a factor 4.

The leaching behaviour for bituminized as well as cemented waste materials was found in most cases to be diffusion controlled, i.e. the leach rate decreases with $\sqrt{t}$. However, exceptions were encountered which makes extrapolation uncertain.

INIS descriptors: BITUMENS; BRINES; CEMENTS; COMPARATIVE EVALUATIONS; DECOMPOSITION; DIFFUSION; HEAT TREATMENTS; INTERMEDIATE-LEVEL RADIOACTIVE; ION EXCHANGE MATERIALS; LEACHING; LOW-LEVEL RADIOACTIVE WASTES; MICRO-ORGANISMS; PARTICLE SIZE; RADIOACTIVE WASTE DISPOSAL; RESINS; SODIUM SULPHATES; SODIUM NITRATES; SOLIDIFICATION; SWELLING; SOLUBILITY; TESTING; UPTAKE; WATER

UDC 621.039.736

ISBN 87-550-0981-6
ISSN 0418-6435

Risø repro 1984

ACKNOWLEDGEMENT

The authors wish to thank Dr. Heinz Hansen and members of the Health Physics Department at Risø for the performance of the tritium analyses, Mr. Peter Bo from the Chemistry Department for advice on membrane chemistry, and other members of the staff of the Chemistry Department and the Waste Management Plant, who in various ways have contributed to this work.

LIST OF CONTENTS

Page

ACKNOWLEDGEMENT 4

1. INTRODUCTION 7

2. BITUMINIZED MATERIALS 8
   2.1. Waste uptake and diffusion in pure bitumen 8
   2.2. Weighing method for determining water uptake in bituminized materials 23
   2.3. Sodium sulphate/bitumen system (early experiments) 26
   2.4. Sodium nitrate/bitumen system (early experiments) 28
   2.5. Example of leaching from and water uptake in bituminized evaporator concentrate from the production plant at Risø 35
   2.6. Cat. on-exchange resin/bitumen system 41
   2.7. Thermal pre-treatment of cation-exchange resin before bituminization 56
   2.8. Combined measurements of leaching, water uptake and cation in-diffusion into bituminized cation-exchange resin 60
   2.9. Leaching from bituminized cation-exchange resin in contact with concrete 79
   2.10. Degradation of bituminized waste by micro-organisms 90

3. POLYMER SOLIDIFIED MATERIALS 111
   3.1. Preliminary experiments with production of samples of polystyrene-solidified ion-exchange resin 111

4. CEMENTED WASTE MATERIALS 113
   4.1. The effect of silica-fume additive and of cracked containers on leaching from cemented sodium nitrate 113

Page

4.2. Influence of sample geometry on diffusion-controlled leaching 122

4.3. An improved leach configuration and leaching from cemented sodium nitrate under various conditions 125

4.4. Leaching from cemented sodium sulphate 141

5. REFERENCES 143

APPENDIX I

Calculation model for the presentation of experimental results concerning wat uptake, water penetration, leaching of solut.e salts and swelling of bituminized waste materials 146

1. INTRODUCTION

Most of the work presented in this Final Report has been described in a preliminary way in Progress Reports (1,2) and in contributions to the Joint Annual Reports from the CEC working group on Characterization of low- and medium-level radioactive waste forms (3,4). However, in this final report some necessary corrections and modifications have been made, which clarifies the results considerably. The work has been performed with financial support from the Commission of the European Communities. It is continuing under a new contract with the CEC.

The objective of the characterization work made at Risø is to contribute to a better understanding of mechanisms determining the long-term behaviour of various types of conditioned low- and medium-level radioactive wastes. This is done by developing new test methods and comparing experimental results from new or established methods when used on various types of conditioned waste materials. Indications on the extent to which the results can be extrapolated in time and to other circumstances are especially important. To understand the mechanisms it is necessary to characterize the system under investigation as a whole. This is because many properties of solidified waste materials cannot be regarded as simple material properties but may change with time in different ways depending for example on the chemical composition of water solutions in contact with the material.

The main emphasis in the study has been on various aspects of the behaviour of bituminized and cemented waste in contact with water. Transport of water and cations in pure bitumen have been investigated. A method for simultaneously measuring leaching, water uptake, and swelling of bituminized materials has been developed. The use of the methodology has been demonstrated on various types of materials. The effect of thermal cracking of ion exchange resin on the tendency of the bitumized material to swell in contact with water has been investigated. Pre-

liminary experiments with leaching from bituminized waste in contact with concrete have been made. Some work has been done on testing and improving methods for leach rate measurements from cemented waste. The improvements of leach rate properties which can be attained by the use of silica-fume as additive to cemented waste have been demonstrated. Preparation of laboratory samples of polystyrene-solidified moist ion-exchange resin for use in the characterization studies has been tried.

An example of characterization of bituminized evaporator concentrate from the waste water evaporator plant at Risø is reported, and some work has been done on reference waste No. 1: Cemented sodium sulphate. Otherwise it has been preferred to work with simplified systems to facilitate the interpretation of the experimental results. This means that the results may not be directly applicable to materials containing wastes with the generally more complicated compositions recommended as reference wastes in the CEC work on characterization of low- and medium-level radioactive waste forms (3). However, some fundamental work with simplified systems is thought to be necessary for understanding more realistic simulation experiments with "real" waste.

2. BITUMINIZED MATERIALS

2.1. Waste uptake and diffusion in pure bitumen

It is of considerable interest for the theoretical interpretation of water uptake in bituminized waste materials to know something about the rate of transport of water in pure bitumen. In a steady-state situation the rate of water transport through undamaged films of bitumen is expected to be proportional to the solubility of water in bitumen, to the diffusion coefficient for water in the bitumen, and to the water concentration gradient over the film. This gradient depends on the chemical prop-

erties of the waste particles and on the concentration of solutes in the surrounding water. It is also dependent on the thickness of the bitumen films which is determined by the waste loading and the size of the waste particles distributed in the bitumen. This is discussed in more detail in (5).

The diffusion coefficient and especially the solubility of water in the bitumen are material constants which may depend on the type and history of the bitumen.

The migration of dissolved salts in pure bitumen will indicate whether the water is taken up in the bitumen as a true solution or is present in form of inclusions in microcracks or pores in the material. The behaviour of dissolved salts is important for understanding osmotic phenomena in the material.

2.1.1. Weight increases due to water uptake in pure bitumen

The weighing method described later in connection with the swelling experiments (Section 2.2) can also be used to determine the rate of diffusion of water into pure bitumen.

In the first experiment 2-cm thick samples of Mexphalte 40/50 cast in Perspex rings were placed in pure water. At suitable intervals each sample was removed from the water and weighed after carefully removing droplets adhering to the surface by wiping the surface with filter paper. Easily measurable weight increases were obtained but it was later found that this was partly due to water uptake in the Perspex ring.

The results of a repeated experiment using a sample cast in a stainless steel ring are shown in Fig. 1. It gave the same rate of water uptake as could be estimated from the original experiments after correcting for water uptake in the Perspex.

The results of a series of experiments based on the same weighing principle but using samples of pure Mexphalte 40/50 cast in glass Petri dishes are shown in Figs. 2 a, b, and c.

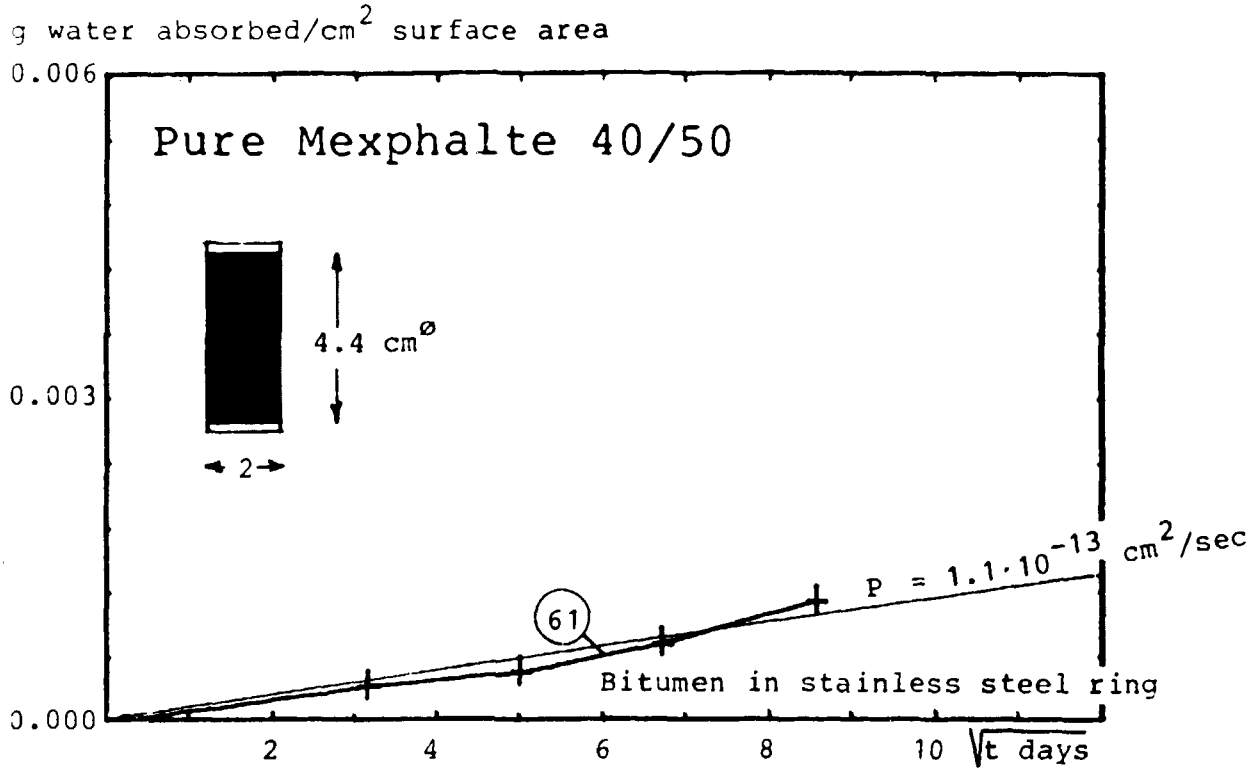

Fig. 1. Weight increase per cm^2 exposed surface area of a sample of pure Mexphalte 40/50 cast in a ring of stainless steel and immersed in pure water at 20°C.

Three sets of samples were used: a) Pure Mexphalte 40/50 as cast. b) Pure Mexphalte 40/50 after heating to 110°C in air in the Petri dishes for 14 days. (This resulted in a weight loss of about 0.2% due to evaporation of volatile components. Some oxidation may possibly have taken place.) c) Pure Mexphalte 40/50 irradiated in air to 10 Mrad using a ^{60}Co-source. (Dose rate about 0.3 Mrad/hour.) d) As a control, empty Petri dishes were also exposed to the various solutions employed in the experiment.

One of each set of samples were placed in pure water at 40°C, pure water at 20°C, pure water with an addition of ~ 10 nCi ^{134}Cs + 13 nCi ^{60}Co per ml, or either nearly saturated NaCl or $NaNO_3$ solution all at 20°C.

The exposure time was up to 180 days. Weight increases between 20 and 100 mg were attained. The variation in the weight of the empty control dishes was less than ±2 mg in all cases indicating that the use of glass containers does not significantly influence the accuracy of the method.

The weight increases are shown as a function of the square root of exposure time in Figs. 2 a, b, and c.

The accumulative amount of water going into a flat semi-infinitely thick sample of bitumen should follow the formula:

$$m = A \cdot c_1 \sqrt{\frac{4 \cdot D \cdot t}{\pi}} \text{ g water}$$

where D cm^2/sec is the diffusion coefficient, A cm^2 is the sample surface area and c_1 g/cm^3 is the (unknown) concentration of water in the surface layer of the bitumen. It is assumed that this layer is saturated with water momentarily at the beginning of the experiment. The term c_1 depends on the type of bitumen and on the concentration of water in the solution in contact with the bitumen. It is seen from the figures that the weight increases that occur after an initial period of about 1 week show a reasonable linear dependence on $\sqrt{t}$ in most cases. Values of $c_1^2 \cdot D$ derived from this later linear part of the curves are given in Table 1.

It is seen from Figs. 2 a, b, and c and the values given in Table 1 that the slopes of the curves are fairly reproducible, and that there is only a slight, if any, difference between the fresh, irradiated, and heated bitumen samples. The rate of water uptake increases considerably with temperature as expected for a diffusion-controlled process. The rate of weight increase diminishes considerably when the samples are placed in strong salt solutions instead of pure water. This is probably an effect of the lower water concentration in the strong solutions which must be reflected in a lower concentration of water in the surface layer of the bitumen sample.

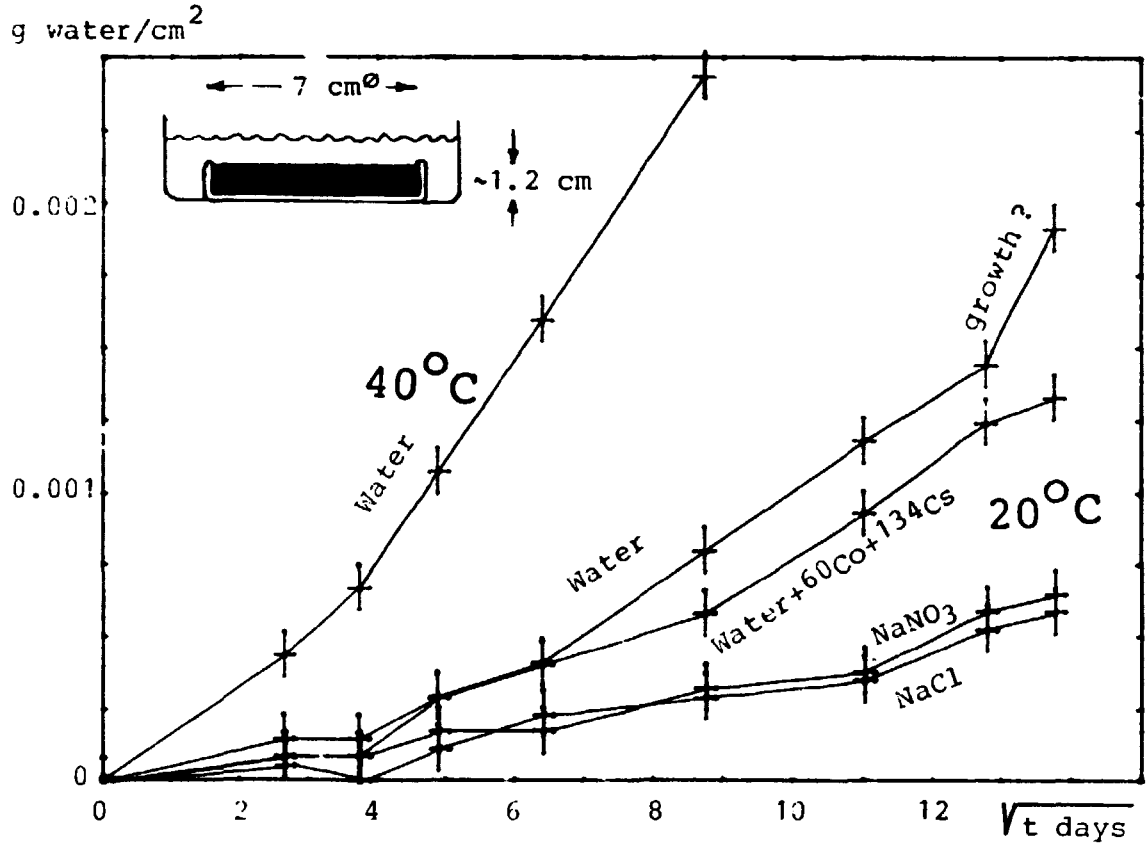

Fig. 2a. Water absorption into pure Mexphalte 40/50 from water and from saturated salt solutions. Weighing method.

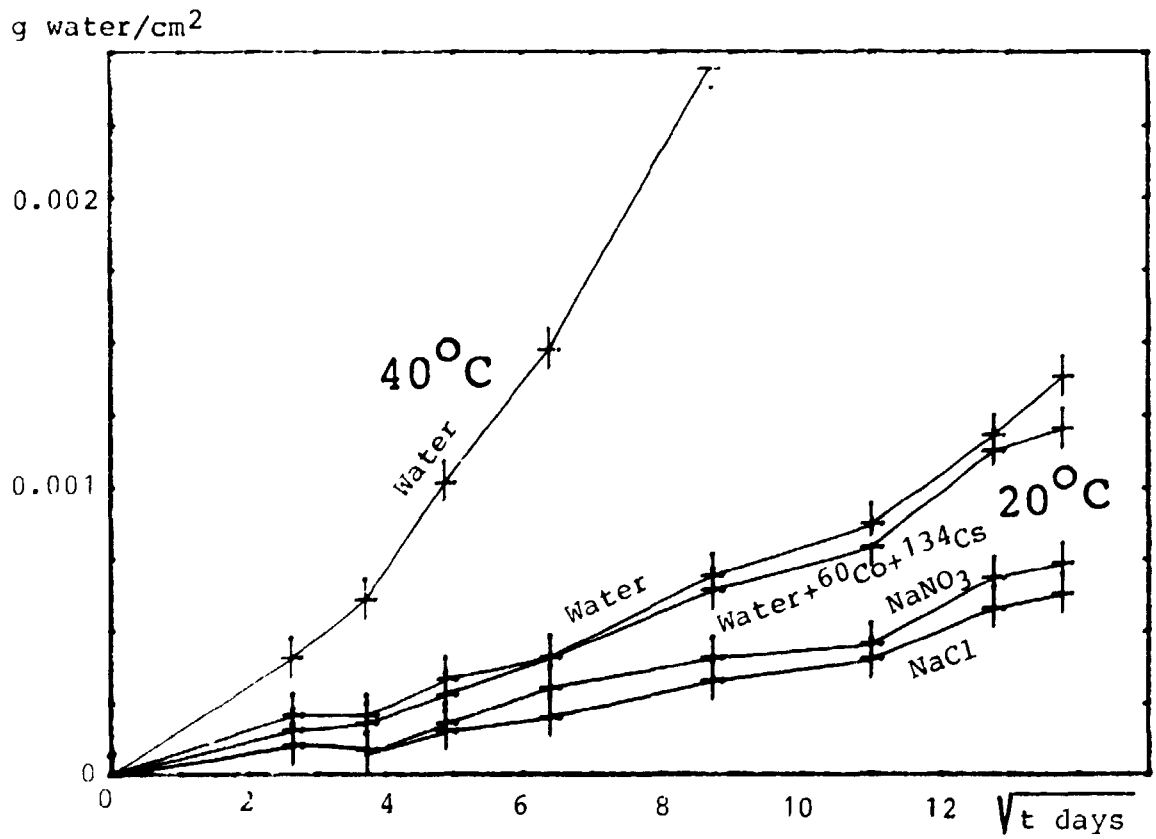

Fig. 2b. Water absorption into pure Mexphalte 40/50 after heating at 110°C in 14 days.

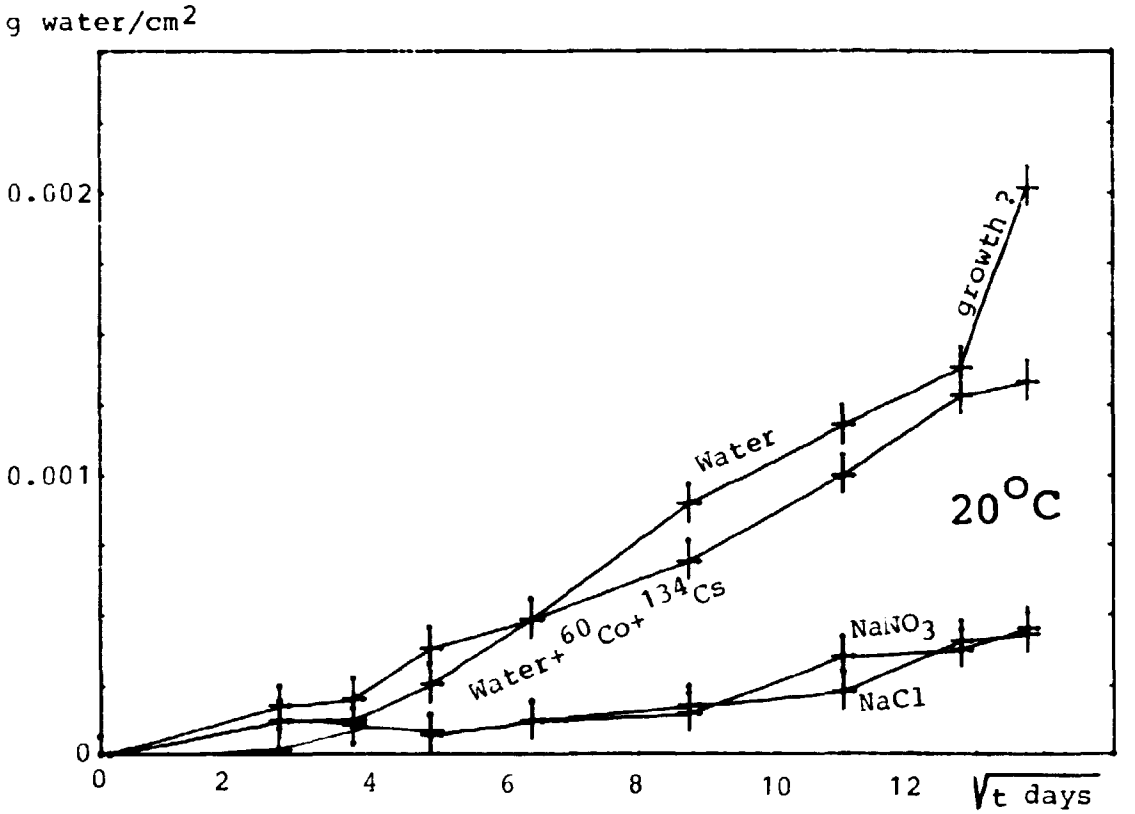

Fig. 2c. Water absorption into pure Mexphalce 40/50 irradiated to 10 Mrad.

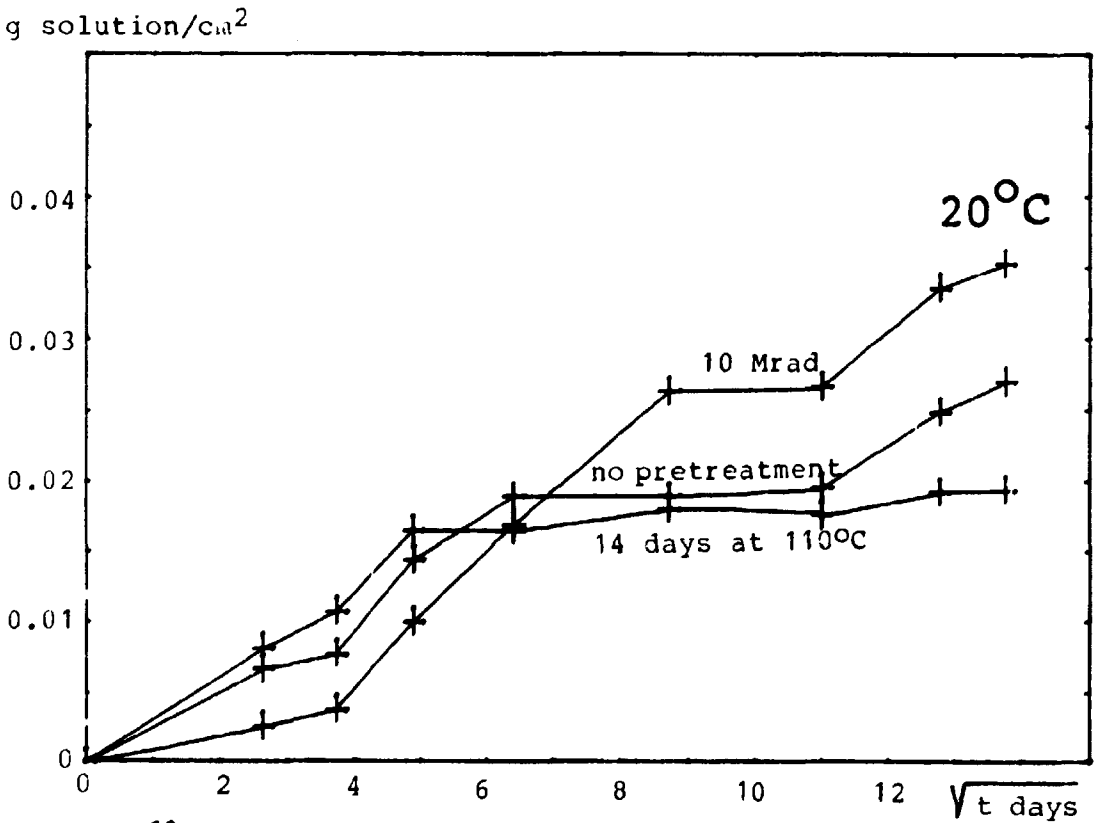

Fig. 3. ^{60}Co absorption in pure Mexphalte 40/50 pretreated in various ways from a solution containing 0.0125 µCi $^{60}Co/cm^3$.

Table 1. Transport coefficients for water in pure Mexphalte 40/50 calculated from weight increase measurements.

Immersed in:	$c_1 \cdot D$ 10^{-12} g^2/cm^4 sec		
	Untreated	Heated at 110°C for 14 days	Irradiated to 10 Mrad
Pure water at 20°C	0.19	0.12	0.16
Water with activity	0.14	0.10	0.14
Pure water at 40°C	1.15	1.22	-
Saturated NaCl solution at 20°C	0.02	0.02	0.01
Saturated $NaNO_3$ solution at 20°C	0.02	0.03	0.01
Pure water at 20°C Experiment in Fig.1.	0.11		

Two of the samples in pure water showed a sudden large increase in weight at the end of the experiment. This is thought to be due to microbial growth since some indications of this phenomenon could be noticed visually especially when the surfaces were dry.

The weighing method can give only the weight increases, i.e. the differences between water (and salt) going into the samples and organic components which may be dissolved from the bitumen by the water. In the case of the 40°C experiments this may be significant since an oily film was noticed on the surface of the water. However, an attempt to quantify this source of error was made only in the case of the 20°C experiments where the concentrations of oxidisable material in the water at the end of the experiments were determined by permanganate titration. The contents were low, corresponding to about 0.005 mg dissolved hydrocarbon/cm^2 surface area in the case of pure water and about 3 times as much in the strong salt solutions. This is only between 1/2 and 3% of the measured weight increases, which therefore must be a reasonably good measure for the water uptake. In the case of the strong salt solutions a contribution due to salt uptake cannot be excluded.

As a supplement to the weight measurements, in one of the experiments it was investigated whether a small amount of radioactive Cs^+ and Co^{++} present in the water from the beginning had any tendency to be adsorbed on the bitumen. This was done simply by gamma-spectroscopy counting of the bitumen samples after removing water adhering to the surface.

The results are shown in Fig. 3 as the accumulative adsorbed activity expressed as the equivalent amount of active solution absorbed per cm^2 exposed surface. Although the concentrations of ^{134}Cs and ^{60}Co were approximately the same in the water, the signal for adsorbed ^{134}Cs was about a factor 40 lower than for ^{60}Co. The control experiment with empty Petri dishes showed that the signal in the case of Cs could be explained by adsorption on the glass surface while only about 10% could be ascribed to this phenomenon in the case of ^{60}Co.

It is seen from Fig. 3 compared with Figs. 2 a, b, and c that the equivalent amount of water corresponding to the amount of ^{60}Co absorbed from the active solution is about a factor 10 higher than the actual amount of water absorbed in the samples as given by the weight increase measurements. Preferential absorption of Co must therefore take place in (on) the bitumen. The high initial rate of adsorption followed by a tendency to a lower rate may indicate that mainly the surface layer is involved. When this is saturated the rate is governed by a much slower diffusion into the interior of the sample. However, the information is insufficient for any firm conclusion to be drawn.

2.1.2. Transport of tritiated water and $^{134}Cs^+$ through bitumen membranes

In a sample of bituminized waste, each individual waste particle is surrounded by a thin film of bitumen which gives some but not complete protection if the material gets into contact with water. The weight increase measurements reported in Section 2.1.1 give some indication of the rate of transport of water into bulk samples of bitumen, but it would be of interest to supplement this information with direct measurements of transport of water

through thin membranes of bitumen. Information about transport of salts in solution is also important for the understanding of osmotic phenomena which seems to play a role in connection with bituminized sodium nitrate and other soluble salts (see Sections 2.3 and 2.4).

Two experiments have been made so far. The membranes were prepared from Mexphalte 40/50, which was cast between two layers of siliconized paper. After cooling to ~ 0°C the paper could easily be removed. The membranes were then reinforced on one side by nylon net (lady's stocking). The two thicknesses, 0.25 and 0.59 mm, were calculated from the weight of the membrane. The preparation was somewhat tricky but visually the membranes showed no defects either before or after the experiment.

The membranes were mounted between two stainless steel chambers with dimensions as indicated in Fig. 4a. A solution containing 0.174 mCi/ml of tritiated water as well as $^{134}Cs^{+}$ was placed in the left-hand chamber while the right-hand one was filled with pure water, which was replaced and analysed at suitable intervals.

During the experiment, which was run for 234 days, only a minor fraction (< 7%) of the activity in the strong solution was transferred to the weak solution, where the concentration in all samples was low compared with the strong solution (< 1%). A reasonably good approximation to steady-state conditions as far as concentrations are concerned have therefore been maintained during the experiment.

In an idealized system migration through a membrane can be described as indicated in Fig. 5.

In a bitumen membrane x cm thick, it is supposed that the initial concentration of the migrating water is $c_o = 0$ while the concentration in the strong solution c_1^* is constant during the whole experime and the concentration in the weak solution is $c_2^* = 0$ also during the whole experiment. The concentration in the surface layer of the sample is assumed momentarily to

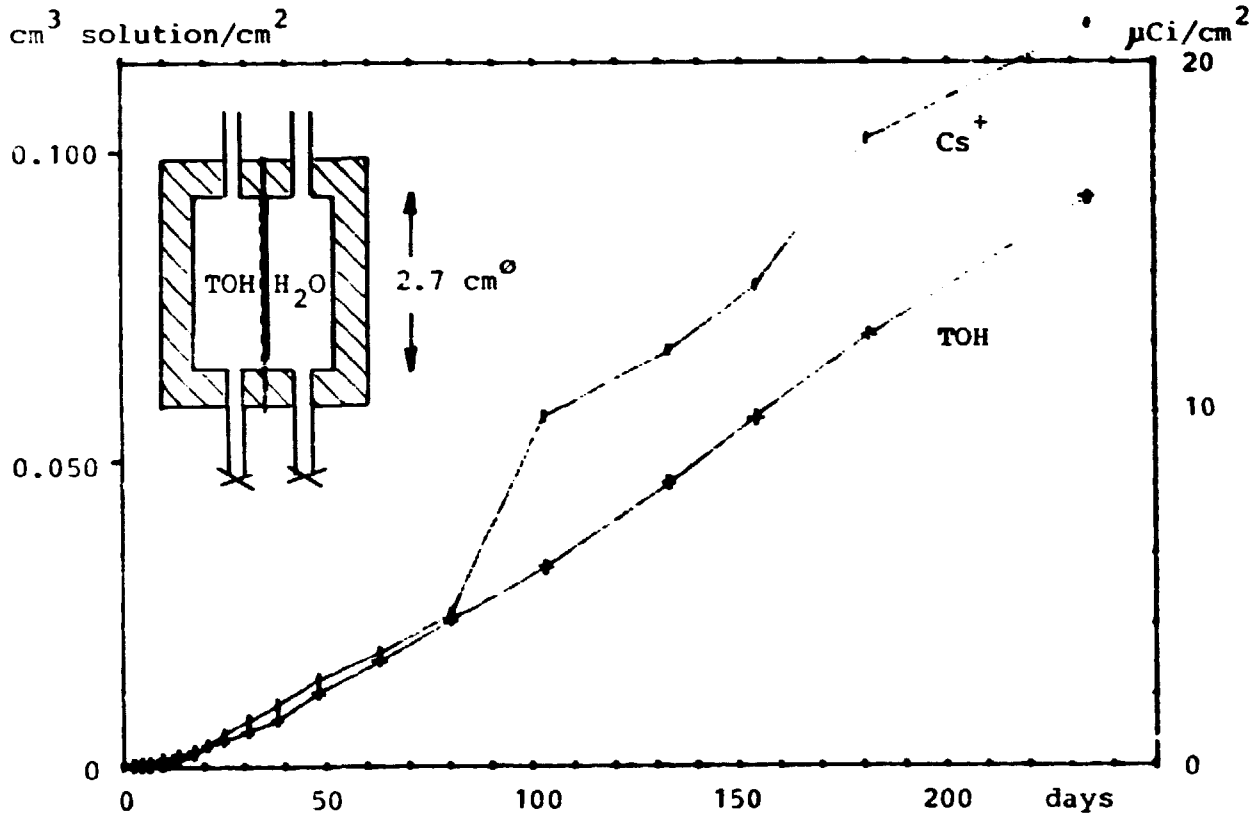

Fig. 4a. Transport of tritiated water and Cs^+ solution through 0.25 mm thick membrane of pure Mexphalte 40/50.

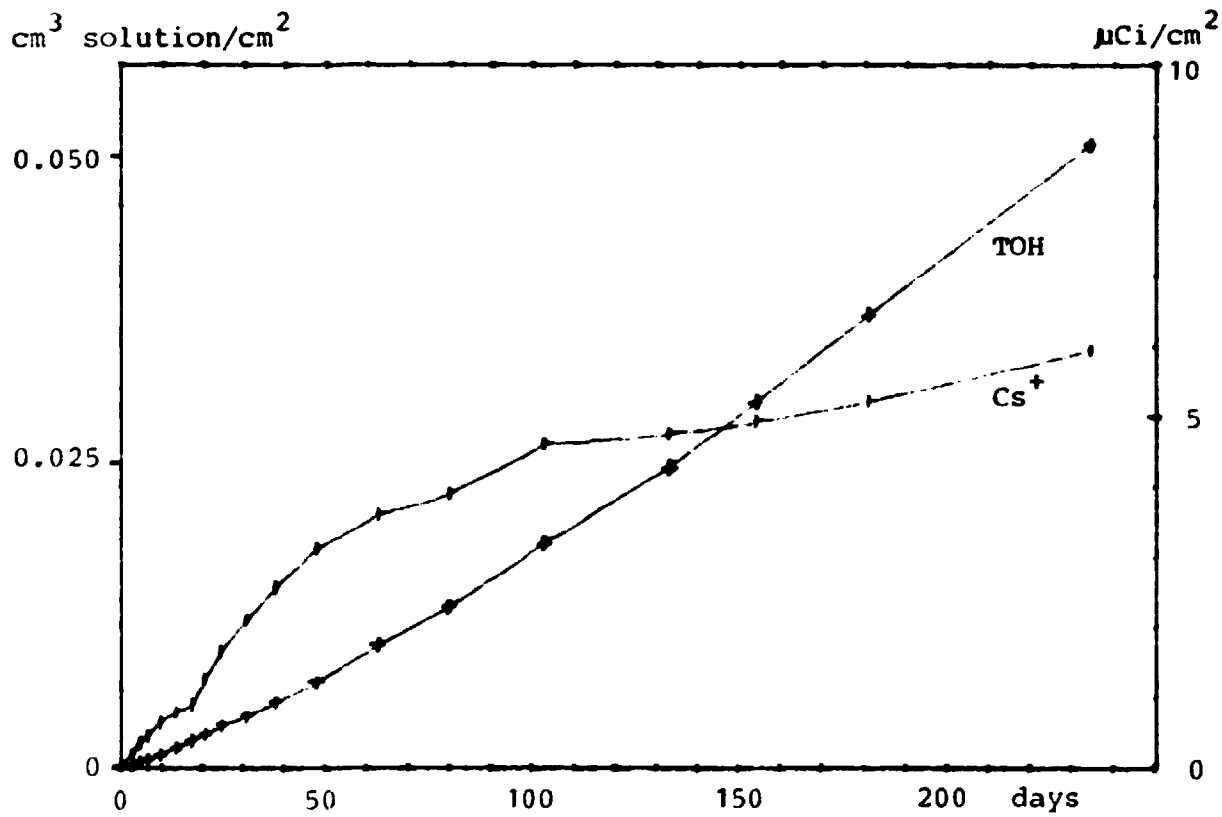

Fig. 4b. Transport of tritiated water and Cs^+ solution through 0.59 mm thick membrane of pure Mexphalte 40/50.

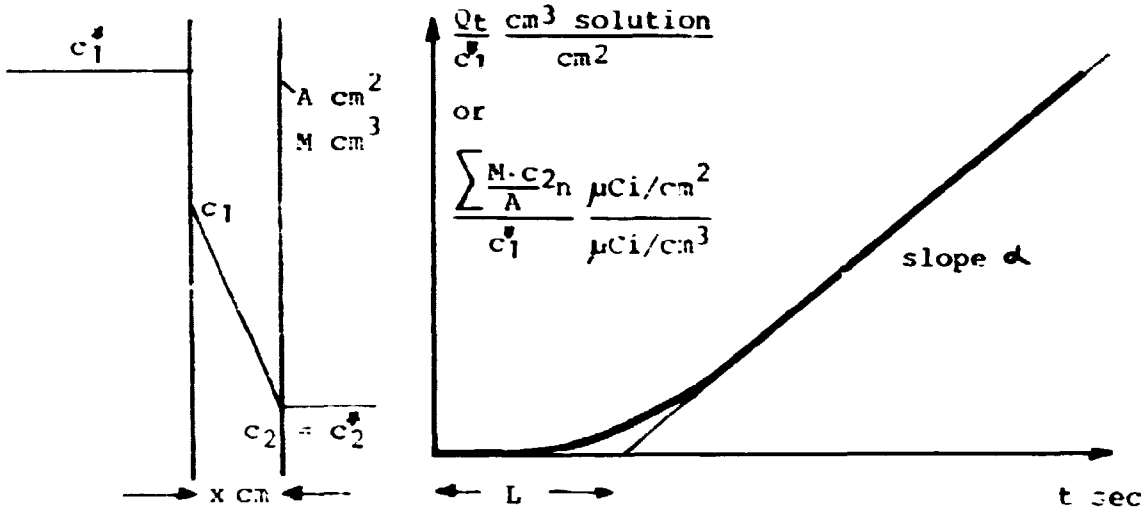

Fig. 5. Concentration profile and penetration curve for an idealized membrane x cm thick.

reach the concentration $c_1 = S \cdot c_1^*$, where S is the solubility of water in bitumen. Similarly is on the weak side: $c_2 = S \cdot c_2^* \cong 0$.

The accumulative amount of material transported through the membrane in such a system should show a dependence on time as indicated to the right in Fig. 5. The straight line with inclination α represents the steady diffusion governed by Fick's 1st law. It follows that

$$\alpha = \frac{(c_1 - c_2) \cdot D}{c_1^* \cdot x} \cong \frac{c_1 \cdot D}{c_1^* \cdot x} = \frac{S \cdot D}{x} = \frac{P}{x}$$

using the usually assumed relationship between the permeability coefficient P, diffusion coefficient D, and solubility S:

$$P = S \cdot D$$

It can be shown (6) that the time-lag L representing the intersection between the steady-state straight-line approximation and the t-axis is dependent only on the membrane thickness x

and the value of the diffusion coefficient D:

$$L = \frac{x^2}{6 \cdot D}$$

This makes it possible in principle to determine the diffusion coefficient independent of the solubility S.

The experimental results are shown in Figs. 4a and b. The accumulative amounts in $\mu Ci/cm^2$ or cm^3 of TOH or $^{134}Cs^+$ solution transferred through each cm^2 membrane area are given as a function of time.

Tritium diffusion through both membranes seems to follow a reasonable approximation to Fick's 1st law, but there is a tendency to an increasing rate of diffusion with time. This is of minor importance for the numerical value of the slope of the straight line approximation to the curve, but it makes the determination of L difficult. Values of 10 to 20 days are upper limits, but L = 1 day or even less is not excluded.

In the case of the 0.25 mm membrane Cs^+ diffusion follows the migration of tritiated water very closely in the initial period, and it would have continued to do so except for the single ^{134}Cs measurement at 105 days which may be an error. The diffusion of tritiated water and Cs^+ at the same rate indicates transport through water-filled pores or cracks in the membrane since Cs^+ should be retarded relative to water if the transport of water took place as a true solution of water in bitumen.

In the case of the 0.59-mm membrane the behaviour of Cs^+ is curious. It seems that the rate of diffusion of Cs^+ solution is faster than the rate of diffusion of the tritiated water at least in the first part of the experiment. This is difficult to explain. The general shape of the curve is also curious giving the impression that the preferential transport channels for Cs^+ disappears (or rather disappear, reappear, and disappear again) during the experiment, so that the rate of Cs^+ transport in the last half of the experiment is considerably lower than the rate

of water transport through the membrane. Numerical values for the permeability coefficients estimated from Figs. 4a and b are given in Table 2. They are in reasonable agreement for the two membranes and of the same order of magnitude for the transport of water as well as Cs^+ ions. This may indicate that transport through the membranes is mainly by pores or cracks. However, further investigation of the transport of water and ions through bitumen is necessary before any firm conclusion can be drawn as far as the mechanism is concerned.

Table 2. Permeability coefficients for tritiated water and $^{134}Cs^+$ in thin membranes of pure Mexphalte 40/50 in (nearly) pure water at 20-25°C.

Membrane thickness	Permeability coefficient from the slope of the curves in Figs 4a and b.		
x cm	P = S·D 10^{-12} cm^2/sec		
	TOH	Cs^+	
0.025	58 130	110 160	Beginning of exp. End of exp.
0.059	82 170	170 40	Beginning of exp. End of exp.

Combining the values from Table 2 for $P = S \cdot D \cong 70 \cdot 10^{-12}$ cm^2/sec for the beginning of the experiments with the values for $c_1^2 \cdot D = S^2 \cdot c_1^{*2} \cdot D \cong 0.16 \cdot 10^{-12}$ $g^2/cm^4 \cdot sec$ for the same material at approximately the same temperature in Table 1, makes it possible to determine the values for S and D for Mexphalte 40/50 exposed to pure water (where $c_1^* = 1$ g/cm^3) at ~ 20°C. The following values are obtained:

$$D = \frac{P^2}{c_1 \cdot D} = 3.1 \cdot 10^{-8} \ \frac{cm^2}{sec}$$

$$S = \frac{c_1^2 \cdot D}{P} = 2.3 \cdot 10^{-3} \ \frac{g \ \text{water}}{g \ \text{bitumen}}$$

Assuming that D and S are independent of the composition of the solution in contact with the bitumen the following values for $c_1^2 \cdot D$ for saturated NaCl and saturated $NaNO_3$ solution can be obtained by introducing $c^*_{1_{NaCl}} \equiv 0.88$ and $c^*_{1_{NaNO_3}} \equiv 0.80$ g/cm^3 into the formula $c_1^2 \cdot D = S^2 \cdot c_1^{*2} \cdot D$:

$$c_{1_{NaCl}} = 0.13 \cdot 10^{-12} \ \frac{g^2}{cm^4 \ sec}$$

$$c_{1_{NaNO_3}} = 0.10 \cdot 10^{-12} \ \frac{g^2}{cm^4 \ sec}$$

These values are somewhat too high compared with the experimentally determined values in Table 1.

Introducing the values for D in the formula $L = x^2/6 \cdot D$ gives for the thickest membrane with $x = 0.059$ cm: $L \equiv 0.2$ days. The breakthrough occurred already during the first few hours and it is therefore not surprising that it is poorly defined in the figures.

The relatively high value of the diffusion coefficient means that saturation of even rather thick bitumen layers will occur within a reasonably short period. A 1-cm thick slab of Mexphalte 40/50 exposed to water from one side will reach more than 90% water saturation in about one year. The rate of water transport through 1 m^2 of such a slab will be about 1 g water/year, assuming that there is a water-removing process on the inside.

2.1.3. Solubility of water in bitumen

The solubility of water in pure Mexphalte 40/50 has also been investigated using an independent method based on tritiated water: Platinum vessels or small cylindrical glass beakers were coated on the inside by molten bitumen in the form of a thin layer with weight m g. After cooling, the containers were filled with water containing a known concentration c_k µCi/ml of tritiated water. The systems were left to equilibrate for 10 to 36

days. Then the tritiated water was removed, the surface of the bitumen film was cleaned fast but efficiently with flowing deionized water, and the bitumen layer was dissolved in a mixture of 10 ml Xylene and 10 ml water. The suspension was separated and the concentration c_v µCi/l of tritiated water in the water phase was determined. The solubility is then given by:

$$S = \frac{c_v \cdot 10}{c_k \cdot m \cdot 1000} \; \frac{\text{g water}}{\text{g bitumen}}$$

The results of the experiments are summarized in Table 3.

Table 3. Determinations of the solubility of water in pure Mexphalte 40/50 at about 25°C.

Bitumen m g	Thickness of layer mm	Time of equilibration days	c_k µCi/ml	c_v µCi/l	S g water/g bitumen	
0.50	0.18	36	77.9	4.8	$1.2 \cdot 10^{-3}$	Pt
0.53	0.18	11		35.0	$8.5 \cdot 10^{-3}$	
0.52	0.18	10		19.0	$4.7 \cdot 10^{-3}$	
0.51	0.18	21		27.0	$6.8 \cdot 10^{-3}$	
0.50	0.08	14	83.8	26.7	$6.3 \cdot 10^{-3}$	glass beaker
1.00	0.16			41.6	$4.9 \cdot 10^{-3}$	
1.50	0.24			45.4	$3.9 \cdot 10^{-3}$	
2.00	0.32			62.9	$3.8 \cdot 10^{-3}$	

In the last 4 experiments there is a systematic trend of increasing solubility with decreasing layer thickness. This may indicate incomplete saturation of the thicker layers, a surface phenomenon which results in a film of tritiated water which is difficult to remove in the rinsing process (growth of microorganisms on the surface would be an extreme case), or possibly a tendency to pore formations in thin layers. Adsorption on the glass surface cannot explain the trend since two control experiments with empty glass beakers showed that the amount of triti-

ated water adsorbed on the glass was insignificantly compared with the activity in the bitumen layers.

Disregarding the possible systematic errors it will be assumed here that the mean of the last 6 experiments is representative for the solubility of water in Mexphalte 40/50 at 25°C, i.e.

$$S = (5 \pm 2) \cdot 10^{-3} \text{ g water/g bitumen}$$

A solubility of about 0.5% water in pure bitumen is surprisingly high, but it is in reasonable agreement with the value for $S \cong 0.2\%$ found in the previous section.

In general, it can be concluded that a method has been developed by which fundamental constants for the transport of water in bitumen can be determined. The transport mechanism as far as ions in solution are concerned is still partly unexplained.

Some further work on pure bitumen/water systems will be made using the method described in the previous sections but supplemented with studies of electrical resistivities of bitumen membranes in contact with water and salt solutions. The intention is to use somewhat thicker membranes made from various types of bitumen.

2.2. Weighing method for determining water uptake in bituminized materials

The method which has been developed at Risø for studying water uptake and swelling of waste materials solidified by bitumen (or polymers) is based on simple weight measurements and mass-balance calculations over the system consisting of the sample together with the water in contact with the sample. Archimedes' principle is used for determining volume changes.

There is nothing advanced in the technique, which can be managed in all laboratories; nevertheless it seems able to give information that is important for understanding the swelling

and leaching phenomena in connection with bituminized and possibly also other types of solidified waste materials. The method may therefore be a valuable supplement to leach-rate measurements using classic methods.

The method has the following main features:

Cylindrical samples, for example, with dimensions as shown in Fig. 6a are cast from bituminized material using as mold a perspex or preferably a stainless steel ring closed at the bottom by a piece of siliconized paper. The paper is easily removed when the sample has cooled to room temperature. The casting is made at the lowest possible temperature (100-120°C) to avoid settling of the waste particles dispersed in the bitumen. The ring with the sample is then placed vertically in water in a beaker so that the two end surfaces are freely exposed. The ring gives sufficient support to the sample when immersed in water so that significant deformation is avoided even with rather soft bituminized materials. The exposure to water of both of the two flat end-surfaces, the one which was upward during the casting as well as the bottom one, tends to diminish the effects of settling of waste particles which may have occurred to some degree regardless of the attempt made to avoid it. Diffusion in and out of a sample where only two flat parallel end-surfaces are exposed is one-dimensional. This facilitates the mathematical interpretation of the experimental results.

Before being immersed in water the samples are weighed in air. After immersion they are weighed again, suspended in and completely covered by water, as indicated in Fig. 6c. The measurements are repeated at suitable time intervals. The weighing in air takes place after removal of water adhering to the sample. This is done with filter paper taking care not to damage the surface. An electronic balance is used for the weight measurements. The weights can be reproduced within about ±0.003 g. This means that also rather small volume changes can be registered. With the sample size employed about 0.01% seems to be the limit, provided temperature and other factors influencing

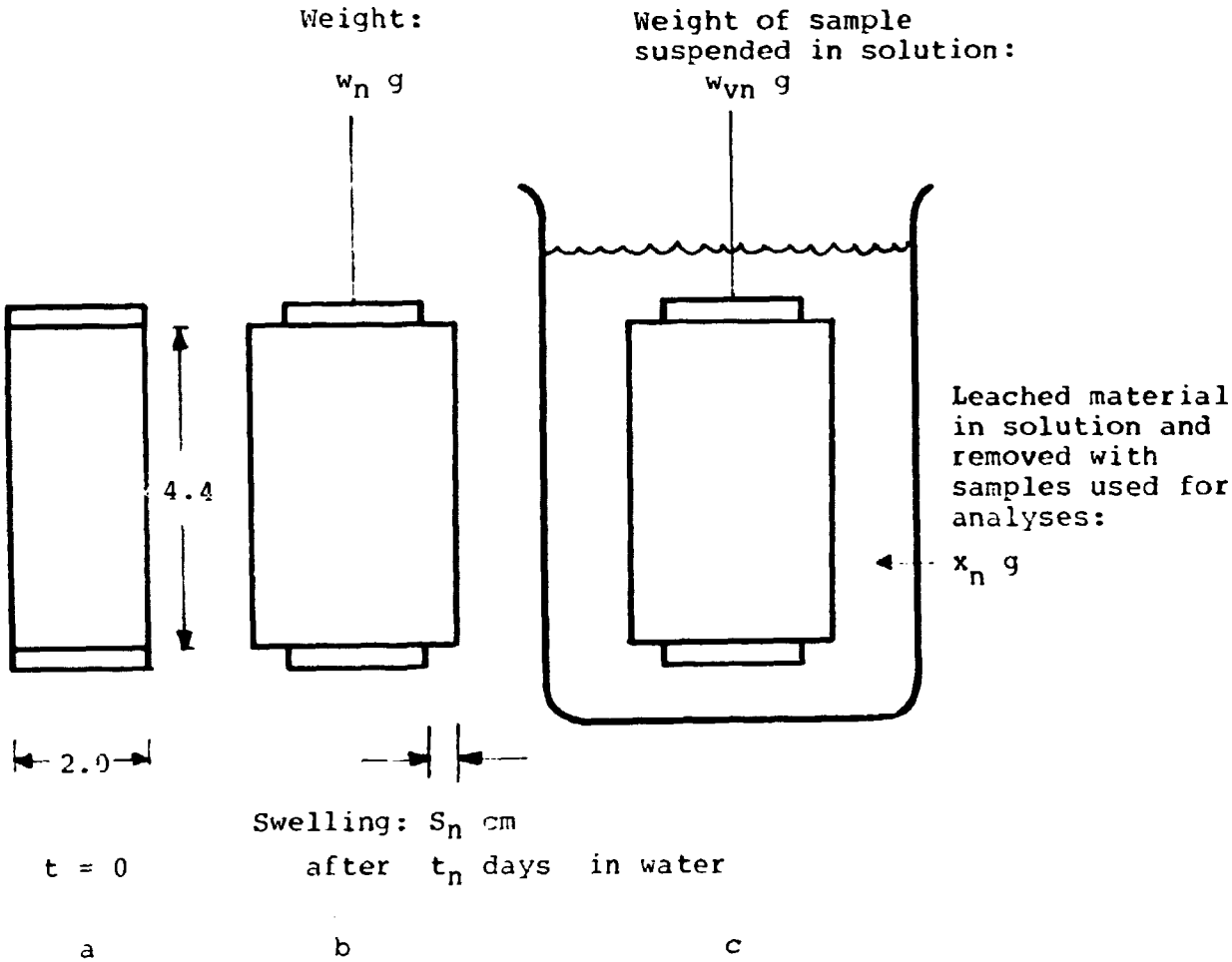

Fig. 6. Weight and concentration measurements necessary for determining weight change, water absorption, leaching of soluble materials, and swelling of a sample of bituminized waste material as function of time of exposure to water.

the density of the solution are controlled carefully.

Material leached from the sample is determined by simple measurement of dry material in the water or by chemical analysis. The amount of water in the system is maintained by adding pure water - as a substitute for evaporated water - until the original weight of beaker + sample is reached. This is done before each sampling. Water removed for analysis is replaced by fresh water or solution of known composition. It is necessary to keep track on the amount of solid material removed with the water samples used for analysis. Density of the solution is determined by calculation from the chemical composition or by direct meas-

urement. From these measurements the volume changes, i.e. swelling of the sample, can be determined together with water uptake and the amount of material leached out in the water. For simple systems and using some simplifying assumptions profiles of water penetration into the sample can be calculated also. For more complex systems, i.e. waste with more than one main component embedded in bitumen, the information tends to be insufficient and should preferably be supplemented by other measurements on the system.

The mass-balance calculation system is described in Appendix 1.

Leach rates can be determined simultaneously with the water uptake by chemical analysis or measurement of activity in the solution. It has been shown in some control experiments that the leach rates are not influenced significantly by wiping the surface before weighing in air. (See Section 2.8).

In the following some examples of the use of the methodology on specific systems will be described. This will give an impression of the various stages of the development of the method and indicate some areas where further investigation is needed.

2.3. Sodium sulphate bitumen system (Early experiments)

(Waste form No. 12)

It is quite normal at the end of a leaching experiment to measure the weight of the sample to get an idea of weight loss or water uptake which might have taken place during the exposure of the sample to water. In some preliminary experiments these weight changes were simply measured as a function of time. An example of the results is shown in Fig. 7.

The samples consisted of 40% sodium sulphate (water-free, crystallized from boiling water) and 60% Mexphalte 40/50. Three different particle sizes of the crystals were used. Such a system is known (7) to be unstable in water, but the figure gives some idea of the degradation rate.

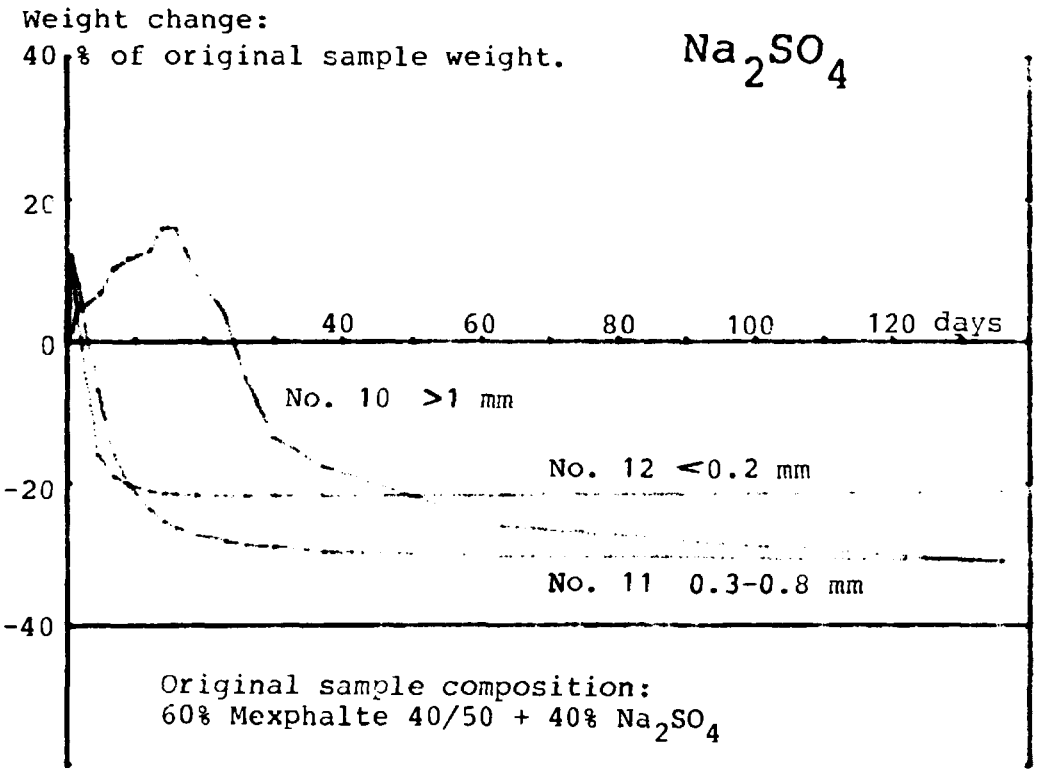

Fig. 7. Weight changes of samples immersed in water for three different particle sizes of the embedded water-free sodium sulphate crystals.

With fine-grained sodium sulphate, an initial weight increase - undoubtedly due to the formation of decahydrate: $Na_2SO_4 10H_2O$ in the sample - is rapidly followed by a large decrease in weight, which must be caused by leaching of sodium sulphate.

With large-grained sodium sulphate the period of weight increase lasted somewhat longer, probably due to the thicker layer of bitumen surrounding each crystal when coarse particles are employed.

The samples swelled considerably but collapsed somewhat again when the sodium sulphate was leached. The water was not changed during the experiment and was therefore converted into a relatively strong sodium sulphate solution. This explains why the weight change did not reach -40%, which corresponds to leaching of the total amount of sodium sulphate and indicates that a

considerable solution-filled porosity remained in the sample.

In Figs. 8a and b results from a repetition of these experiments are shown, again using a coarse- and a fine-grained sodium sulphate, but this time with determination of the concentrations in the solutions. This permits calculation of the water content in the samples. It is seen that the pore structure of the coarse-grained material collapsed nearly completely and that practically all the sodium sulphate had left the sample at the end of the experiment.

The swelling of fine-grained material proceeds faster, but the swelled material is more stable and seems able to retain a considerable amount of water. The ratio between remaining sodium sulphate (3.5 g) and water in the sample (7 g) corresponds to a nearly saturated sodium sulphate solution in the pores, i.e. concentrations about 10 times higher than in the surrounding solution. This situation cannot be stable in the long run, and the slight weight increases of the two fine-grained samples: No. 19 in Fig. 8 and No. 12 in Fig. 7, which can be noticed in the last period of the experiments, may indicate diffusion of water into a closed pore structure containing a strong solution, but where the solute is not or only to some degree able to penetrate the bitumen films surrounding each droplet. Experiments related to the phenomenon were described in Section 2.1.2, but further investigations are necessary before the mechanisms are understood.

Similar osmotic phenomena have also been observed in the experiments with sodium nitrate described in the following.

2.4. Sodium nitrate/bitumen system (Early experiments)

(Ref. Waste No. 7)

The sodium nitrate/bitumen system is generally supposed to be volume-stable in contact with water as sodium nitrate forms no hydrates. However, osmotic phenomena can also be expected in this system. Similar experiments as with the sodium sulphate/

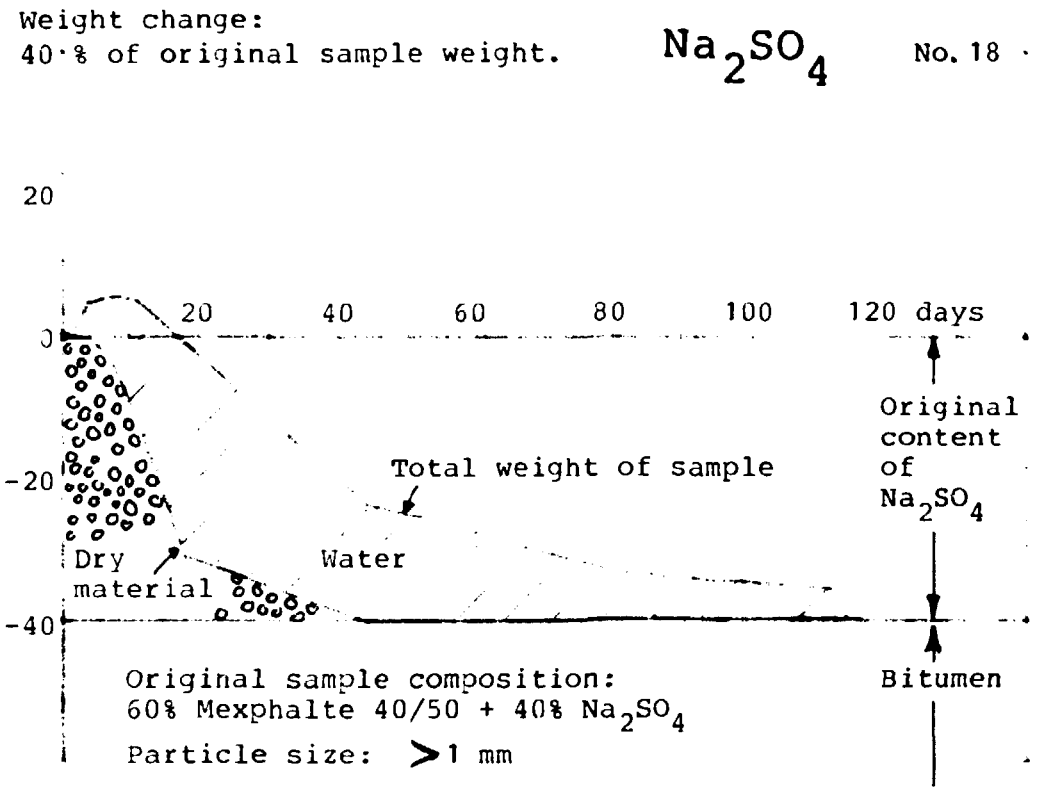

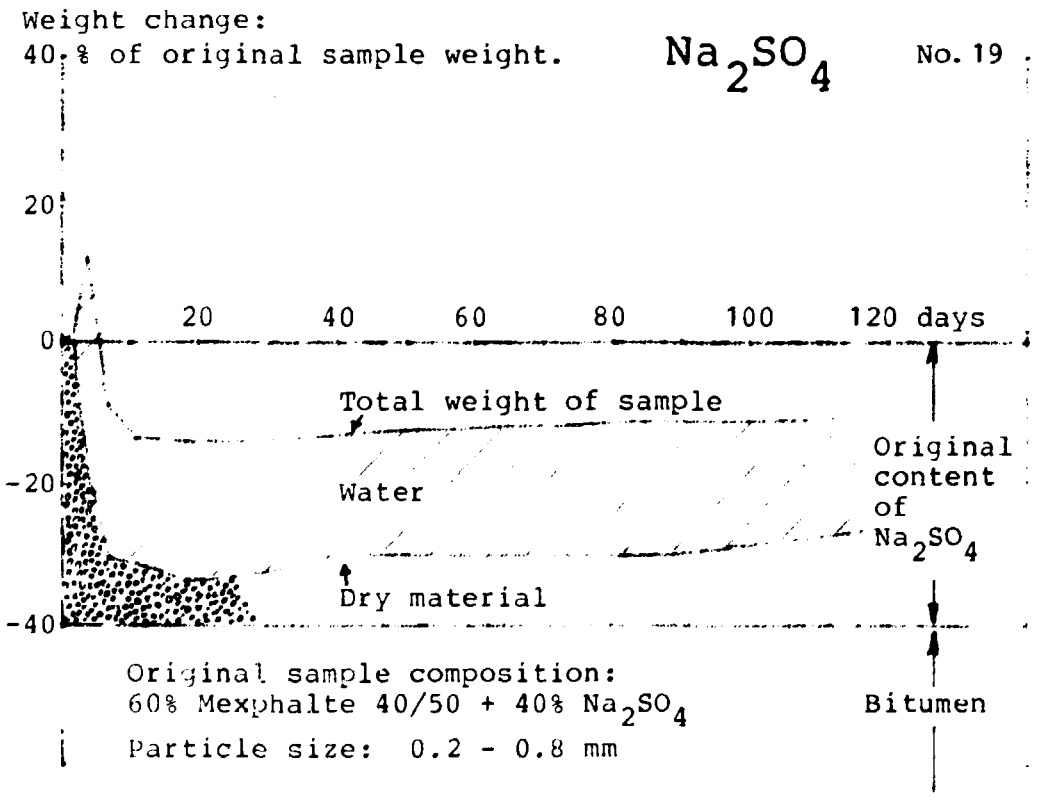

Fig. 8a and b. Weight changes and water absorption in samples immersed in water for two different particle sizes of the embedded water-free sodium sulphate crystals.

bitumen system were therefore made using samples containing 40% $NaNO_3$ and 60% Mexphalte 40/50. The measured weight changes and water uptakes are shown in Figs. 9a, b, c and d for 4 different particle sizes of the embedded sodium nitrate crystals. The weight changes are much smaller than in the case of sodium sulphate but by no means insignificant. Some trends depending on particle size can be observed immediately:

- There is an initial fast decline in content of dry material in the samples followed by a period with much slower release rates as indicated by the slopes of the lower lines in the figures. The leach rates for sodium nitrate tend to diminish with decreasing particle size of the embedded material.

- All the systems contain water, from 0.9 to 1.8%, after 116 days in water. This water must be present as a solution of more or less saturated sodium nitrate in pores in the material.

- Except in the case of the most coarse-grained material, the water absorption generally tends to compensate for the weight loss due to leaching of sodium nitrate. In the case of the fine-grained material, the water uptake was even larger and resulted in a weight increase of the sample. This is only possible with this system if some swelling takes place, but the volume increases were not measured directly.

Leaching, together with the water-sampling manner used, resulted in the case of the experiments shown in Fig. 9 in water concentrations from 1 - 6 g sodium nitrate per litre. In Figs. 10a and b, results are shown from two similar experiments using a material with particle size corresponding to a mixture of b and c in Fig. 9. In the new experiments the initial release of solid material is somewhat larger than in the previous ones. This may be associated with slight differences in sample preparation in the two cases. The tendency to absorb water seems to be slightly less than in the previous cases, but it should be noted that the

new experiments were run for only about 60 days against the 116 days in the first experiments.

The difference between experiments a and b in Fig. 10 is the use of a different sampling method for the water in the two cases. In experiment a only a small fraction of the water was removed and replaced by pure water at each sampling which was made twice every week. This resulted in typical concentrations of 5-3 g $NaNO_3$/l in the water during this experiment. In experiment b the total amount of water was replaced at each sampling resulting in very low $NaNO_3$ concentrations in the water after the first replacement. The result seems to be a slightly higher water absorption than in case A. This agrees with the tendency which must be expected if the driving force for water absorption is the dilution of a strong sodium nitrate solution contained in closed pores in a semi-permeable matrix-material. The rate of diffusion of water into the system is probably proportional to the concentration difference between the strong solution in the pores and the concentration in the surrounding water.

Strong sodium chloride solutions, which would be typical of accident conditions in disposal in salt formations, will probably also diminish the tendency to water uptake in bituminized sodium nitrate or other soluble salts.

The release of sodium nitrate from the samples in Fig. 10 was determined by atomic absorption analysis of Na^+ in the water. This gives greater accuracy than the determination of total dry material used in the first experiments shown in Fig. 9

For comparative purposes ordinary leach curves based on releases of dry material given in Figs. 9 and 10 have been calculated and are shown together for all 6 samples in Fig. 11. The accumulative equivalent leached thickness in cm is shown as a function of the square root of leaching time. The leach rates at 100 days: S_{100} is given by the slopes where the curves intersect the line $\sqrt{t} = 10$. Values from $3 \cdot 10^{-4}$ to $0.2 \cdot 10^{-4}$ cm/day ($\sim 7 \cdot 10^{-4}$ to $0.5 \cdot 10^{-4}$ g/cm^2·days) are obtained, with the lowest

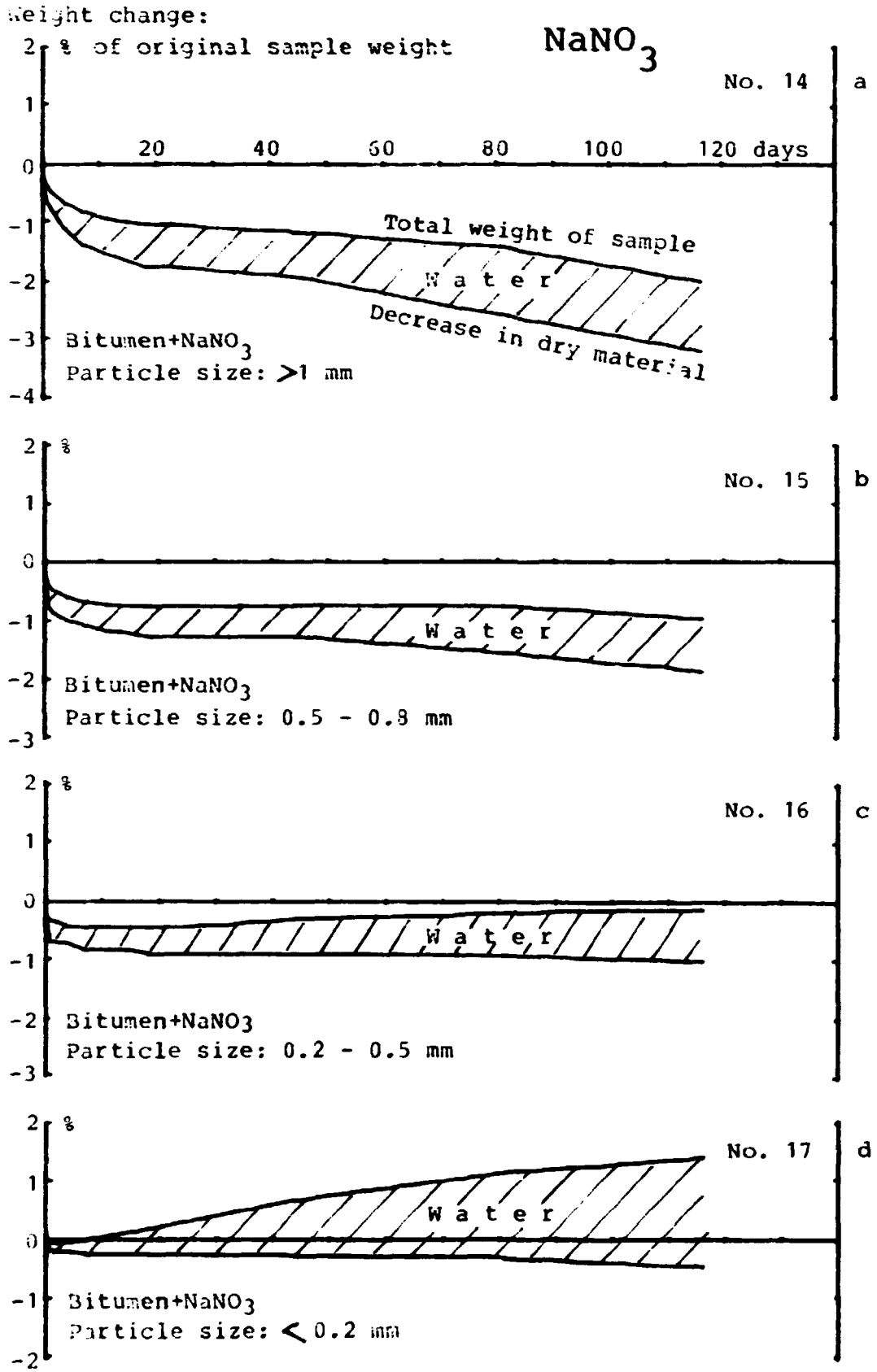

Fig. 9. Weight changes and water absorption in samples immersed in water for four different particle sizes of the embedded sodium nitrate crystals. (Corrected for a slight water uptake in the Perspex rings holding the samples.) Original Composition: 60% Mexphalte 40/50 + 40% $NaNO_3$ crystals.

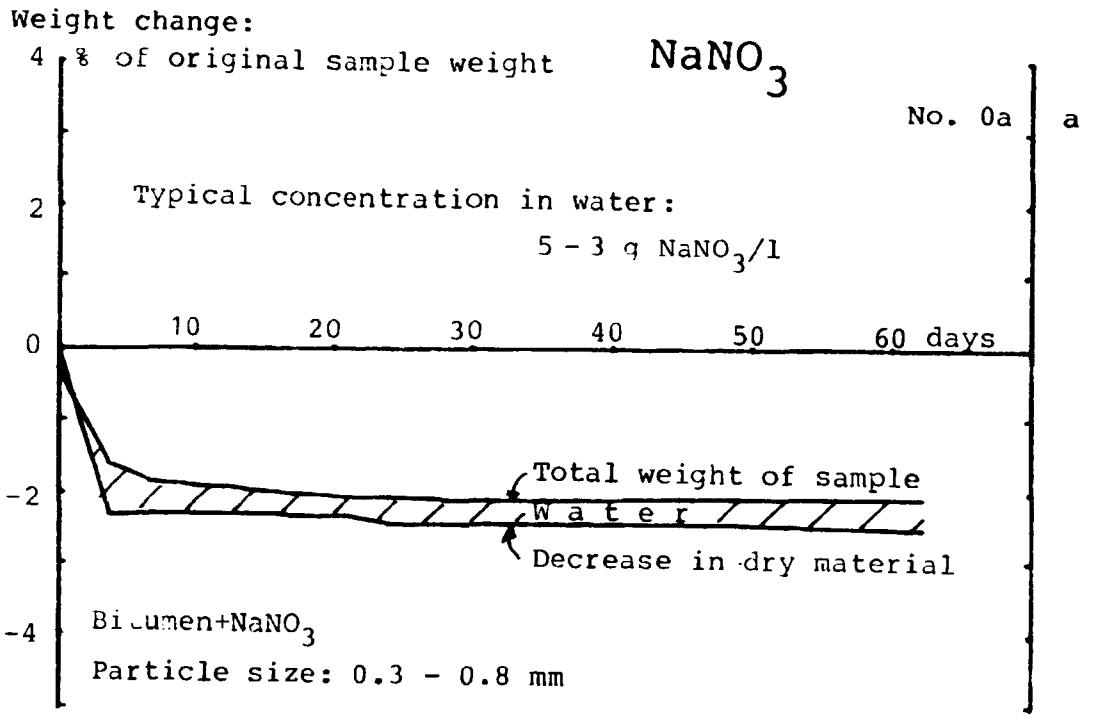

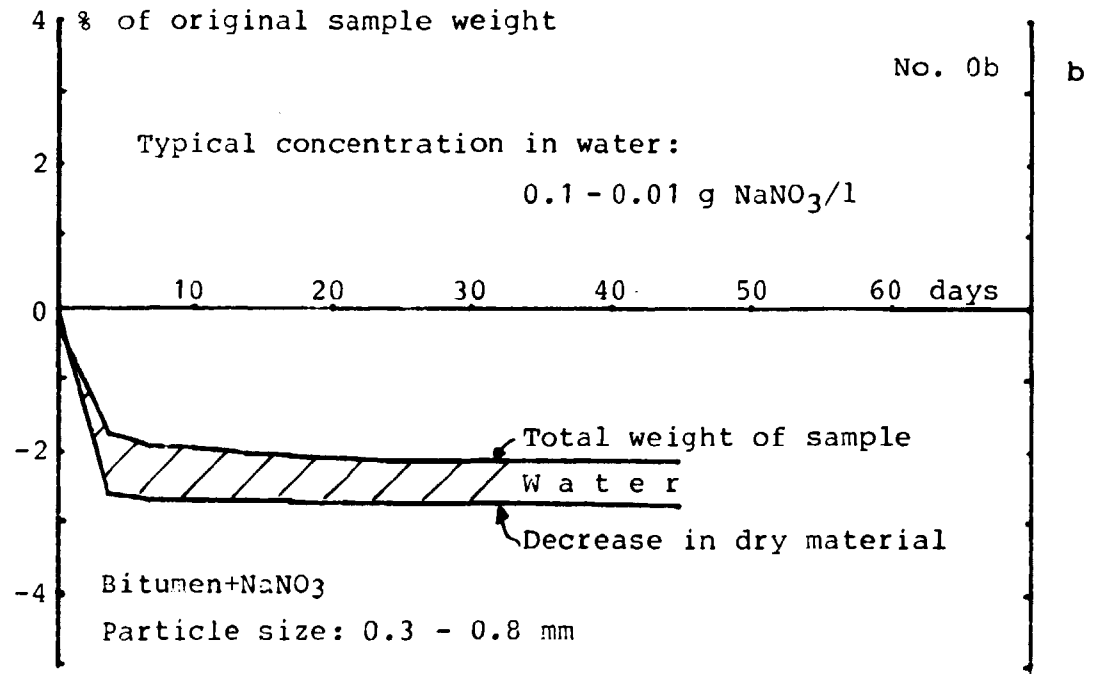

Fig. 10a, b. Weight changes and water absorption in two identical $NaNO_3$-containing samples immersed in water using respectively partial sampling or complete renewal of the water twice a week, resulting in very different sodium nitrate concentrations in the water in contact with the sample. (Corrected for a slight water uptake in the Perspex rings.)

Original composition: 60% Mexphalte 40/50 + 40% $NaNO_3$ crystals.

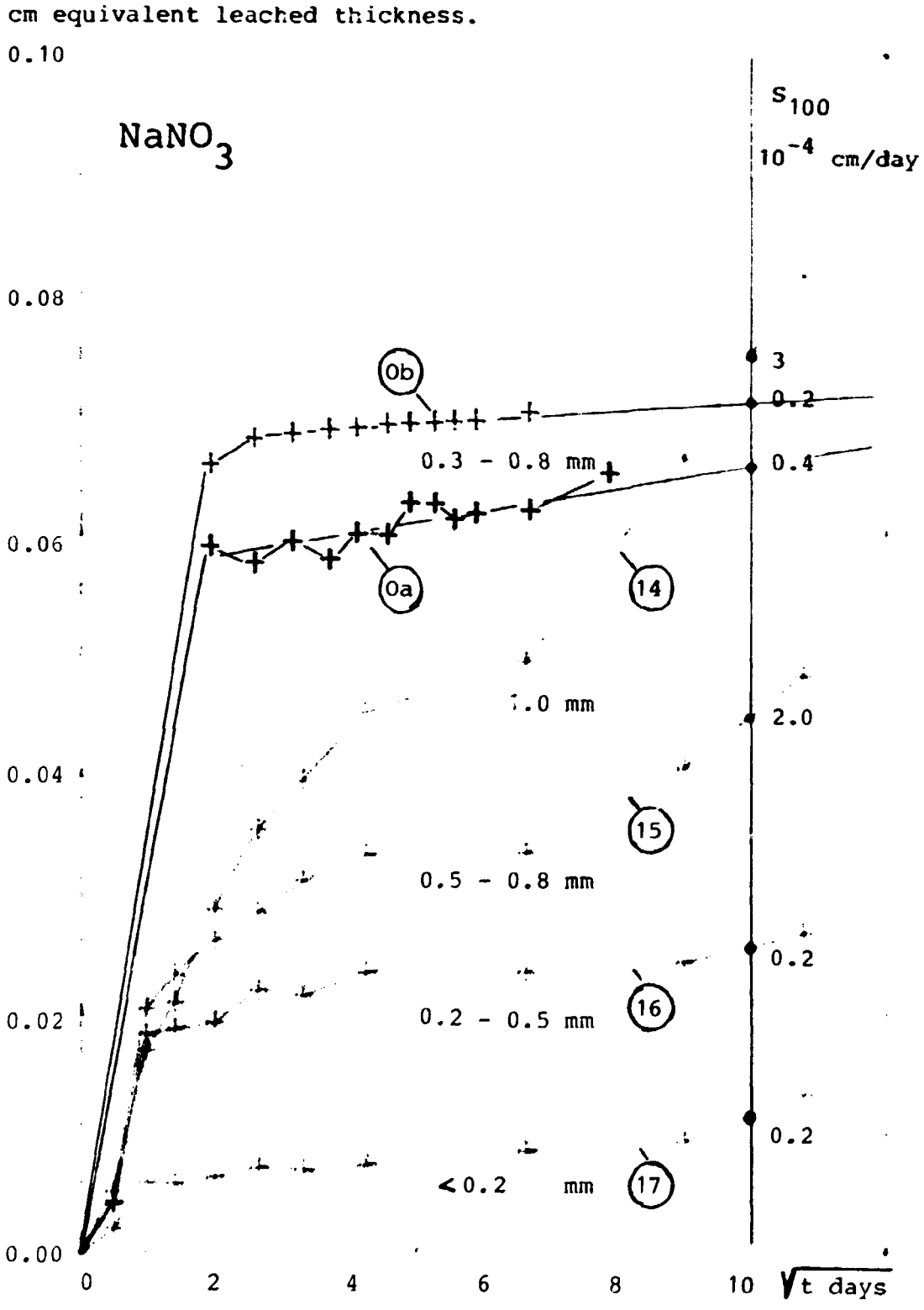

Fig. 11. $NaNO_3$ leaching from samples containing 60% Mexphalte 40/50 and 40% pure sodium nitrate in the form of crystals with different particle sizes. Samples Nos. 14 to 17 and Ob in a relatively strong sodium nitrate solution, Oa in a thin solution.

values for the fine-grained materials. The same trend with grain size has also been observed for sodium chloride in German investigations (8). The shape of the curves for sample Nos. 14 and 17 is interesting, and it should be investigated whether the trend to increasing leach rates after about 50 days is a real phenomenon.

The samples were prepared simply by mixing various sieve fractions of dry sodium nitrate crystals with molten bitumen at about 100° to 120°C. The crystals in the coarse fractions were considerably larger than is typical of real bituminized sodium nitrate waste. A crystal size of about 40 µm is mentioned in (8) for sodium nitrate bituminized in extruders. The large crystals, and the possibility that the simple preparation method may result in a somewhat unefficient dispersion of the crystals in the matrix, can be used to argue that the results are not relevant to real waste. However, inefficient dispersion, with chains of sodium nitrate crystals touching each other, would result in an increased leach rate and not in the observed increase in water uptake and decrease in leaching with decreasing particle size.

Recent Belgian experiments with real medium-level bituminized reprocessing waste containing sodium nitrate have shown that water uptake and swelling of such materials may occur (9).

Due to the practical importance of the sodium nitrate/bitumen system further investigations should be conducted of the phenomena described above. Some work is in progress at Risø within the frame of the CEC cooperation projects.

2.5. Example of leaching from and water uptake in bituminized evaporator concentrate from the production plant at Risø

(Waste form No. 13)

The materials used in the experiments described so far have all been of a synthetic type, i.e. simulated waste of simple composition which was mixed with bitumen in primitive laboratory

equipment. To demonstrate the use of the characterization method on real radioactive waste, a few experiments have been made with materials produced by the bituminization facility which is a part of the waste management plant at Risø. An example of such an investigation is described below.

The bituminization plant at Risø is a relatively small facility operated after a batch principle (10). When in use it converts in a one-day cycle about 300 l concentrate from the waste-water evaporator plant into bituminished material containing about 40% dry waste. The rest is Mexphalte 40/50 delivered by Danish Shell. The plant has been used for about 13 years without any significant technical troubles.

The material chosen for the characterization study contains waste from operation period No. 74 of the evaporator plant. An approximate composition of the concentrate is given in Table 4. The inorganic components are mainly sulphates and chlorides of the alkali metals. A considerable amount of sludge is normally present but the content is rather low in this particular concentrate. No additives are used to precipitate sulphates. A high content of organic materials of only a partly known type is present. This is rather typical for evaporator concentrate waste from nuclear research laboratories. The organic fraction contains considerable amounts of detergents from laboratories, laundry and decontamination operations. Another major component is an organic foam suppressing agent used in rather large amounts in the evaporator plant. It has been found that the stability of the bituminized product in water is improved by heating for about one hour to 200°C. This results in considerable cracking or distillation of organic materials.

A sample of the bituminized evaporator concentrate was collected from the outlet of the apparatus in connection with the emptying of a batch. The material had the approximative composition given in Table 5. The specific activity of the material is low. This gave some measurement problems in the leaching experiments especially in the case of cesium.

Table 4.

Major components in concentrate from the waste-water evaporator plant at Risø. Period No. 74. 80-11-22 to 81-03-27.

		g/l		g/l
Dry material (105°C)		124		
Mostly organic	Weight loss by heating to 200°C	11		11
	Xylene extractable	8		8
Soluble in water		102	SO_4^{--}	42
			Cl^-	12
			NO_3^-	0.2
			NO_2^-	0.7
			PO_4^{---}	4.5
Sludge, soluble in HNO_3 (atypically low)		2	Na^+	24
			K^+	6
			Ca^{++}	0.05
			Uranium	0.4
Insoluble		0.5		0.5
Total:		123.5		109.3

pH: 8.9

Density: 1.073 g/cm^3

Activity: ~0.01 $\mu Ci\alpha/cm^3$ ~40 $\mu Ci\beta/cm^3$

Table 5.

Approximate composition of sample of bituminized evaporator concentrate from period No. 74. Collected 81-04-13.

	Weight %
Organic materials, mostly Mexphalte 40/50	~67
Water soluble, Na_2SO_4, NaCl, etc.	25
HNO_3 extractable, sludge etc.	3
Insoluble	~ 5
Density:	1.185 g/cm^3
Specific activities:	0.0014 $\mu Ci\ ^{134}Cs/cm^3$
	0.059 $\mu Ci\ ^{60}Co/cm^3$

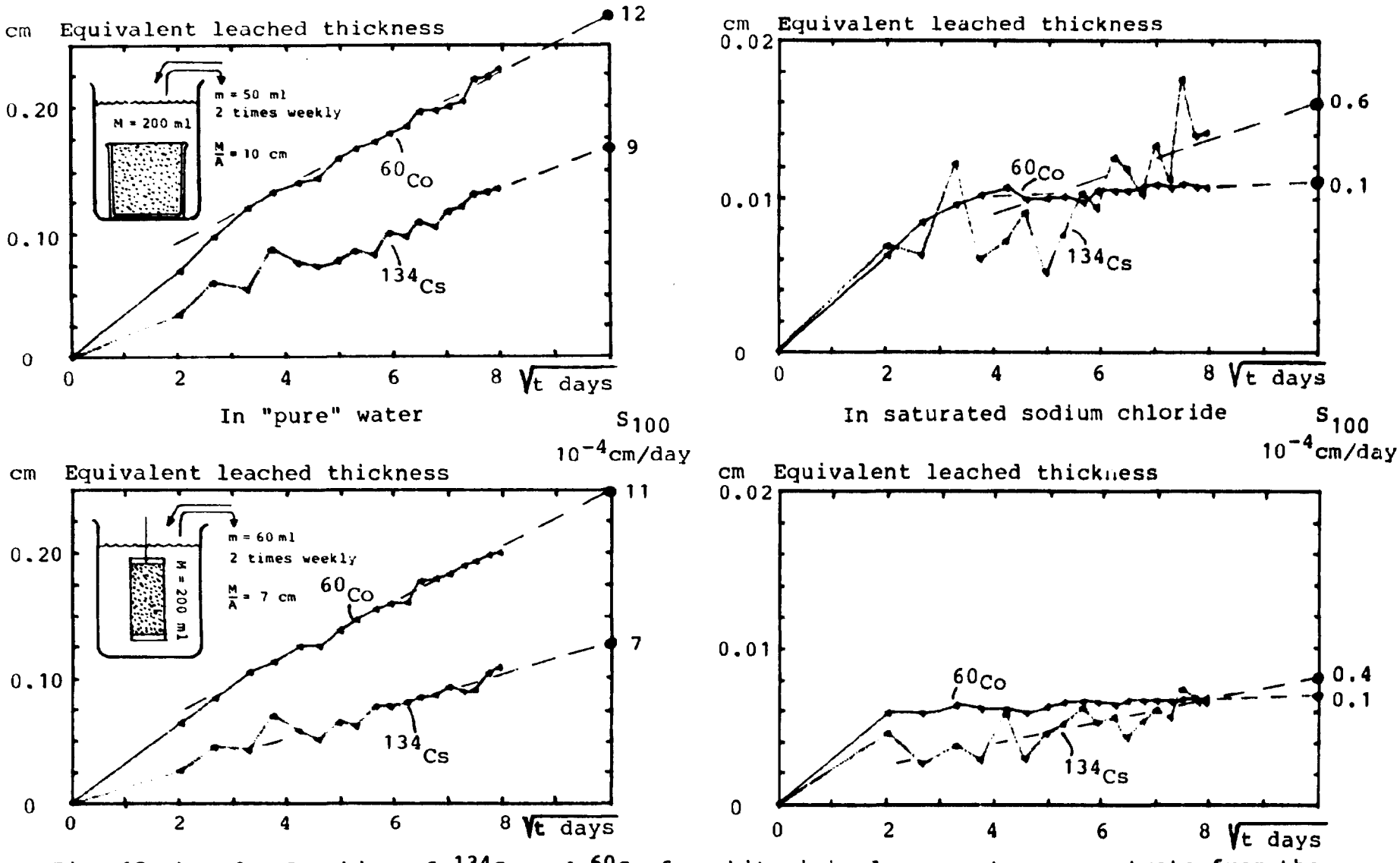

Fig. 12a,b,c,d. Leaching of ^{134}Cs and ^{60}Co from bituminized evaporator concentrate from the Risø plant. Period 74, sample collected 81-04-13.

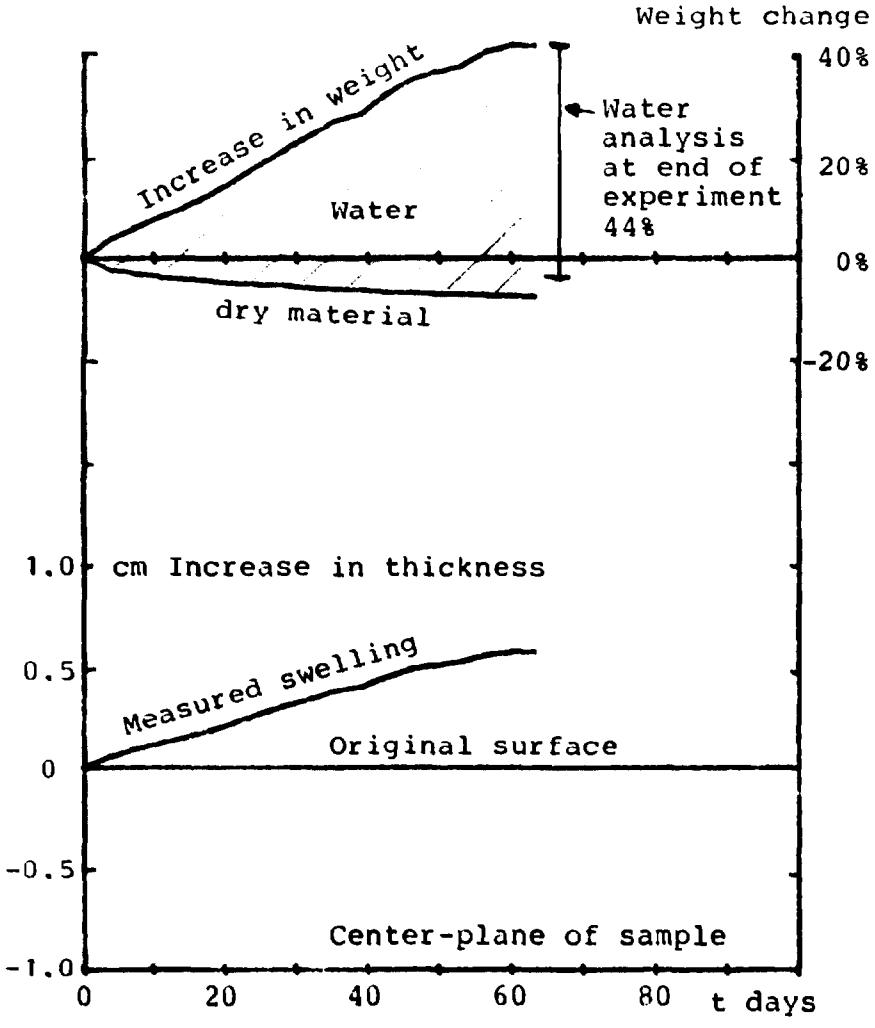

Fig. 13a. In "pure" water

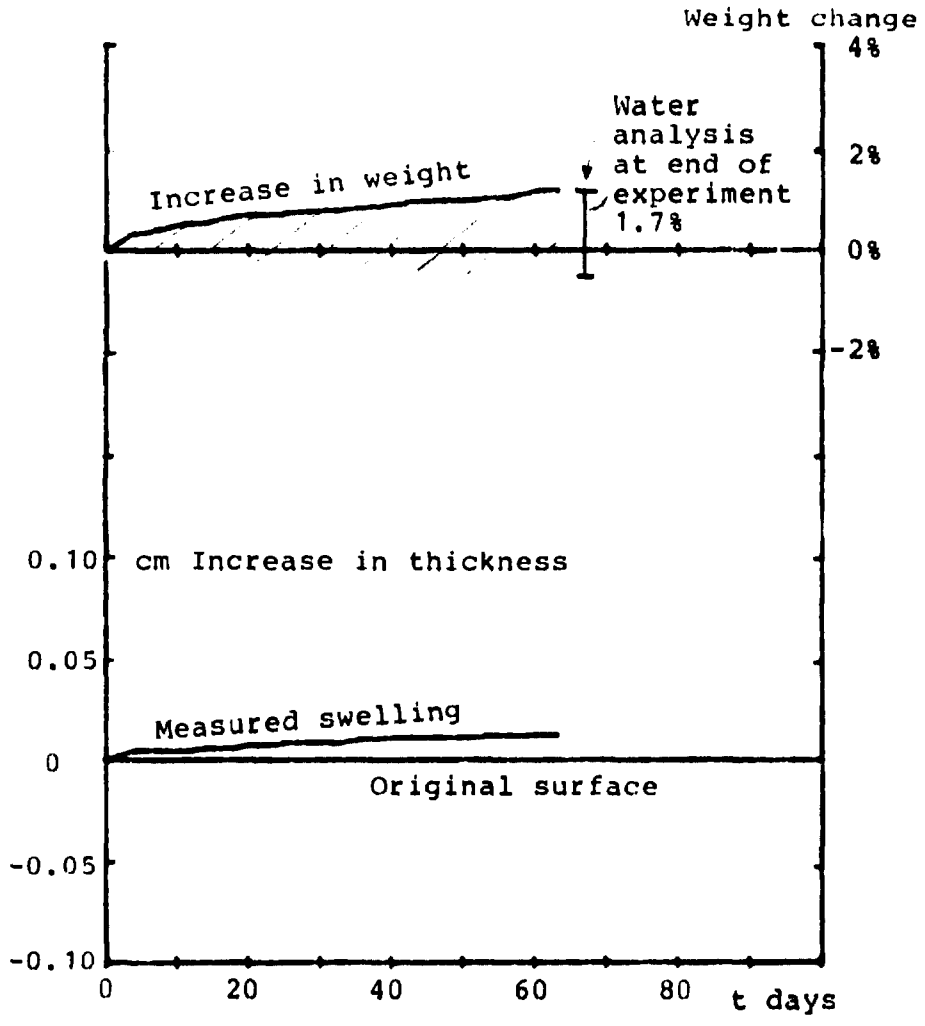

Fig. 13b. In saturated NaCl solution

Water uptake and swelling of samples of bituminized evaporator concentrate from the Risø plant. Period No. 74.

The material was remelted and cast into the shape appropriate for the intended leaching experiments:

1) A classical IAEA-Hespe configuration with leaching only from the horizontal upper surfaces of the samples.

2) The configuration used in the water uptake measurement system described in Section 2.2, i.e. leaching from two plane parallel surfaces of a 2-cm thick sample with the surfaces placed in vertical position.

Leaching and swelling were measured in saturated NaCl solution and in "pure" water, i.e. water with a composition determined by the leached components from the sample. The concentration in the water (5-1 g dry material/l) is dependent on the leach rate and the sampling schedule for the system. The results are shown in Figs. 12 and 13.

It is seen that there are no significant differences between the leaching behaviour of the two configurations.

The leach curves for the samples in nearly pure water indicate diffusion-controlled leaching while the mechanism in saturated NaCl solution is more uncertain. Values for S_{100} - the leach rate expected after 100 days of leaching - are given in Table 6.

The leach rates are considerably lower in saturated sodium chloride than in the weak solutions typical of leaching in "pure" water. This must be associated with the much lower water uptake in the samples kept in saturated NaCl solution as illustrated by Figs. 13a and b. However, even in saturated sodium chloride there is a slight but steadily increasing water uptake.

In the "pure"-water systems the leach rates for ^{60}Co are higher than for ^{134}Cs. This is a relatively uncommon feature and could be associated either with a fixation of Cs to particles in the waste or to the formation of more mobile Co species, for example, by complexation with the organic components in the waste.

Table 6. Leach rates after 100 days immersion in water or saturated NaCl solution for bituminized evaporator concentrate from the Risø plant. Period No. 74

Configuration:	IAEA	Risø	IAEA	Risø
Leach solution:	"Pure" water		Saturated NaCl	
Leach rate:	S_{100} 10^{-4} cm/day			
^{134}Cs	9	7	0.6	0.4
^{60}Co	12	11	0.1	0.1

The weight of the samples and the measured swelling increases within the time frame of the experiment approximately linearly with time. The swelling of the samples kept in "pure" water is considerable: up to 50%. This may give problems in the disposal of such a material, if contact with ordinary ground water cannot be avoided. When disposal takes place in salt the swelling is hardly important, even if flooding of the mine should take place.

The water uptake in the material is larger than for the pure sodium sulphate/bitumen systems reported in Section 2.3. This could be an effect of the small particle size of the crystals in the bituminized evaporator concentrate, but it may also be due to changes in the bitumen properties caused by the contents of organic materials or sludges in the waste.

2.6. Cation-exchange resin/bitumen system

(Waste form No. 16)

Bituminized ion exchange resin is not produced as a major industrial waste material at nuclear installations within the EEC. The system is therefore not included between the 10 major reference waste materials selected for detailed characterization under the research program of the Commission (3). However, it

is produced industrially (although the production may be discontinued) at power plants in Sweden and Finland. The experiments reported in this section can therefore be regarded as a follow-up on previous leaching experiments performed within the frame of a Nordic Cooperative project (11). Furthermore, the material has some properties which, from a more fundamental point of view, makes it well suited as model material for study of swelling problems without complications from simultaneous leaching of major components, as the case is with salt-containing materials.

Used ion exchange resin from water purification systems in LWR's is normally a mixture of cation and anion-exchange resin. The capacity is normally not completely exhausted when the resin is discarded so that a considerable part is still on the H^+ and OH^- form. However, to simplify the system we have selected to work mainly with fresh cation-exchange resin saturated with sodium, i.e. the thermally most stable form of resin. The results may therefore not be directly applicable on real bituminized reactor waste containing partly degraded and only partly saturated mixed bed resin.

2.6.1. Swelling behaviour of cation-exchange resin

Polystyrene-based strong-acid cation-exchange resins are dehydrated but not destroyed when heated in the bituminization process. The dehydration is associated with a considerable volume decrease of the resin beads. The process is reversible and some swelling must therefore be expected when a dehydrated sample of bituminized ion exchange resin remains in contact with water for an extended period.

The density of a typical cation exchange resin Amberlite IR 120 has been determined by immersion in mixtures of the two organic liquids: Tetrachloretan and xylene. The relative proportion of the two liquids was changed until a density was achieved where the resin particles no longer rose to the surface or settled to the bottom. The density of dry IR 120 on sodium form was found to be $\rho = 1.151$ g/cm^3. The density of the same material com-

pletely rehydrated by contact with pure water was ρ_{hyd} = 1.27 g/cm^3 and the water content was q = 0.51 g water per g hydrated material. This can be used to calculate the swelling factor F, i.e. the ratio of the volumes of a resin bead before and after rehydration:

$$F = \frac{d^3_{hyd}}{d^3} = \frac{\rho}{(1-q)\cdot\rho_{hyd}} = 2.43$$

The theoretical swelling due to complete rehydration of the originally dry beads of resin in a sample of bituminized ion exchange resin is dependent on F, on the waste loading w g dry waste/g bituminized product and on the density of the pure bitumen $\rho_{bit} \cong 1.0$ g/cm^3. The swelling defined as the fractional volume increase of the sample is given by (5):

$$S = \frac{F-1}{1 + \frac{1-w}{w} \cdot \frac{\rho}{\rho_{bit}}}$$

In the experiments reported here, the value of w has always been 0.4, i.e. 40% dry resin mixed with 60% bitumen. Inserting in the formula gives: S = 0.43, i.e. a theoretical volume increase of about 43%.

2.6.2. Water uptake as a function of particle size (early exp.)

The weight increase of a sample of bituminized ion exchange resin stored in pure water is a direct measure of the water uptake since there is no leaching of major components from such a sample.

In a first set of experiments samples containing 40% cation-exchange resin on Na^+ form in 60% Mexphalte 40/50 were exposed to deionized water. The weight increases were followed simply by weighing the samples in air at suitable times during the experiment. The sample materials were prepared using various size fractions of cation-exchange resin. Mainly sieve fractions of Amberlite IR 120, but also a commercialy available IRP 69 Powdex type resin.

The results of the experiments are shown in Fig. 15. The weight increase is in some cases considerable, up to more than 100%. The arrows on the figure indicates 43% water uptake corresponding to complete saturation of the resin in the sample. The water content above that value must be present as free water in pores in the material. That this is the case, at least to some extent, was obvious for the more water-containing samples, since water could be squeezed out of them by a slight pressure on the surface.

The swelling of some of the samples was rapid and rather spectacular as indicated on the photograph Fig. 14. The mushroom-shaped form of the sample to the right is rather typical for samples with large degrees of swelling. The assumption about one-dimensional swelling and diffusion into the samples is therefore only an approximation.

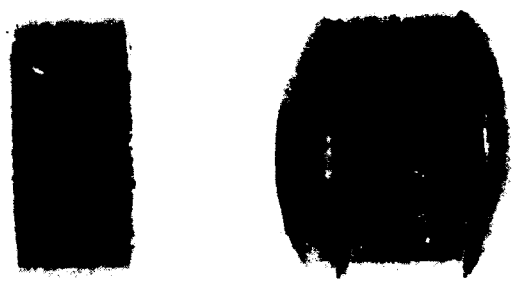

Fig. 14. Samples with 40% IR 120 (un-shieved) or IRP 69 Powdex after 28 days in water.

It is seen from Fig. 15 that the rate of water uptake is dependent on the size of the resin particles. The rate is increasing rapidly with decreasing particle size, probably due to the decreasing thickness of the bitumen films between the individual resin grains. The shape of the particles may also be important, i.e. whether they are spherical or irregular as in crushed resin.

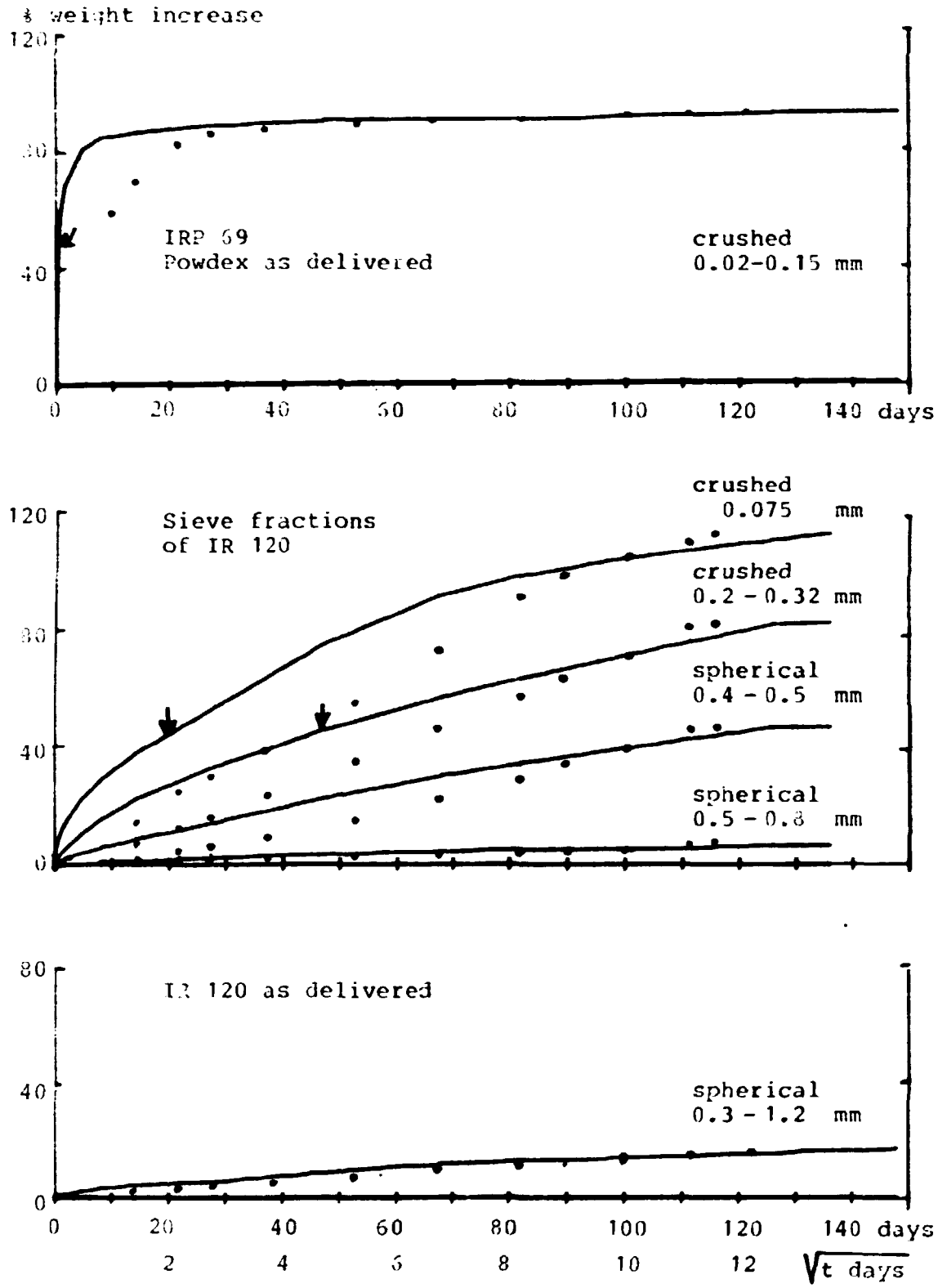

Fig. 15. Weight increase of samples immersed in water for different particle sizes of cation-exchange resin, 40%, embedded in 60% Mexphalte 40/50.

Replotting of the weight increase measurements against $\sqrt{t}$, the square root of exposure time (the dots in Fig. 15) gives approximately straight lines indicating diffusion-controlled water uptake, when the water content is not too high. However, it can be about two times higher than corresponding to theoretical saturation of the resin before significant deviations from straight line behaviour are observed.

From the slopes of the lines effective diffusion coefficients D_e can be calculated using theory derived in (11). The results are given in Table 7 together with calculated values for volumetric swelling and an estimate of the amount of water-filled pores in the samples after about 150 days in water. For comparative purposes the bottom 4 lines in the table show similar results for the repeated experiments described in Section 2.6.3.

Table 7. Summary of main results from test series on water uptake in bituminized cation-exchange resin of various grain size.

After about 150 days in water	Water uptake weight increase % of original weight	Swelling volume increase % of original volume	Water-filled porosity % of total volume	Effective diffusion coefficient 10^{-9} cm^2/sec
IRP 69 as delivered Powdex 0.02-0.15 mm	92%	104%	29%	780
IR 120 crushed 0.005-0.075 mm	115%	131%	38%	160
IR 120 crushed 0.2 - 0.32 mm	85%	96%	26%	68
IR 120 spherical 0.4 - 0.5 mm	48%	51%	5%	18
IR 120 spherical 0.5 - 0.8 mm	7%	7%	0%	0.2
IR 120 as delivered 0.3 - 1.2 mm	17%	18%	0%	2.9
IR 120 as delivered 0.3 - 1.2 mm No. 24	20%	19%	0%	5.3
IR 120 as delivered 0.3 - 1.2 mm No. 25	56%	59%	11%	32
IR 120 crushed 0.005-0.075 No. 26	112%	123%	41%	280
IR 120 crushed 0.005-0.075 No. 27	114%	125%	43%	280

Calculated

Measured

2.6.3. Improved method including direct swelling measurements

In the experiments described in Section 2.6.2 only the weight increase of the samples was measured. A theoretical swelling can be calculated from these data and some additional assumptions about the behaviour of the water in the samples. However, it is preferable to have some direct measurements of the swelling as a control on the calculations. The experiments with bituminished cation-exchange resin have therefore been repeated using the improved method with weighing in water as well as in air. The materials were of the same type as in the first experiments, i.e. 60% Mexphalte 40/50 mixed with dry IR 120 on sodium form either as spherical beads with diameter 0.3 to 1.2 mm or crushed to powder with grain-size 0.005 to 0.075 mm. The bituminized material was cast in Perspex rings and the samples kept immersed in pure water for a period of up to 220 days. They were weighed at suitable intervals most frequently at the beginning of the experiment. The water was changed with fresh demineralised water in connection with each weighing and analysed for sodium.

Calculations based on the weight measurements are shown in Figs. 16, 17 and 18. The format of these figures is generally usable for the presentation of this type of more comprehensive results.

The upper curve in the figures represents the weight increase as a percentage of the original sample of weight. In the case of ion-exchange resin, the weight increase is nearly identical with the water uptake since only very slight leaching of soluble material takes place. This is confirmed by the sodium analyses of the water, which showed that only relatively small amounts - calculated as NaCl - of material were leached from the samples.

The specific water uptake in g water/cm^2 sample surface can therefore be obtained directly from the weight increase curve and the weight and exposed area of the samples. (The upper left scale on the figures).

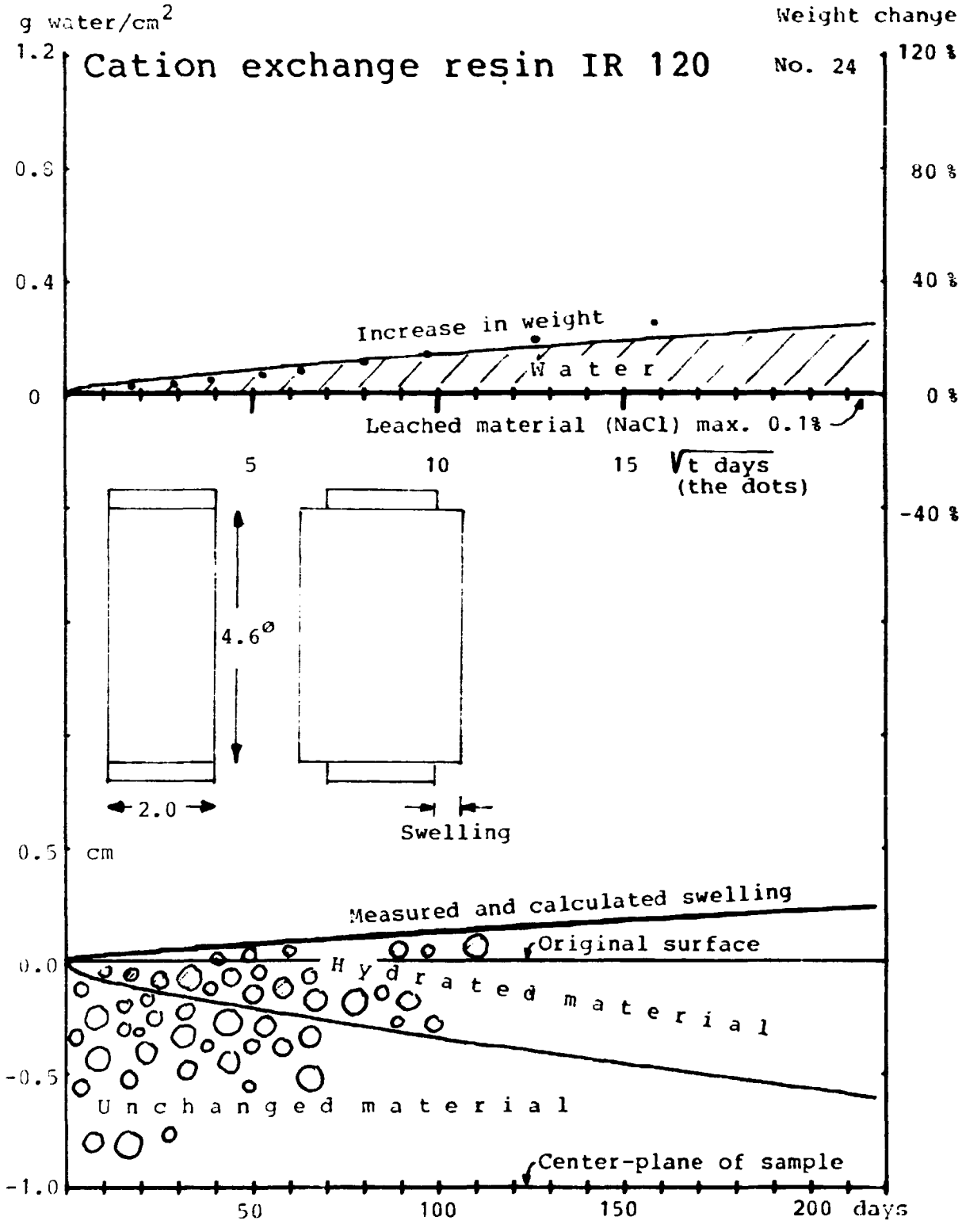

Fig. 16. Weight change, swelling and water penetration as a function of time for a sample of bituminized grain-formed cation-exchange resin immersed in pure water.

Original composition: 60% Mexphate 40/50 + 40% dry IR 120 on Na^+ form. Particle size: 0.3-1.2 mm.

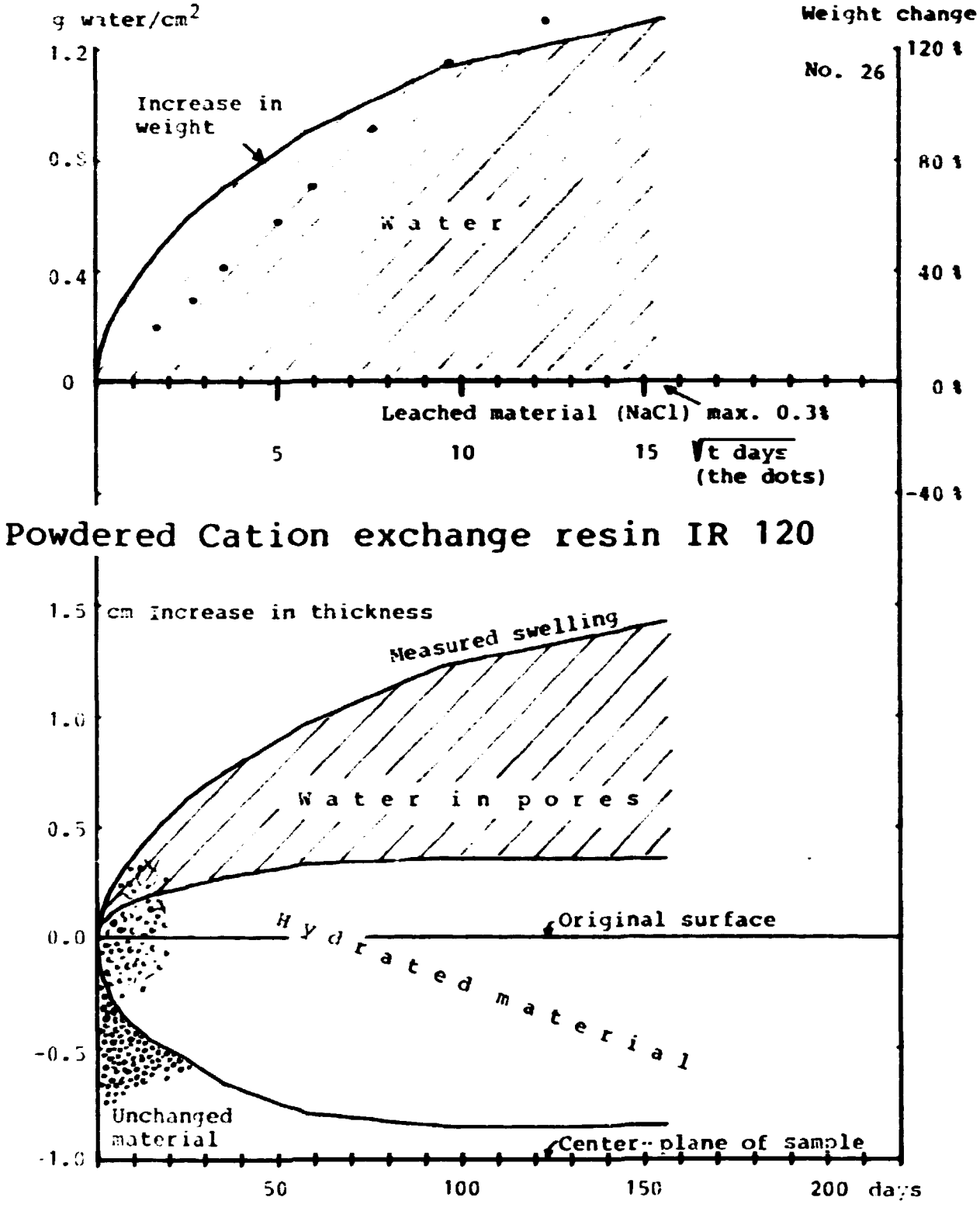

Fig. 17. Weight change, swelling and water penetration as a function of time for a sample of bituminized powdered cation-exchange resin immersed in pure water.

Original composition: 60% Mexphate 40/50 + 40% dry crushed IR 120 on Na^+ form. Particle size: 0.005-0.075 mm.

The curves presented in the upper part of Figs. 16 and 17 contain the same information as is given for the previous experiments in Fig. 11. It is confirmed that the rate of water uptake as well as the total amount of water taken up are considerably higher in samples with powdered resin than in samples with granular resin.

Replotting the weight increase measurements against $\sqrt{t}$ gives approximately straight lines. (The dots in the figures.) Effective diffusion coefficients D_e were calculated from the slope of these lines. The results are given in Table 7 together with the results of the previous experiments.

The lower part of the figures shows in a somewhat idealized form the development of the geometry of the sample as a function of time. The measured swelling is given as the increase in thickness of the sample, but since the half-thickness of the fresh sample is 1 cm, the numerical value of the swelling is the same as for the swelling S defined as the fractional volume increase. It is assumed that swelling takes place only in the direction perpendicular to the surface. This is not strictly correct especially if the swelling is large and the area of the sample relatively small. The shape of the swelling samples under such circumstances is typically as shown by the photo Fig. 14.

As shown in Fig. 16, the measured swelling of sample No. 24 is practically identical with the swelling which can be calculated from the volume increase corresponding to complete rehydration of the resin in the layer which is designated "hydrated material" in the figure. In reality, there will not be a sharp division between layers with unchanged and with completely hydrated material, as shown in the figure. An intermediate zone with some kind of water-concentration gradient must be present, but the sharp dividing line is a convenient way to show the progression of hydration into the material. In sample No. 24 the rate of penetration of the postulated hydration front is about 0.0027 cm/day, i.e. considerably higher than typical leach rates for radioisotopes from such materials. The sample would probably be completely hydrated after about 400 days in water. A swelling

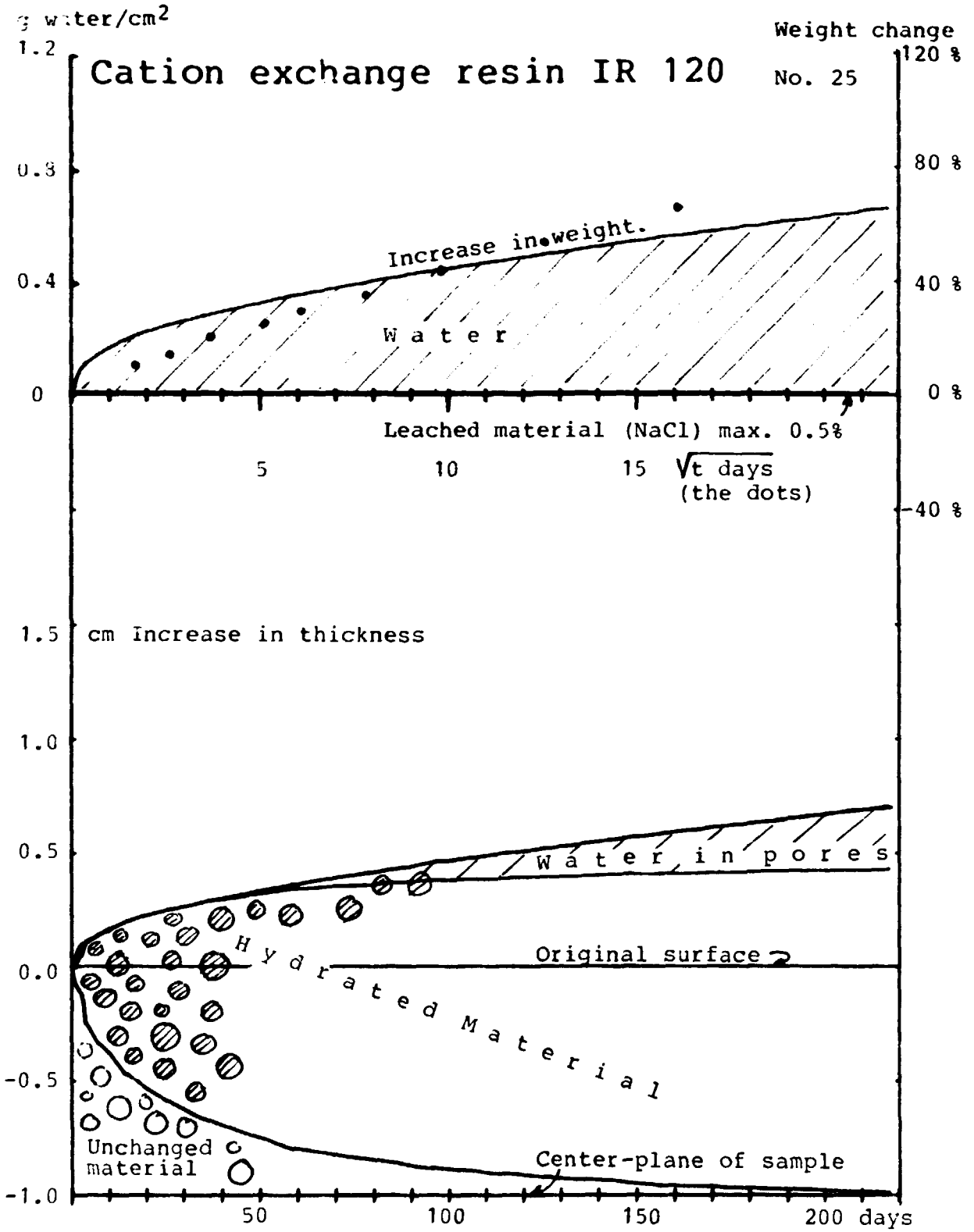

Fig. 18. Weight change, swelling and water penetration as a function of time for a sample of bituminized grain-formed cation-exchange resin immersed in pure water.

Original composition: 60% Mexphate 40/50 + 40% dry IR 120 on Na^+ form. Particle size: 0.3-1.2 mm. (Identical with sample No. 24, Fig. 8.)

near the theoretical value of a 43% volume increase can be expected.

In the case of crushed resin the picture is quite different as shown in Fig. 17. The sample swells to about 2.5 times the original volume and the rate of hydration is high: from 0.1 to 0.01 cm/day. The sample is probably completely hydrated after less than 100 days in water. The small amount of remaining unchanged material shown in the figure after 150 days is thought to be due to measurement difficulties or to the use of the same values for ρ, ρ_{hyd} and q as determined for IR 120 on grain-form (see Section 2.6.1). This could be incorrect if crushing and sieving result in separation of the material in fractions with slightly different properties, which could happen if, for example, the interior and outer shell of the spherical resin beads have somewhat different mechanical strength and chemical properties. There was excellent agreement between measured and calculated swelling.

As mentioned in Section 2.6.2 it is not possible to explain the high degree of swelling by rehydration of the powdered resin alone. A considerable amount of water must be present as free water in pores or cracks in the material. The excess water is shown in Fig. 17 as a layer on top of the hydrated material. This is again only a convenient way to present the volume of free water, which in reality will be present in cracks and pores distributed more or less homogeneously in the combined thickness of the two layers designated "water in pores" and "hydrated material" in the figure.

The thickness of the bitumen films surrounding the individual particles in bituminized waste decreases proportionally with the diameter of the particles and is somewhat dependent on the waste loading. The mean thickness of the films are therefore much less in bituminized powdered resin than in material with a similar waste loading of granular resin. This could be part of the explanation of the high rate of water uptake in bituminized powdered resin, but cannot in itself explain the tendency to form water-filled pores. A possible reason could be that a

higher fraction of the available bitumen is used to fill "empty holes" between the grains instead of forming films of reasonably uniform thickness around the waste particles when mixed with the irregular particles in crushed resin contrary to the spherical particles typical for granular resin. It may also be easier for the smooth spherical particles and the thicker bitumen films in bituminized granular resin to participate in the flow necessary to accommodate the volume changes of the particles. In the case of powdered resin a semi-rigid structure may develop with particles touching each other. Further swelling of the individual particles in such a structure will then result in the formation of water-filled cracks. Some model calculations connected with these phenomena are presented in (5).

The experiments were made in duplicate with two identical samples of each material. The two samples with powdered resin, viz. Nos. 26 and 27, gave almost exactly identical results and can both be represented by Fig. 17. The two samples with granular resin behaved somewhat differently from each other, however, as can be seen by comparing the results for sample No. 24 shown in Fig. 16 with those for No. 25 in Fig. 18. The rate of water uptake is much higher in the last sample which is completely hydrated after about 200 days in water. After about 60 days some water is present in the form of water-filled cracks. This phenomenon is therefore not only associated with powdered resin but may occur, in a less pronounced form, also with granular resin. The effect was observed earlier in an experiment reported in Section 2.6.2. The sample contained a sieve fraction of spherical IR 120 particles with grain size 0.4-0.5 mm, i.e. a slightly lower mean size and a more narrow size distribution than the unsieved IR 120 resin used in samples 24 and 25.

The poor reproducibility of the water uptake in bituminized granular resin, illustrated by Fig. 16 compared with 18 and by the variation in the values for the effective diffusion coefficient given in Table 7, agrees with the generally poor reproducibility of the leach rates for samples of this material, a problem which has also been encountered in other connections (see, for example, Section 2.1). The large variability is

thought to be caused by the inhomogeneous nature of the material: The waste particles are relatively large compared with the sample dimensions. The risk of formation of "channels" of resin particles touching each other may show considerable statistical variation. Furthermore, the material has a tendency to form a bitumen-rich layer on the upper surface of the sample due to a slight settling immediately after casting. The thickness etc. of such a layer is extremely difficult to reproduce from sample to sample.

The tendency to crack formation is probably related to a combination of waste loading, particle size, shape and density, the swelling ratio F of the particles, and maybe the flow properties of the bitumen. It would be interesting to investigate whether or not swelling in excess of the theoretical value corresponding to complete hydration of the particles disappears at lower waste loadings.

Conventional leach curves for sodium leaching from the two types of bituminished IR 120 in pure water are shown in Fig. 19. The accumulative equivalent leached thickness is calculated as a function of the square root of time from the sodium analyses of the leach water and an approximate sodium content in the dry resin of 13.7%. However, it has been found that only about 4.4% of the total Na^+ in untreated resin is leached easily by deionized water. This makes the concept of an equivalent leached thickness based on the total sodium content in the resin rather artificial. The leached sodium will represent only a small fraction of the sodium contained in a much thicker layer. The right-hand scale in Fig. 19 corresponds to $13.7 \cdot 0.044 = 0.6\%$ leachable Na^+ in the dry resin and gives probably a more realistic estimate of the thickness of the layer from which leaching has taken place. The shape of the curves shows considerable deviation from ideal diffusion-governed leaching. By comparison with Figs. 16, 17 and 18, it is seen that a high degree of water uptake corresponds to a high degree of leaching.

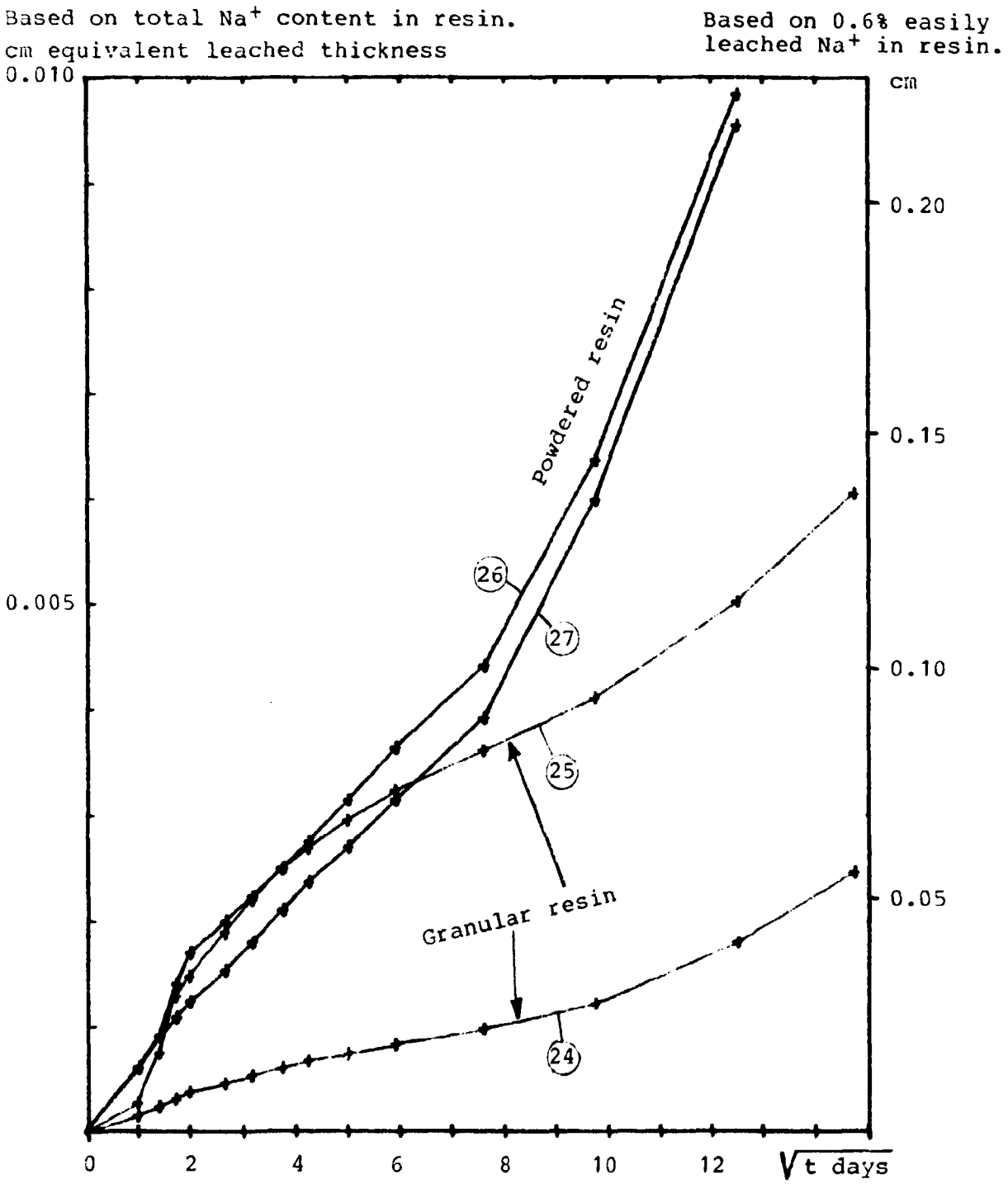

Fig. 19. Na^+ leaching in pure water from samples containing 60% Mexphalte 40/50 and 40% dry granular or powdered IR 120 cation-exchange resin on sodium form.

cm equivalent leached thickness refers to the thickness of the samples before swelling.

2.7. Thermal pre-treatment of cation-exchange resin before bituminization

The swelling of dry ion exchange resin in water is due to the presence of the hydrophilic functional groups. It is well known that the quaternary amine groups in strong base anion-exchange resins are thermally unstable. Heat treatment below 150°C will decrease the swelling tendency and the capacity of such resins considerably (13). Due to the explosion hazards associated with the liberated amines it is usually thought desirable to avoid this decomposition by the use of low bituminization temperatures and short residence time in the bituminization apparatus.

Strong acid cation-exchange resins are much more thermally stable but can of course also be destroyed by heating to sufficiently high temperatures. This will result in degradation of the functional $-SO_3^-$ groups, but also in some destruction of the polystyrene matrix material in the resin beads.

It is a possibility that such thermally treated cation-exchange resin after bituminization will have a decreased tendency to swell in contact with water. A few experiments have been made to investigate this possibility:

About 50 g dry granular or powdered cation-exchange resin of type Amberlite IR 120 on sodium form was placed in porcelain crucibles inside cylindrical steel containers with close-fitting but not completely air-tight lids. The containers were heated slowly in an electrical oven to 300, 350 or 400°C and kept there for about 3.5 hours. The lids did not prevent escape of the decomposition gases but were supposed to ensure a neutral or reducing atmosphere in the containers. The weight losses due to the heat treatment are given in Table 8.

A considerable increase in decomposition seems to occur between 300 and 350°C. In all cases the material was black and cinder-like. The individual particles were still visible but were sticking together so that the material had to be crushed to obtain particles suitable for mixing with bitumen. Careful crush-

Table 8. Weight loss when dry cation-exchange resin on Na^+ form is heated to various temperatures without access of air.

Dry resin	300°C	350°C	400°C
Granular IR 120	6.9 %	22.3 %	24.7 %
Crushed IR 120	6.9 %	26.7 %	32.4 %

ing of the thermally treated granular resin gave about 2/3 of the material as a sieve fraction with a grain size between 0.3 and 1.2 mm. The thermally treated powdered resin was crushed to < 0.075 mm. These two size fractions were used for the preparation of samples. This was done by mixing 40% of the heat-treated, crushed and sieved materials with 60% Mexphalte 40/50 at about 120°C and casting the mixture in Perspex rings. The procedure used here is of course not applicable if the thermal degradation had to be made on a technical scale. The crushing stage is especially a nuisance.

The samples were placed in pure water and weighed at suitable intervals. The contents of leached dry material in the water were determined occasionally together with the density of the solution.

The water in contact with the samples with resin treated at 300 and 350°C was rapidly turned into a deep brown to nearly black solution, indicating that some partially decomposed organic material was going into solution. The water in contact with the samples with resin treated at 400°C remained clear, which probably means that the cracking of the organic material has reached some kind of final stage, with components which do not have any affinity to water. The concentrations of leached material in the water were also considerably lower than with the samples treated at lower temperatures. The type of the solute which is leached has not been determined, but it must be some kind of sodium salt, for example Na_2SO_3 from decomposition of the sulphonic acid groups in the original resin.

The results of the weighing measurements are presented in Figs. 20a, b and c. Only the weight increases due to water uptake and the weight losses due to leaching are shown. The values for two identical samples of each type of material are given in the figure. The reproducibility of the measurements are in all cases excellent.

Compared with similar information about bituminized untreated IR 120 given in the upper part of Figs. 16, 17 and 18, it is seen that heat treatment at 300 and 350°C do not result in an improvement of the volume stability of the material in contact with water. In fact the water uptake tends to be worse than for untreated resin. The extremely high degree of water uptake in samples with powdered resin is also maintained.

The samples with material treated at 400°C show water uptakes which are about the same as for samples with untreated granular resin, but in this case the excess water uptake typical for bituminished untreated powdered resin is nearly eliminated.

It is difficult on the basis of these experiments to reach a conclusion about the possibility of quality improvements of bituminished ion exchange resin by heat treatment of the resin before bituminization. In the case of cation-exchange resins temperatures of at least 400°C seem to be necessary, but the swelling properties are still not satisfactory even after treatment at 400°C. It is possible, but perhaps improbable, that treatment at higher temperatures will result in further improvements which, together with the higher waste loadings made possible by the partial thermal destruction, may justify the technical complexities of such a treatment.

Anion-exchange resin is more likely to be stabilized by thermal treatment, but this has not been investigated.

An improved laboratory technology (a fluidized bed ?), which do not produce materials with particles sticking together due to the thermal treatment, would be desirable if further investigation of the systems has to be made.

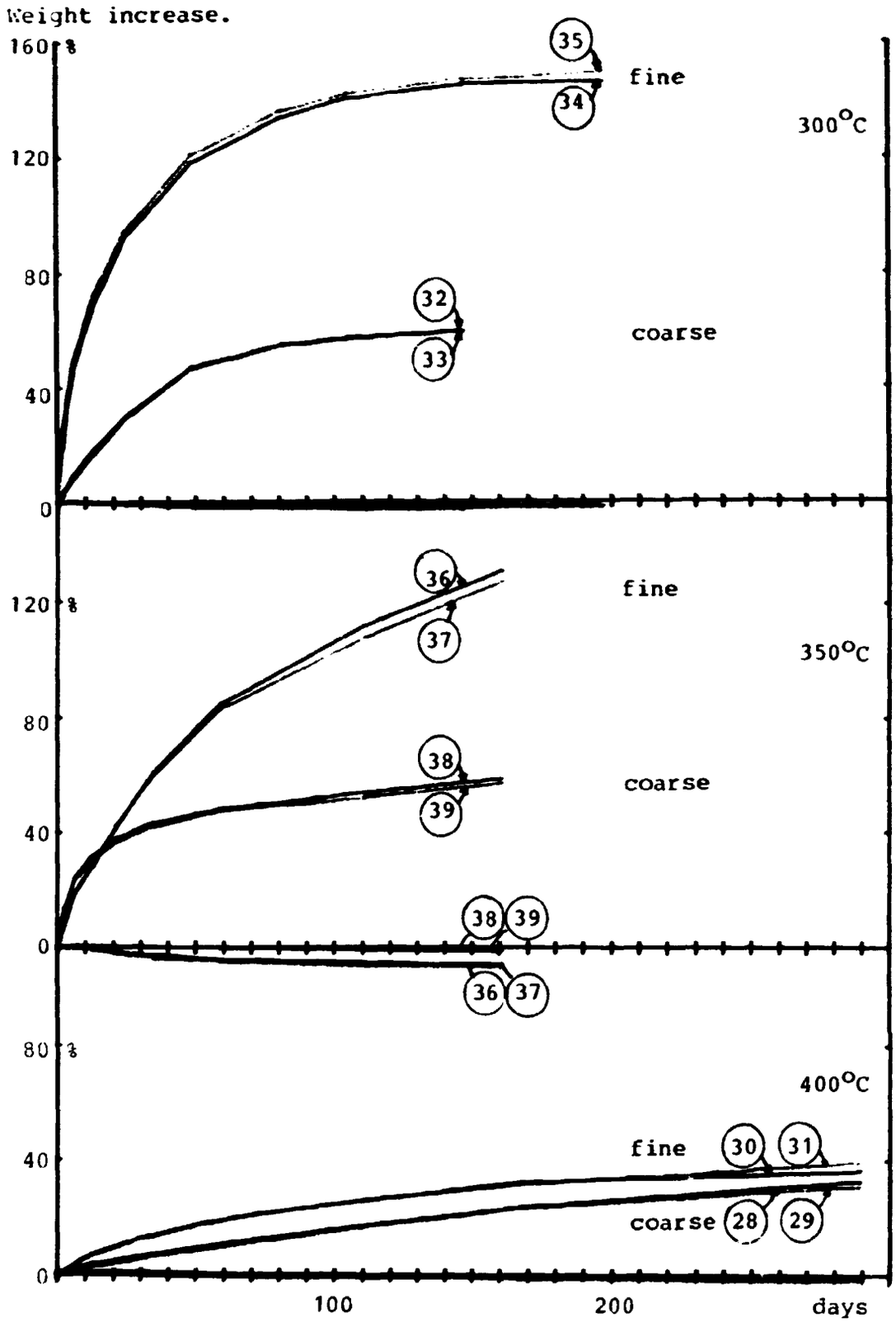

Fig. 20a,b and c. Weight increases due to water absorption in samples containing 60% Mexphalte 40/50 and 40% of either a fine or a coarse sieve fraction of IR 120 ion exchange resin on sodium form after heat treatment without access of air at 300, 350 and 400°C.

2.8. Combined measurements of leaching, water uptake and cation in-diffusion into bituminished cation-exchange resin

It is an advantage to measure water uptake and leaching simultaneously for the same sample since this eliminates the influence of possible variations in properties between individual samples. There is, however, a risk that the wiping of the sample surface with filter paper, which is necessary to remove adhering water before the weighing in air, may have some influence on the surface properties resulting in a changed leach rate compared to an undisturbed sample.

An experiment to investigate this possibility has been made using 8 identical samples of bituminished cation-exchange resin cast in Perspex rings as described in Section 2.2. A material containing 60% Mexphalte 40/50 and 40% granular IR 120 on sodium form was used as in previous experiments. The resin was contaminated with ^{134}Cs and ^{85}Sr so that the activity concentrations in the product at the beginning of the experiment were, respectively, a_o = 1.59 μCi $^{134}Cs/cm^3$ and 3.16 μCi $^{85}Sr/cm^3$. The amounts of carriers used correspond to about 0.1 μeq/cm^3 for Sr^{++} as well as Cs^+.

4 different leaching conditions were investigated:

Series A:	Leaching in 0.01 M NaCl	With weighings
	Leaching in 5 M NaCl	With weighings
Series B:	Leaching in 0.01 M NaCl	Without weighings
	Leaching in 5 M NaCl	Without weighings

Each experiment was made in duplicate.

The exposed area of the samples was A = 30.0 cm^2 and the amount of leach solution M = 200 ml, 50 ml of which was removed for γ-spectroscopy analysis at each sampling and replaced by fresh

solution. The sampling and weighing frequencies were once every week at the beginning of the experiment decreasing to once every month at the end.

As a supplement to this investigation a sort of reversed experiment was also made:

Series C:	Uptake from 0.01 M NaCl	With weighings
	Uptake from 5 M NaCl	With weighings

4 samples of an inactive material which otherwise was identical with the bituminized active cation-exchange resin used in series A and B, were placed in either 200 ml 0.01 M NaCl or 200 ml ~ 5 M NaCl solution (in practice a saturated sodium chloride solution was used, i.e. ~ 5.3 M NaCl) containing at the beginning about 0.07 μCi ^{85}Sr/ml and 0.04 μCi ^{134}Cs/ml. The carrier concentrations were about 0.1 μeq/ml for Sr^{++} as well as Cs^{+}. The solutions were not sampled during the experiment. The water uptake in the samples was measured by weighing as in the case of series A. In connection with the weighings the activity of the samples were measured by γ-spectroscopy. This gives some information about the rate of diffusion of Sr^{++} and Cs^{+} into samples of bituminished ion-exchange resin instead of out, as in the case of leaching experiments.

The three types of procedures are shown schematically in Fig. 21.

2.8.1. Water uptake and swelling

The results of the weighings of the samples from series A and C are shown in Figs. 22 and 23. Each figure is divided into a figure a and b, where a shows the water uptake from 0.01 M NaCl solution, i.e. nearly pure water, and b shows the water uptake from saturated sodium chloride solution. The presentation follows the same principles as in Figs. 15, 16 and 17, but the scales are different since the rates of water uptake were somewhat smaller in the later experiments.

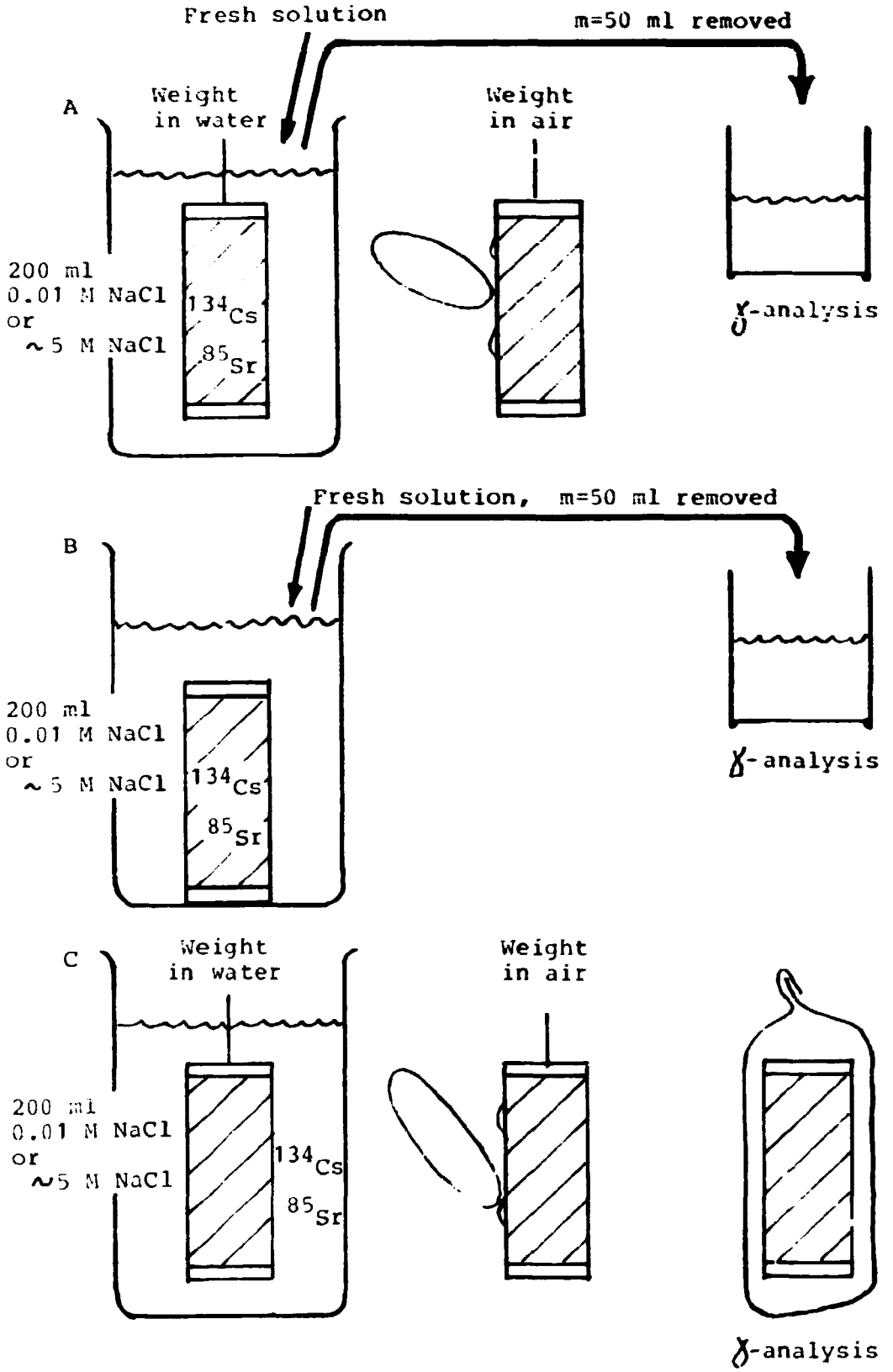

Fig. 21. Three different versions of the method used for measuring leaching and/or water or isotope uptake.

The composition of the samples as far as major components are concerned and the particle size distribution of the solidified ion-exchange resin is the same in all cases. It is hardly probable that there should be any difference between the rate of water uptake from pure water or from a very thin sodium chloride solution. There is, therefore, no particular reason for any difference between the rate of water uptake for the 4 samples shown in Figs. 22a and 23a and the two samples shown in Figs. 16 and 17. However, the measurements show considerable variation which must be ascribed to difficulties in reproducing the properties of samples of this heterogeneous material.

The weight increases at 100 days and the rate of water penetration into the samples are summarized in Table 9 together with the results for the samples which were kept in saturated NaCl solution. The table also includes values for the effective diffusion coefficient for water transport into the material obtained from plots of the weight increase measurements against $\sqrt{t}$.

Table 9. Summary of water uptake measurements in samples of bituminized granular cation-exchange resin on sodium form.
Composition: 60% Mexphalte 40/50 + 40% IR 120
Particle size: 0.3-1.2 mm.

Solution	Fig.	Sample No.	Weight increase after 100 days in water. % of original weight	Rate of water penetration at 100 days 10^{-4} cm/day	Effective diffusion coefficient $10^{-9} cm^2/sec$
Pure water	16	24	14	27	5.3
	17	25	44	nearly saturated	32
0.01 M NaCl	22a	47	3.0	3	0.10
		49	3.0	3	0.10
	23a	55	7.5	13	0.6
		57	9.5	15	0.9
5 M NaCl Saturated	22b	48	1.2	1	0.02
		50	1.2	1	0.02
	23b	56	1.3	1	0.02
		58	1.4	1	0.03

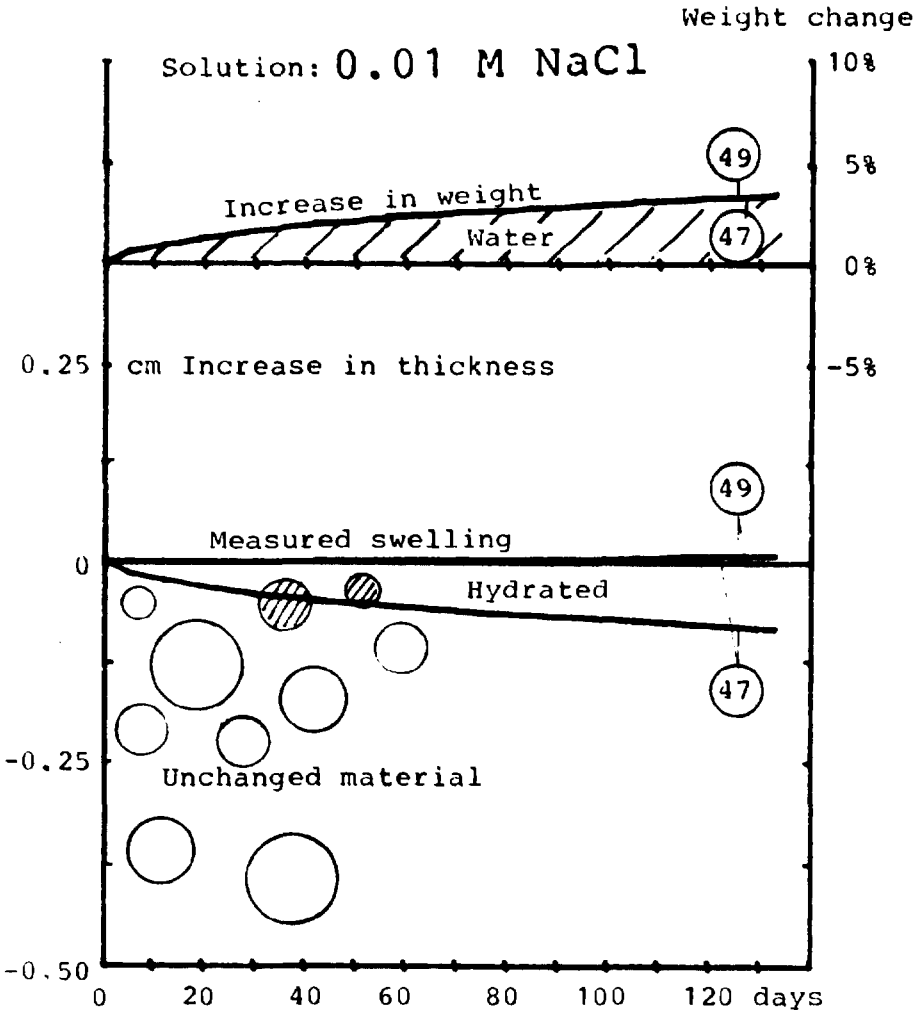

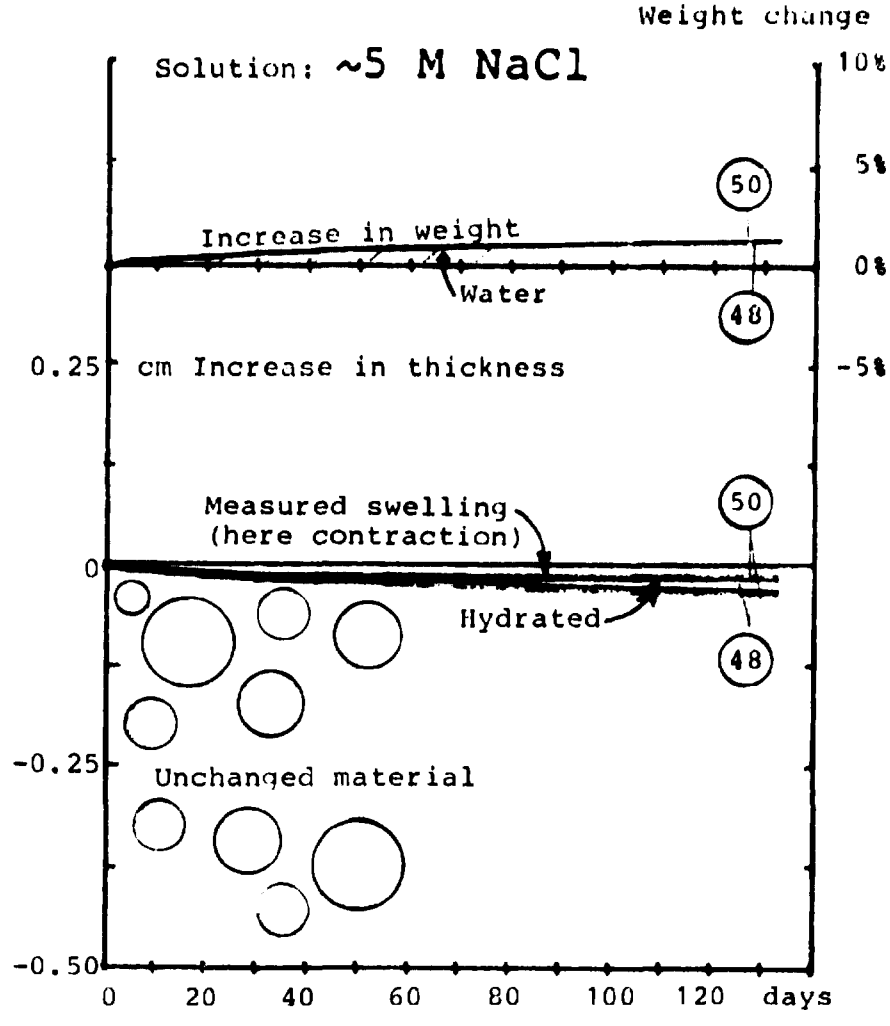

Fig. 22a.

Fig. 22b.

Weight change, swelling and water penetration as a function of time for 4 samples of bituminized cation-exchange resin. Composition: 60% Mexphalte 40/50 + 40% IR 120 on sodium form. Particle size: 0.3-1.2 mm. Procedure A: Active samples in inactive solutions.

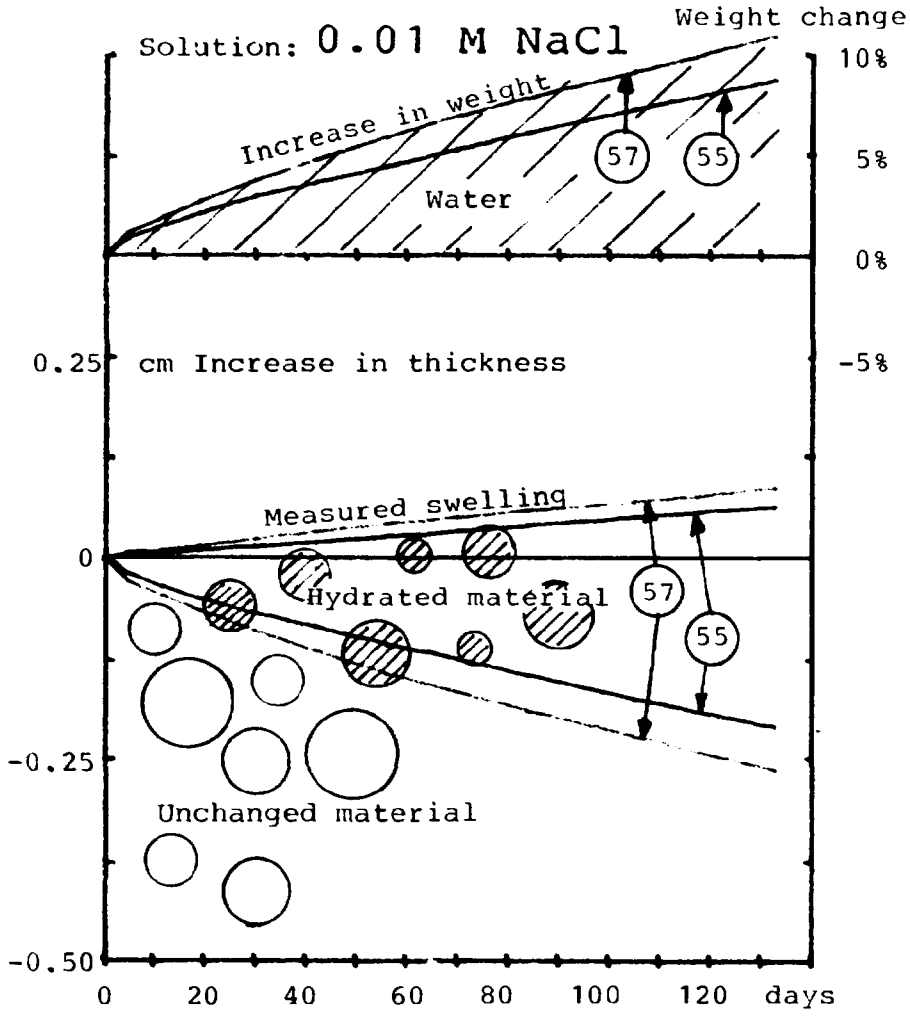

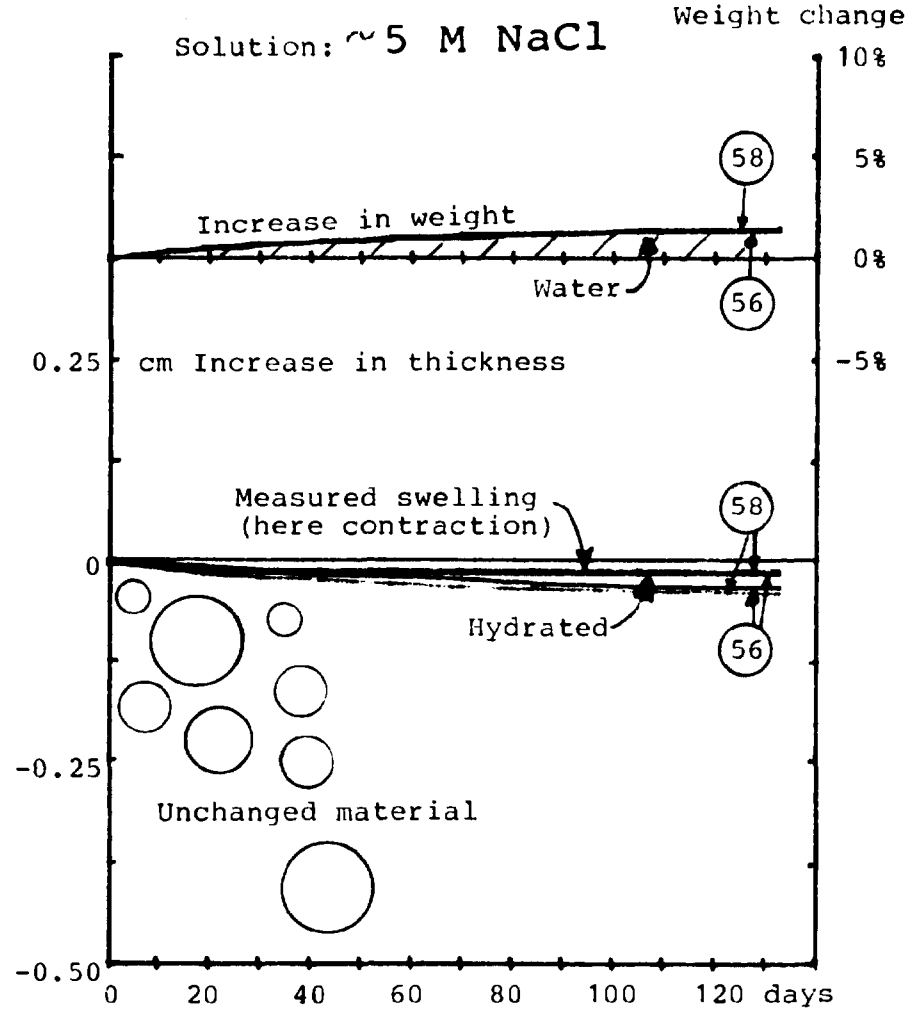

Fig. 23a.

Fig. 23b.

Weight change, swelling and water penetration as a function of time for 4 samples of bituminized cation-exchange resin. Composition: 60% Mexphalte 40/50 + 40% IR 120 on sodium form. Particle size: 0.3-1.2 mm. Procedure C: Inactive samples in active solutions.

The amounts of water taken up in the 4 samples in saturated sodium chloride are lower, much more uniform from sample to sample and show a pronounced tendency to decreasing rate of water uptake with time.

A curious phenomenon can be noticed as far as swelling of the samples is concerned: The volume measurements based on weighings of the samples submersed in saturated sodium chloride solution indicate, as can be seen from the upper curve in the lower part of Figs. 22b and 23b, that the samples contract at the same time as the weight increases due to the water uptake. The contraction is slight, only about 1% of the sample thickness, and could be associated with physical aging of the bitumen, i.e. increased ordering of the structure of the bitumen matrix material.

Later experiments have shown that mixtures of bituminished dry cation-exchange resin also contracts somewhat when stored in air without access of water. A very slight contraction of pure bitumen seems to occur during storage at room temperature and below, but the volume decrease is considerably less than the 1% mentioned above (14).

2.8.2. Leaching and in-diffusion of ions

The mechanism of in-diffusion of ions is rather important in the case of bituminised (or polymer-solidified) ion exchange resin since the release of radioactive isotopes from the resin is a sort of regenerative process dependent on the availability of inactive ions from the outside. This will be Na^+ ions in the cases investigated here and in practical disposal situations normally Na^+, Ca^{++} and/or Mg^{++} ions. The Cs^+ and Sr^{++} ions used in the series C type of experiments can be regarded as a sort of stand-in for these inactive mono- or divalent ions, but there is also some interest in the study of in-diffusion of Cs^+ and Sr^{++} themselves, especially in connection with systems with low water flow and therefore high concentrations of leached species in the water.

Measurements of accumulative leaching are often reported as the thickness of a surface layer from which the original content of a radioactive isotope or another waste component has been completely removed, i.e. the equivalent leached thickness shown, for example, in Figs. 14 and 19. This is not reasonable if the material has ion-exchange properties. In this case a completely leached layer in contact with a solution with a final concentration is not possible. A certain amount of the material corresponding to equilibrium with the concentration in the solution must remain on the ion-exchange resin particles in the leached layer.

If it is assumed that this equilibrium is determined by the K_d values for the untreated resin in contact with the same type of solution as used in the leaching experiment, and, furthermore, if it is assumed - in parallel with the concept of an equivalent completely leached thickness - that the concentration gradient, which must exist over the thickness of the leached layer, can be represented by an equivalent layer of somewhat smaller thickness where the total content of resin is leached to a level corresponding to equilibrium with the solution, then a simple expression based on readily measureable properties can be derived for the thickness of the layer. The system is shown in Fig. 24.

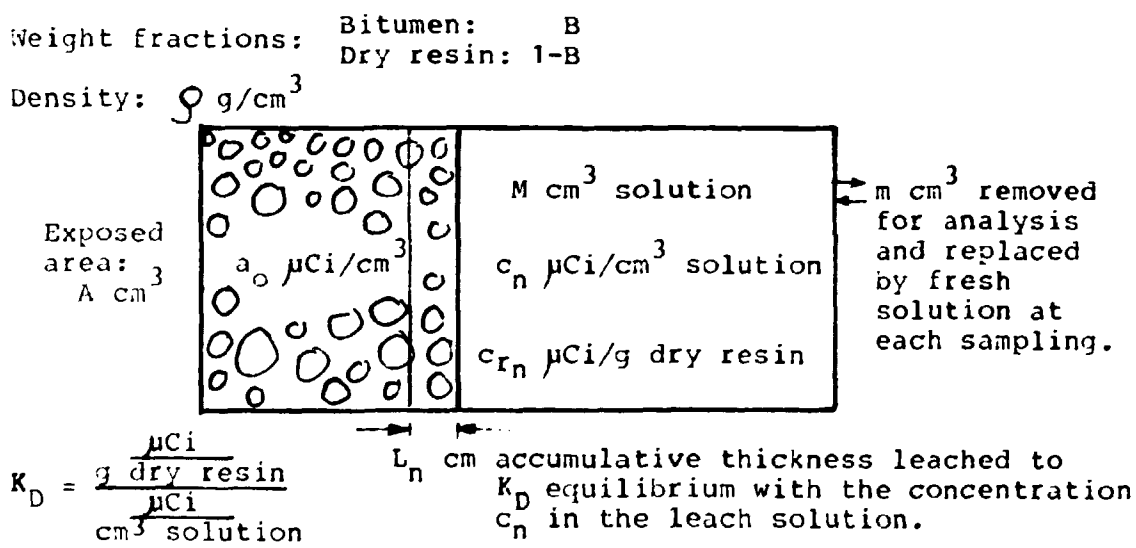

Fig. 24. K_D-modified leaching, calculation system.

An activity balance over the system gives:

$$A \cdot L_n \cdot a_o - L_n \cdot A \cdot \rho \cdot (1-B) \cdot c_{r_n} = M \cdot c_n + \sum_{1}^{n-1} m \cdot c_n$$

where the measured activity concentrations c_n are corrected for decay back to t = 0. Introducing $c_{r_n} = K_d \cdot c_n$ yields:

$$L_n = \frac{M \cdot c_n + \sum_{1}^{n-1} m \cdot c_n}{A \cdot (a_o - \rho(1-B) K_D \cdot c_n)} \text{ cm} \qquad \text{(I)}$$

which describes the situation in an ordinary leaching experiment where c_n is measured.

In an in-diffusion experiment with inactive samples, i.e. $a_o = 0$, placed in a solution with an initial concentration c_o $\mu Ci/cm^3$ the expression for the activity taken up in a sample of bituminised ion exchange resin is:

$$a_{sample_n} = (L_n \cdot A \cdot \rho)(1-B) \cdot c_{r_n} = M(c_o - c_n) \quad \mu Ci$$

which gives:

$$c_n = c_o - \frac{a_{sample_n}}{M} \quad \mu Ci/cm^3 \qquad \text{(II)}$$

It is easy to generalize formula (I) so that it covers in-diffusion as well as leaching:

$$L_n = \frac{M(c_o - c_n) + \sum_{1}^{n-1} m \cdot c_n}{A \cdot (a_o - \rho(1-b) K_D \cdot c_n)} \text{ cm} \qquad \text{(III)}$$

where L_n is negative in the case of leaching and positive in the case of in-diffusion.

Introducing (II) together with $a_o = m = 0$ gives:

$$L_n = \frac{a_{sample_n}}{A \cdot \rho \cdot (1-B) K_D (c_o - a_{sample_n}/M)} \text{ cm} \qquad \text{(IV)}$$

which can be used on the samples from series C.

In this case c_n is calculated from formula (II) as a difference, and c_n is therefore difficult to determine if the uptake in the sample is high. This was the case with the samples from series C, and a direct determination of the activity in the solution would therefore have been a valuable supplement to the measurement of the sample activity. Unfortunately, measurements of the solution activities were made only at the end of the experiments.

K_D values for Cs^+, Sr^{++} and Co^{++} in 0.01, 0.1, 1 and 5 M NaCl solutions were determined experimentally by mixing 1 g washed and newly regenerated IR 120 resin on Na^+ form (2 g material with 50% moisture) with 60 ml sodium chloride solution containing ^{134}Cs, ^{85}Sr or ^{60}Co activity and 0.2 meq of carriers. The activity on the resin and in the solution was determined by analysis after 2 days equilibration of the system. Contact times above 1 day was shown to be necessary to reach complete equilibrium. The K_D values given in Table 10 were obtained.

Table 10. Experimentally determined K_D values for cation-exchange resin IR 120 on sodium form.

K_D ml/g	NaCl solution			
	0.01 M	0.1 M	1 M	5 M
Cs^+	900	100	10	2.4
Sr^{++}	60000	3000	40	5.5
Co^{++}	10000	1300	24	7.5

The K_D values for Cs^+ and Sr^{++} in 0.01 and 5 M NaCl given in Table 10 were used in the calculation of the K_D-modified leaching curves discussed in the following:

The results of the leaching experiments with samples in Series A and B are shown graphically in Figs. 25 and 26. The left-hand figures show Cs^+ leaching and the right-hand figures Sr^{++} leaching.

Each figure shows results from 4 identical samples. In the case of Cs the upper two are for the samples in 0.01 M NaCl and the lower two for the samples in ~ 5 M NaCl. In the case of Sr the position is reversed.

Figures 25a and b show for comparative purposes the accumulative leaching presented as ordinary equivalent leached thickness, i.e. the thickness of a completely leached layer corresponding to the amount of activity found in the leach water.

Figures 25c and d show the same measurements but calculated according to Eq. (I) on p. 68. It is seen that the thickness of the layer in K_D equilibrium with the solution is larger - as it should be - than the thickness of the equivalent thickness of the completely leached layer. The difference between the two forms of presentation is quite pronounced for Cs-leaching in 0.01 M NaCl, but only slight in 5 M NaCl due to the low K_D value in this medium. Sr-leaching is not much affected due to the generally low Sr concentrations in the water which is a consequence of the low leach rates for this isotope.

Figures 26a and b show the results from the samples in series B presented as K_D-modified equivalent thickness. No systematic tendency to lower leach rates in series B compared with series A can be observed. It is therefore concluded - at least for the material investigated here - that it is possible to determine water uptake by the weighing method simultaneously with the determination of leaching properties. The drying of the sample surfaces in series A has not influenced the leach rates significantly compared with the undisturbed samples in series B.

The results from series C, i.e. diffusion of $^{134}Cs^{+}$ and $^{85}Sr^{++}$ from solution into samples of inactive bituminized ion-exchange resin, are shown in Figs. 27a, b, c and d. The thickness of the layer in which the ion-exchange resin is supposed to be in equilibrium with the remaining activity in the solution was calculated by Eq. (IV).

It is seen that the depths of penetration of Cs^{+} and Sr^{++} are different. A comparison with Figs. 25 and 26 shows that the thickness of the layers with indiffused isotopes in K_d equilibrium with the surrounding water is a factor 10 to 30 higher than the K_d modified thicknesses of the leached layers for the two isotopes. This can also be seen from Table 11, which gives a summary of the layer thicknesses after 100 days immersion. The thicknesses of the hydrated layers - obtained from Figs. 19 and 20 - are also included in the table.

In the weak salt solution is the layer with indiffused Cs^{+} of the same thickness as the hydrated layer. Sr^{++} seems to penetrate much less into the material in agreement with the much higher K_D value for this ion. This is also reflected in the much lower leaching of ^{85}Sr than of ^{134}Cs in 0.01 M NaCl.

In the nearly saturated salt solution the leaching of Cs^{+} is reduced about a factor 2 compared with that in 0.01 M NaCl. The reason is probably the lower water uptake from the strong salt solution. On the other hand, the leaching of Sr is increased so that there is no significant difference between leaching of the divalent $^{85}Sr^{++}$ and the monovalent $^{134}Cs^{+}$ ions which is in agreement with general theory for regeneration of ion-exchange resins with strong salt solutions.

The layer with indiffused Cs^{+} is considerably thicker than the hydrated layer when in-diffusion takes place from the strong salt solution. This seems rather improbable, but it should be noticed that the shape of the curve in Fig. 27c is different from the shape of the other in-diffusion curves shown in Figs. 27a, b and d: Practically the whole uptake takes place before the first sampling. An experimental error is a possibility,

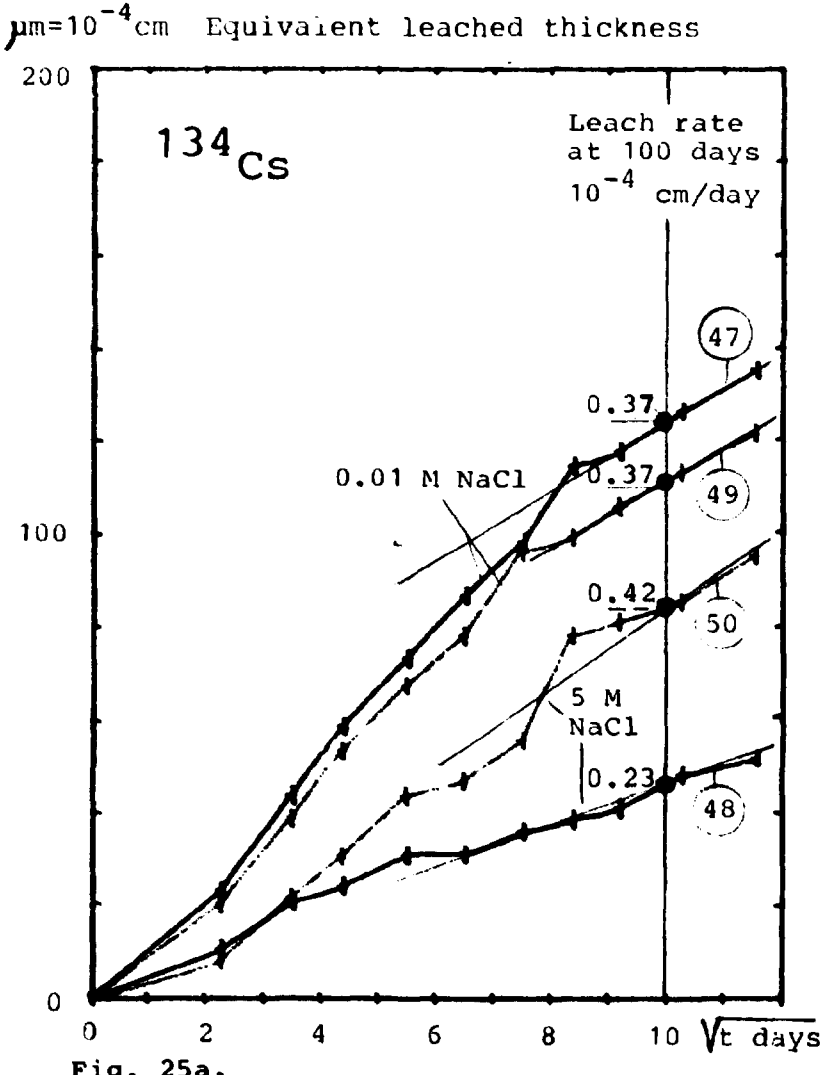

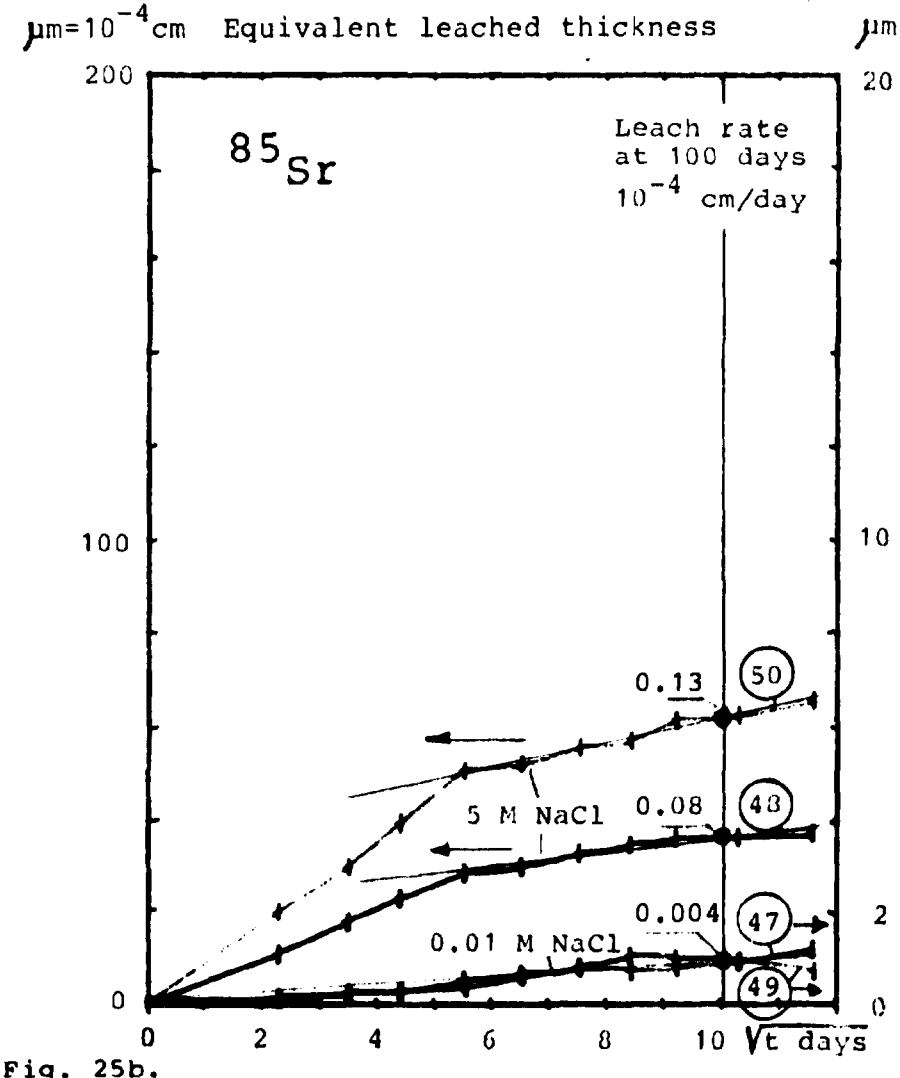

Fig. 25a.

Fig. 25b.

Procedure A. ^{134}Cs and ^{85}Sr leaching presented as the equivalent thickness of a completely leached layer. Sample composition: 60% Mexphalte 40/50 + 40% IR 120 on sodium form. Particle size: 0.3-1.2 mm

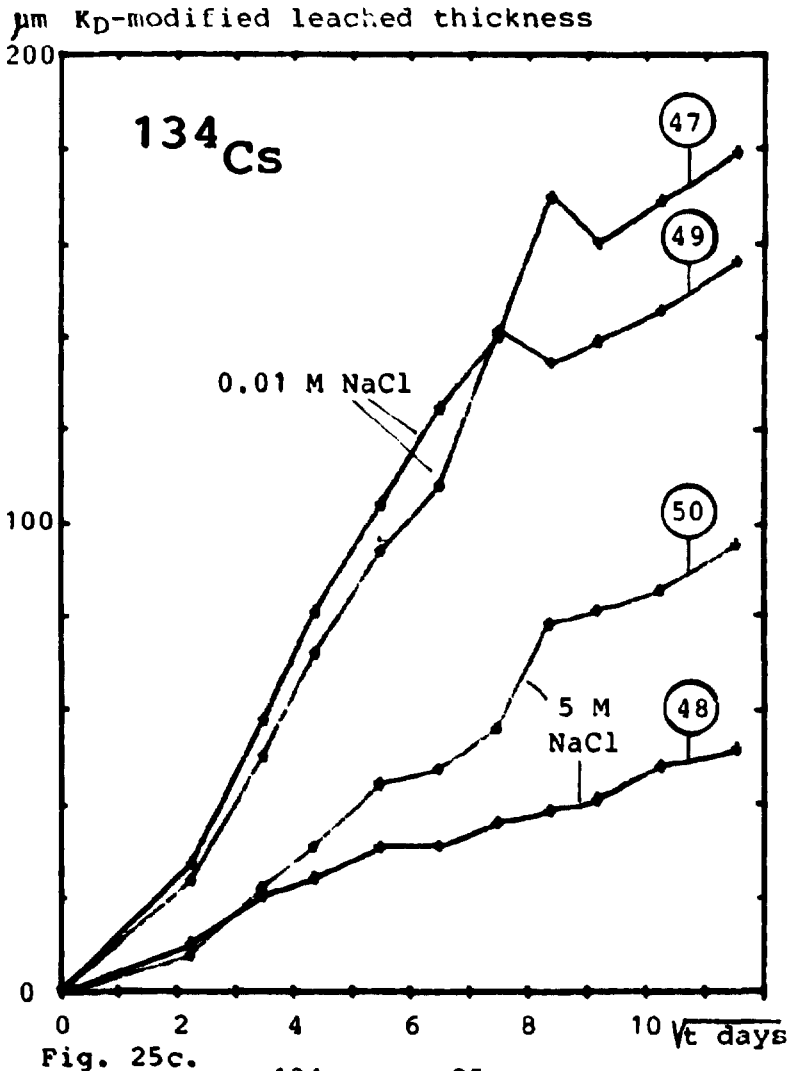

Fig. 25c.

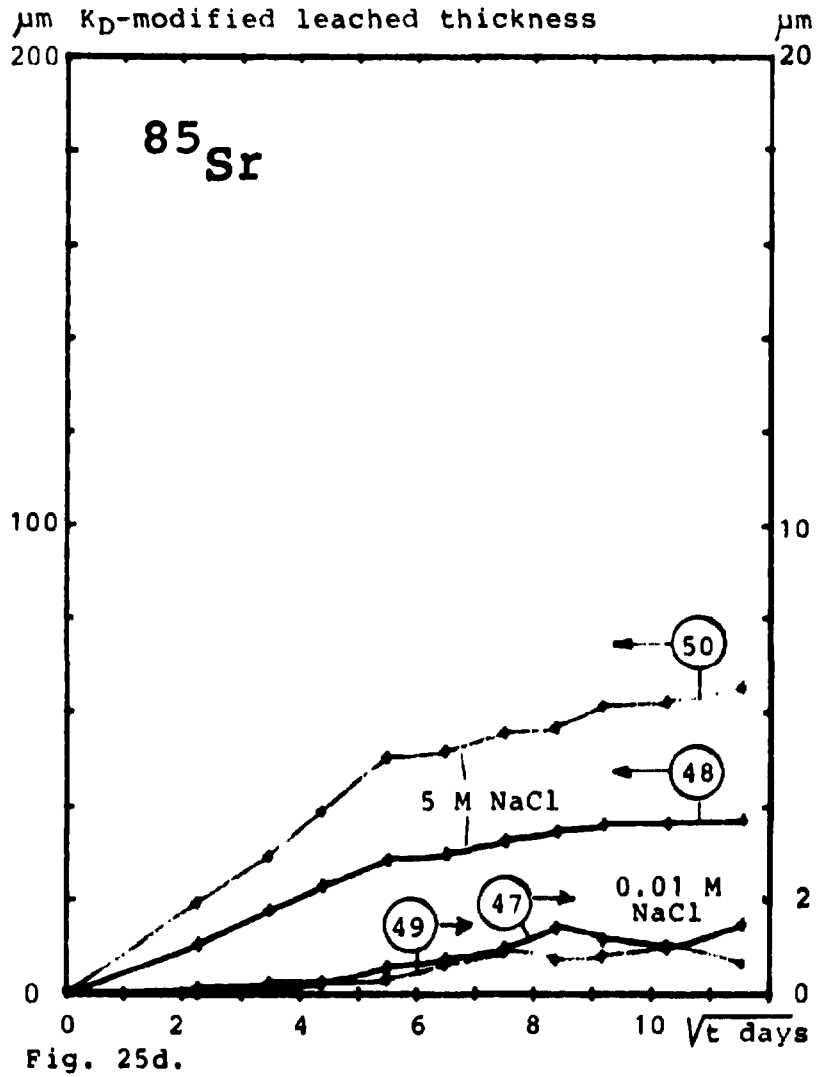

Fig. 25d.

Procedure A. ^{134}Cs and ^{85}Sr leaching presented as the thickness of a leached layer in K_D equilibrium with the solution. Leaching determined together with water uptake measurements.

Table 17. Thicknesses of leached layers, layers with in-diffused activity and layers with hydrated resin on samples of bituminized IR 120 on Na^+ form after 100 days in 0.01 or 5 M NaCl solution.

Procedure	Layer thicknesses after 100 days.	μm = 10^{-4} cm				Fig.
		0.01 M NaCl		5 M NaCl		
		Cs^+	Sr^{++}	Cs^+	Sr^{++}	
A	Equivalent completely leached layer	123 110	0.9 0.8	83 45	60 35	25 a,b
A	K_D modified leached layer	164 140	1.0 1.0	84 46	61 35	25 c,d
B	K_D modified leached layer	166 116	2.3 1.8	52 37	39 31	26 a,b
C	Layer with in-diffused activity	3000 2000	20 10	4000 3000	370 350	27 a,b c,d
A	Layer with hydrated resin	600 600		200 200		22 a,b
C	Layer with hydrated resin	2800 2400		200 250		23 a,b

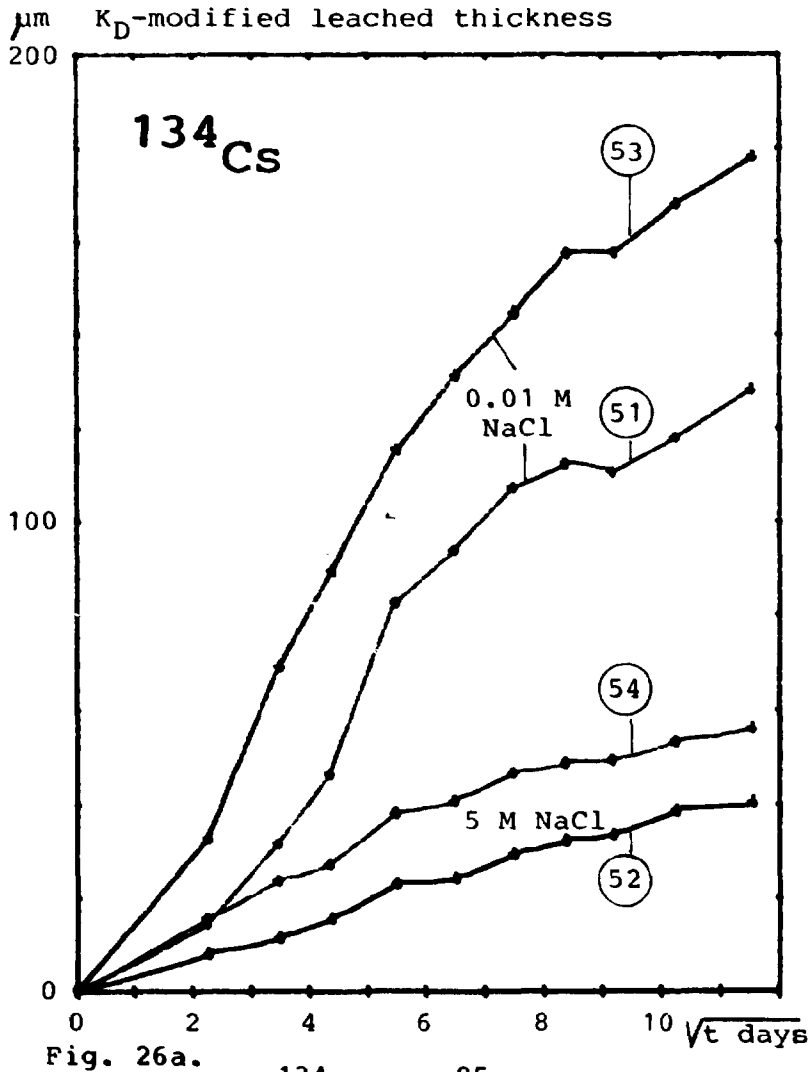

Fig. 26a.

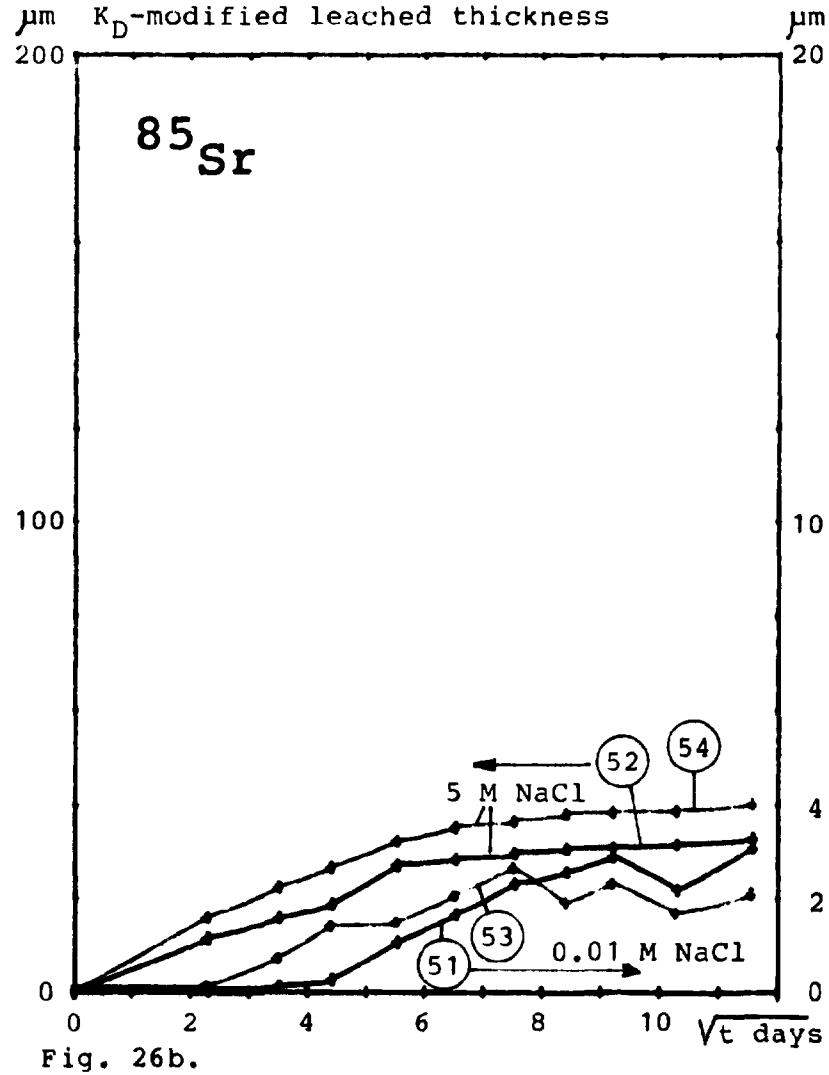

Fig. 26b.

Procedure B. ^{134}Cs and ^{85}Sr leaching presented as the thickness of a leached layer in K_D equilibrium with the solution. Undisturbed samples.

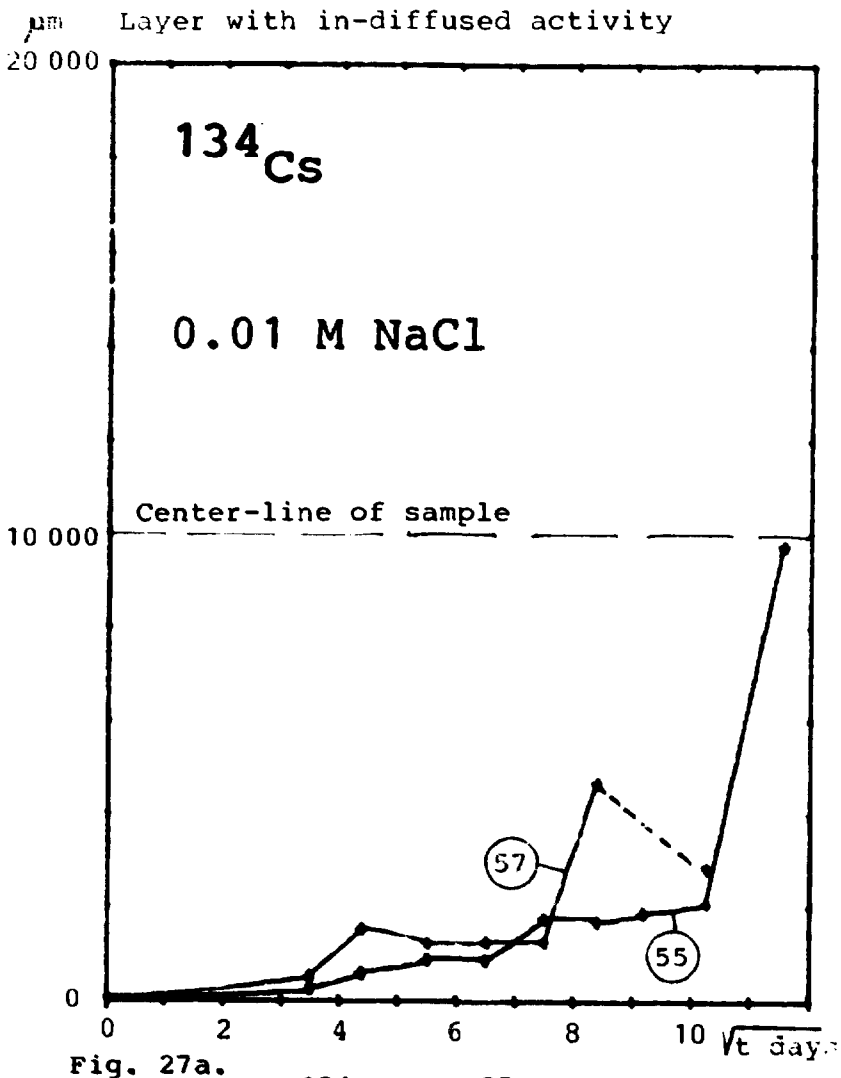

Fig. 27a.

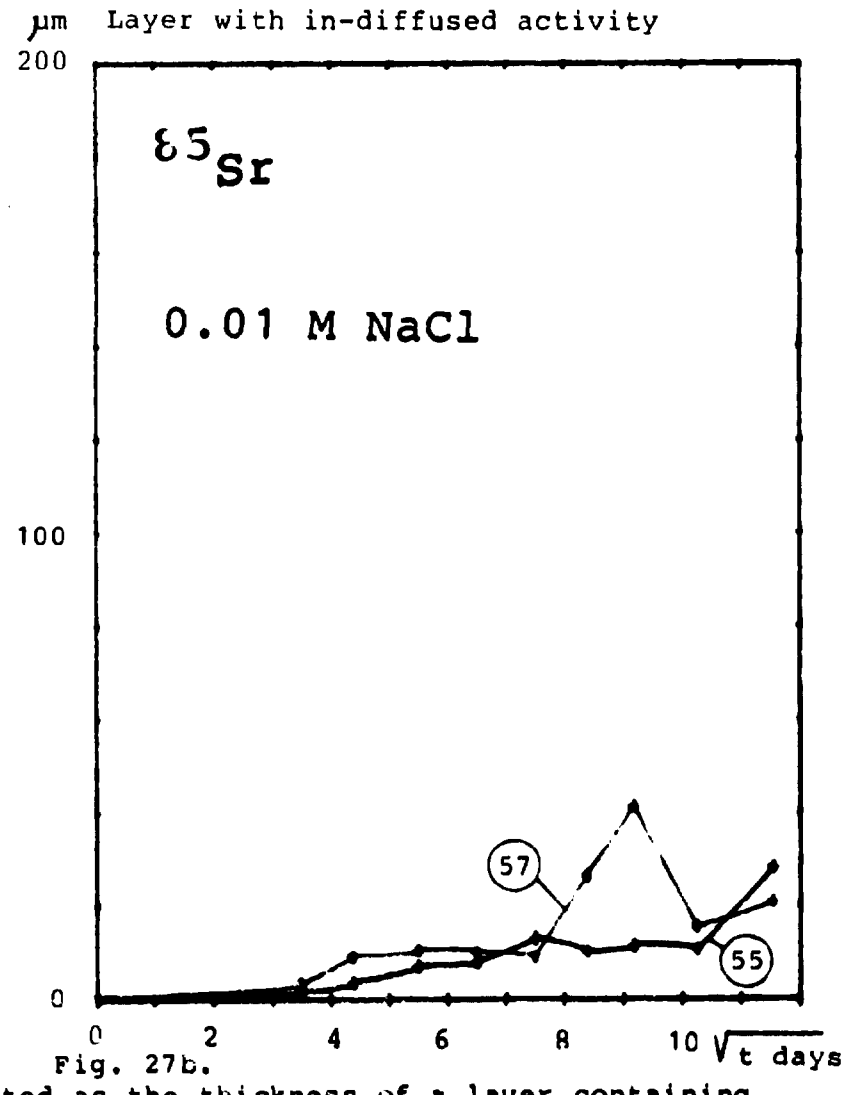

Fig. 27b.

Procedure C. ^{134}Cs and ^{85}Sr in-diffusion presented as the thickness of a layer containing the absorbed amount of isotopes in K_D equilibrium with the amounts remaining in solution.

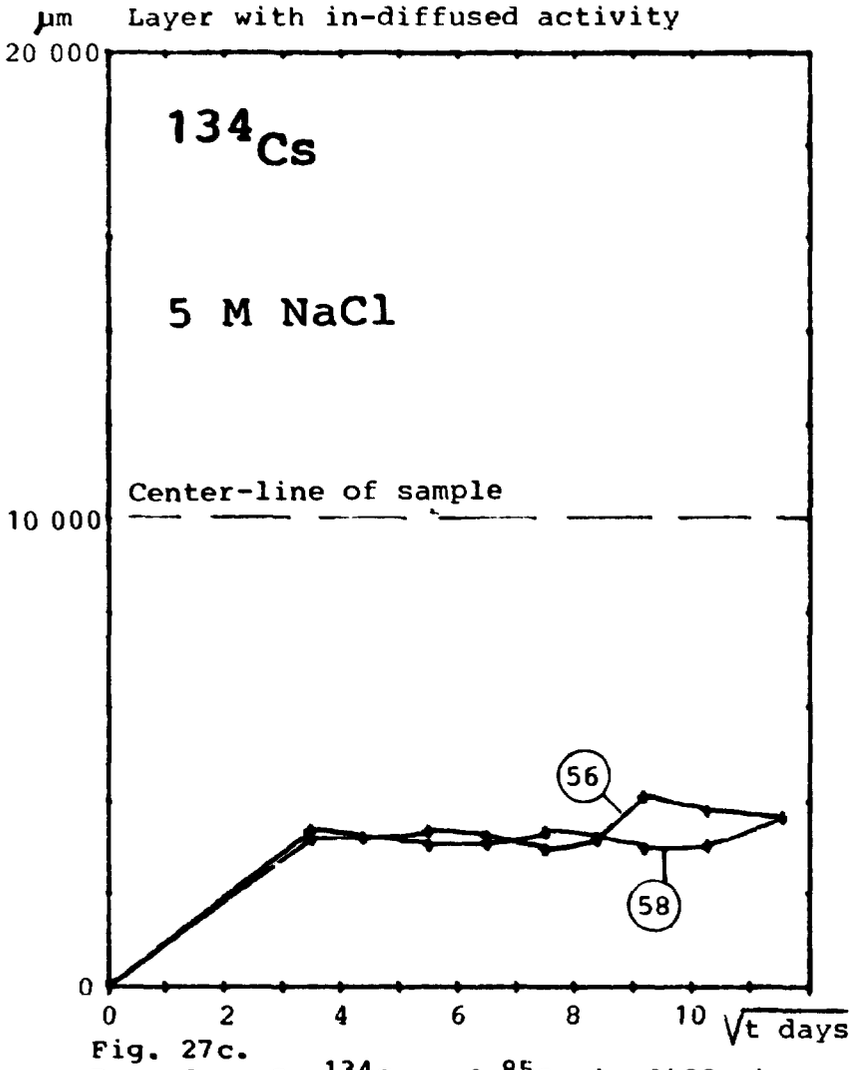

Fig. 27c.

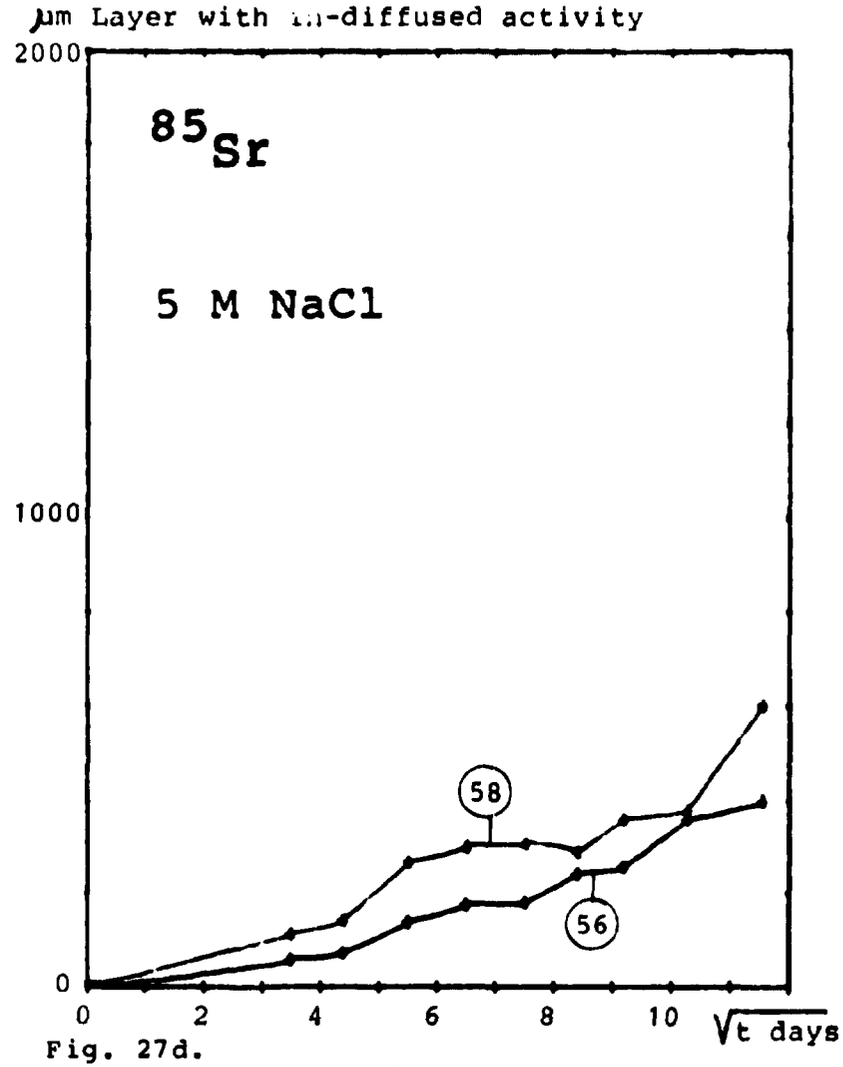

Fig. 27d.

Procedure C. ^{134}Cs and ^{85}Sr in-diffusion presented as the thickness of a layer containing the absorbed amount of isotopes in K_D equilibrium with the amounts remaining in solution.

although the reproducibility between sample Nos. 56 and 58 is good. Another explanation could be that the solution penetrating into the sample from the nearly saturated solution is depleted in salt, so that the Na^+ concentration is less than 5 M. To reduce the calculated thickness of the layer with indiffused Cs from 4000 µm to about 200 µm requires that the K_D for cesium be increased from 2.4 to about 100 ml/g. This would be the case (see Table 10) if the solution penetrating into the material was about 0.1 M instead of 5 M in sodium chloride.

When the experiments were stopped, a few additional investigations were made on sample Nos. 56 and 58 from series C. Both of them had been kept in saturated NaCl solution. The water content in No. 58 was determined by distillation with xylene after the classic principle. A water content of 1.3 ml was found. This is about twice as much as expected from the weight increase measurements, but may include some water which was not completely removed during bituminization of the resin. Sample No. 56 was removed from the ring, the bitumen extracted with xylene and the solution and released cation exchange resin particles were washed carefully with water. The water was analysed for Cl^-, but practically nothing was found: less than 1% of the chloride in 1.3 ml saturated NaCl solution. This supports the theory - if the analysis is correct - that it is mainly water which is diffusing into the samples and not the NaCl solution as such. This is, however, somewhat in conflict with the Cs^+ and Sr^{++} in-diffusion which also has been demonstrated in these experiments.

As a conclusion it can be said that the experiments have thrown some light on mechanisms which influence leaching from bituminized ion-exchange resin. However, the system is still not completely understood. The investigation should be supplemented with further experiments using, for example, $^{22}Na^+$ as a tracer for sodium uptake in the material.

In general, it is felt that the type of combined measurements described in this section is a valuable tool for investigating the mechanisms which influence the behaviour of bituminized

ion-exchange resins. The methods can probably also be used on polymer-solidified materials.

2.9. Leaching from bituminized cation-exchange resin in contact with concrete

Concrete, used as a construction or fill material, will in most cases be a major component in repositories for solidified low- and medium-level waste, at least in repositories of the more advanced types (with the possible exception of repositories in salt). This means that water, which may come in contact with the waste, is conditioned by previous contact with concrete to a large extent, i.e. has a composition dominated by high pH and high content of Na^+, K^+ and/or Ca^{++}. It follows that the leaching behaviour of bituminized materials in such types of water is of considerable interest.

There are many problems involved in establishing a reasonable leaching system using concrete-conditioned water, as for example: 1) The ratio of alkali to Ca^{++} ions in the water, which will depend on the amount of water which has been conditioned by a given amount of cement, 2) the influence of the leached material from the waste on the water chemistry, and 3) the presence or absence of carbon dioxide.

Four different types of leaching experiments involving bituminized ion-exchange resin in interaction with concrete and concrete-conditioned water are described below. They are possibly not the best systems which can be developed, but they give a first impression of what can be achieved by relatively simple means. The four systems are shown in Fig. 28.

The waste material is the same in all cases: 60% Mexphalte 40/50 + 40% IR 120 granulated cation exchange resin on sodium form, the same material as used in many of the experiments described previously in this report. The ion exchange resin was contaminated with ^{134}Cs, representing easily leached radioisotopes, and ^{60}Co, as an isotope where the leach rate was likely

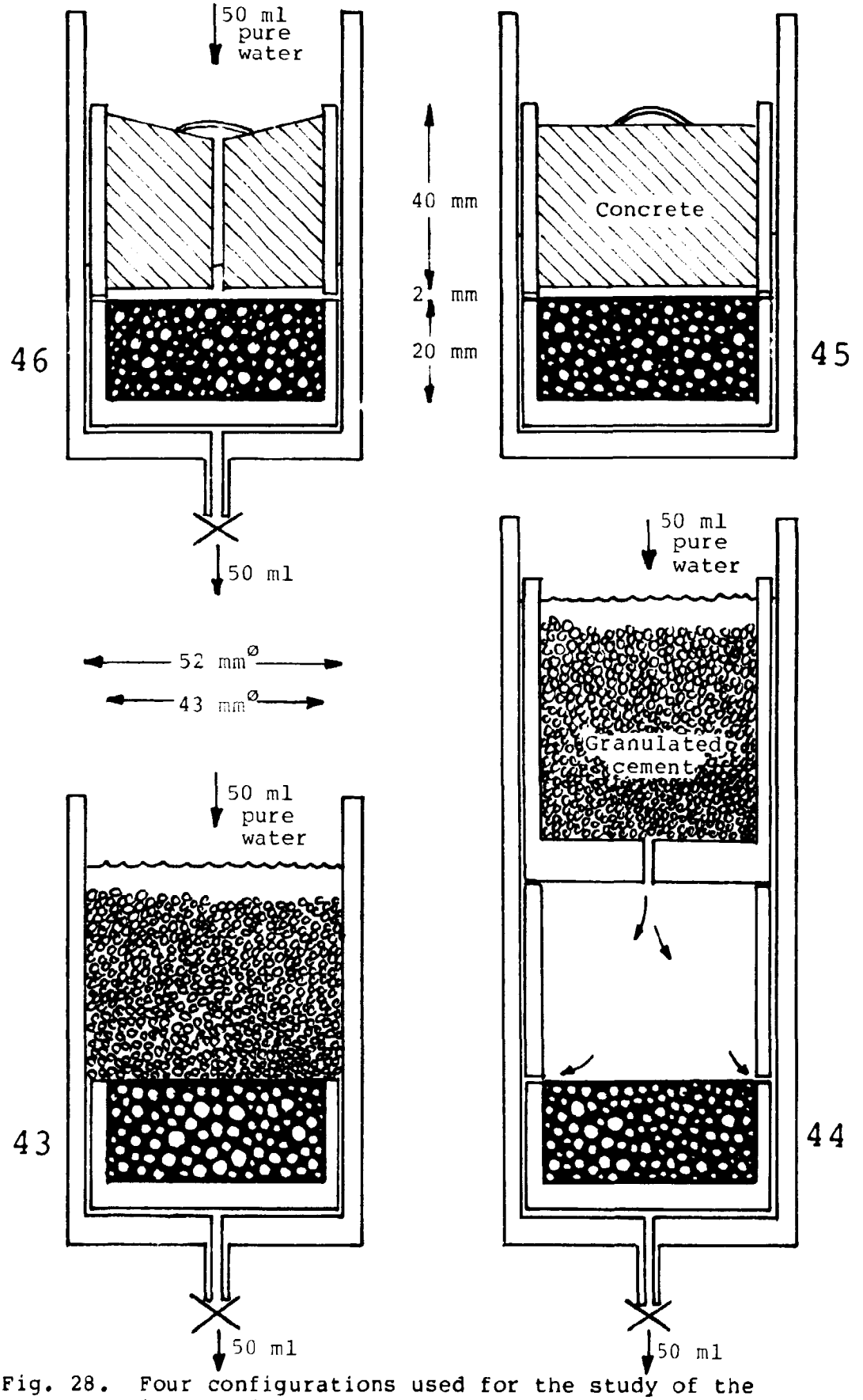

Fig. 28. Four configurations used for the study of the interaction between concrete and bituminized ion-exchange resin.

to be influenced by the high pH in the system. The specific activities were 3.13 μCi $^{134}Cs/cm^3$ and 3.18 μCi $^{60}Co/cm^3$ at the beginning of the experiment. The amounts of carriers correspond to 0.1 meq Cs^+ and Co^{++} per litre product.

The concrete used in the experiments was either in the form of pure granulated hardened cement paste (Danish SRPC: Sulphate Resistant Portland Cement containing 25.0% SiO_2, 1.7% Al_2O_3, 1.8% Fe_2O_3, 67.7% CaO, 0.7% MgO, 0.11% Na_2O, 0.20% K_2O and 1.5% SO_3, moistened with water corresponding to a water/cement ratio of 0.2 and granulated through a sieve with 1.5-mm openings), or in the form of concrete cylinders cast from 50% SRPC + 50% sand using a water/cement ratio of 0.25 and a small amount of superplasticizer.

The containers for the four systems were made of Perspex tubes. They were normally covered by lids, but no special precautions were taken to prevent CO_2 from entering the systems. However, it is probable that carbon dioxide will be unable to penetrate deep into the systems with granulated cement. It will be absorbed in the upper layers.

Only the horizontal upper surface of the waste samples was exposed to water.

In two of the systems (samples Nos. 43 and 44) water was withdrawn for γ-analysis from the bottom outlets and replaced by a similar amount of pure water at the top, where it was conditioned by contact with the granulated cement before it reached the surface of the waste sample. The only difference between the two systems is that in one of them there is direct contact between the granulated cement and the waste, while the other one, in principle, should expose the sample to cement-conditioned water without the complications of the presence of a second solid phase.

In the third of the systems (sample No. 46) pure water was added at the top and immediately withdrawn again from the bottom outlet, thus effecting a sort of washing of the system. About

10-15 ml water is left in the container between samplings so that the surface of the waste sample and the lower surface of the concrete cylinder are always covered with water. The system can be regarded as a discontinuous version of simulated water flow in a crack between concrete and bituminized waste.

The fourth system (sample No. 45) is similar to the third one except that the water was stagnant, i.e. the same water - about 15 ml - was present in the container during the whole experiment. No analyses of the water in this system were made before the end of the experiment.

At each sampling time the concrete cylinders in the third and fourth systems were removed, counted for ^{134}Cs and ^{60}Co in the γ-spectrometer and replaced in their respective containers. This gives an indication of the amount of isotopes transferred to the concrete although the penetration depth and therefore the counting efficiency is somewhat uncertain.

At the end of the experiment the contents of isotopes in solution in the remaining water in the systems were determined together with the activity in the granulated cement.

The two concrete cylinders were etched with successive portions of 1/3 concentrated HCl. The fractions were counted and analysed for Ca^{++}. From this information it is possible to get a rough idea about the penetration of the activity into the concrete since the thickness of the etched layer can be calculated from the calcium analysis and the known content of calcium in the concrete.

The results of the experiments are shown in Figs. 29, 30, 31 and 32. To make it easier to visualize what is going on, the cummulative leach curves are in this case "turned upside down", since a downward direction is the actual direction of the increase in thickness of the leached layer on a horizontal surface of a sample facing upwards. Different scales are used for the leaching of Cs and Co. The thickness of the equivalent leached layers are about 100 times larger for Cs than for Co.

Figures 29 and 30 show the results for samples Nos. 43 and 44, the systems with granulated cement. They are not very different, except that a higher fraction of the leached isotopes are removed with the water samples from No. 44, while they tend to remain absorbed on the cement in the case of No. 43 with the direct contact between the bituminized waste and the granulated cement. Slight amounts of radioisotopes were also found in the granulated cement in the system with sample No. 44 indicating that some transport has taken place through the small hole connecting the upper and the lower part of this system. For both systems the leach rate: S_{100} for ^{134}Cs and ^{60}Co at 100 days are about 10^{-4} and 10^{-6} cm/day, respectively, when the amounts of isotopes on the cement are included.

Figures 31 and 32 show the results for samples Nos. 46 and 45. In these cases the penetration curve obtained from the etching of the concrete cylinder at the end of the experiment is also shown as the upper figure. The step curves show the thickness of the etched layer and the concentrations of the two isotopes found in the various layers by acid extraction. The orientation of the figure is the same as the orientation of the cylinder during the experiment.

The leach rates for sample No. 46, where the water was changed, are seen to be approximately the same as those obtained in the systems with granulated cement. However, since analyses of the water as well as the concrete cylinder are available at each sampling for this system, it is possible to get a better impression of how the leaching and penetration into the concrete proceed. It is seen that most of the cesium is removed with the water, while about 2/3 of the leached cobalt seems to be absorbed on the concrete.

As could be expected the concentrations and penetration depth in the concrete cylinder were largest in the system with sample No. 45 and no water change during the experiment. The absence of water flow seems to result in a slight decrease in Cs leach rate. The total amount of leached Co is the same as for sample No. 46, but about twice of the amounts found in the systems with

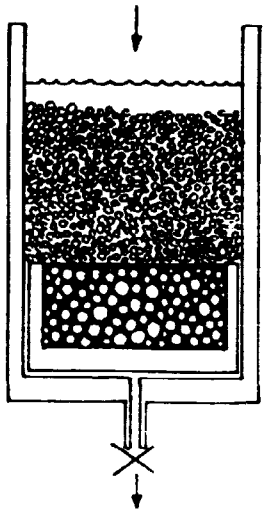

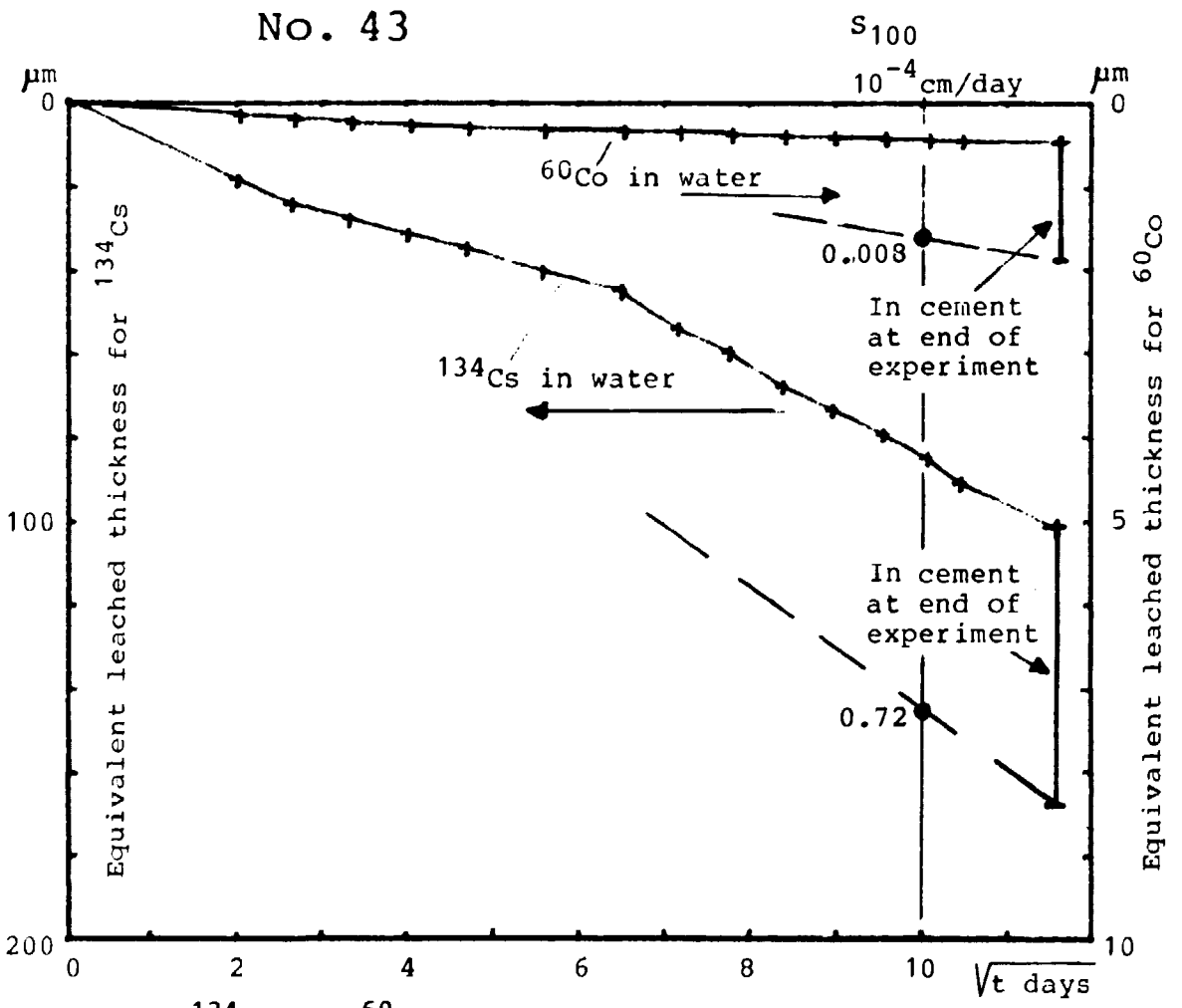

Fig. 29. ^{134}Cs and ^{60}Co removed with leach water conditioned by contact with granulated hardened cement paste in direct contact with the surface of a sample of bituminized cation-exchange resin.
60% Mexphalte 40/50 + 40% granular IR 120 on sodium form.

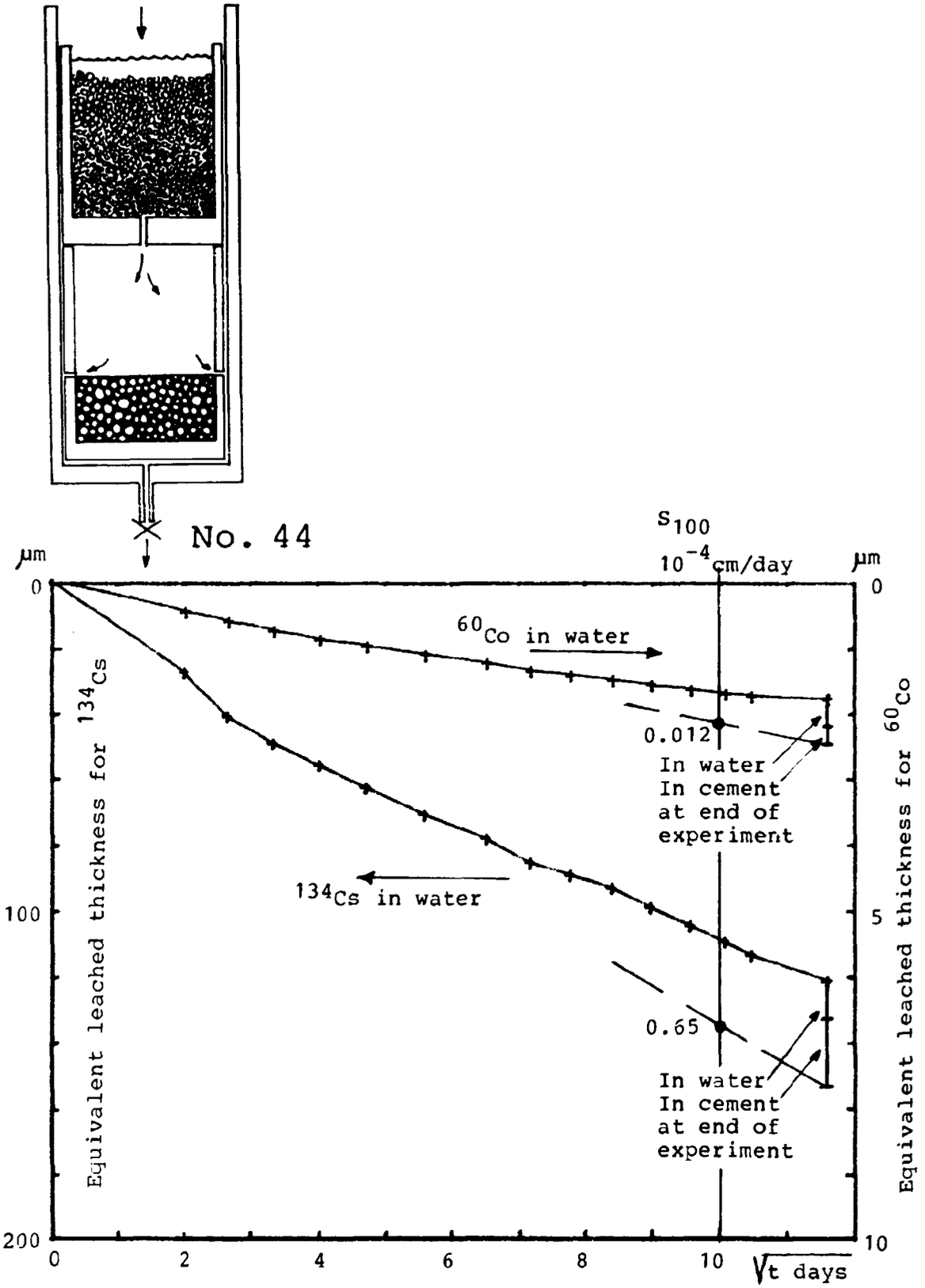

Fig. 30. ^{134}Cs and ^{60}Co removed with leach water conditioned by contact with granulated hardened cement paste from a sample of bituminized cation-exchange resin. 60% Mexphalte 40/50 + 40% granular IR 120 on sodium form.

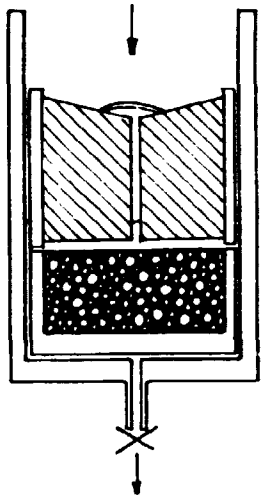

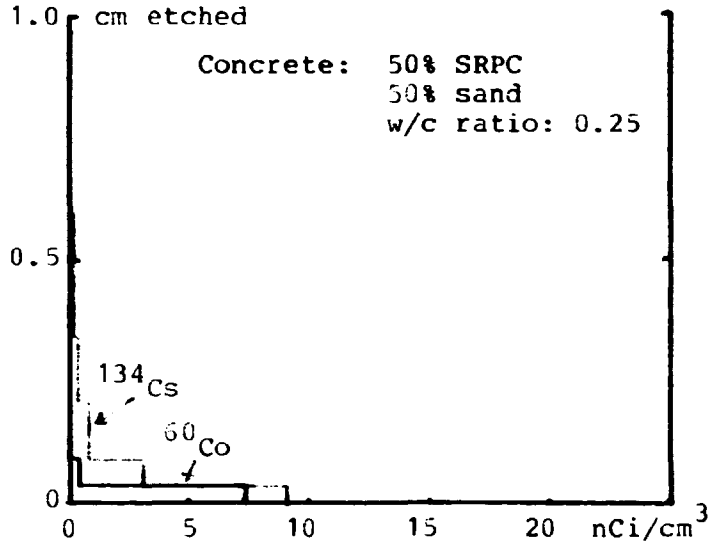

Concentration profile in concrete cylinder at the end of the experiment.

No. 46

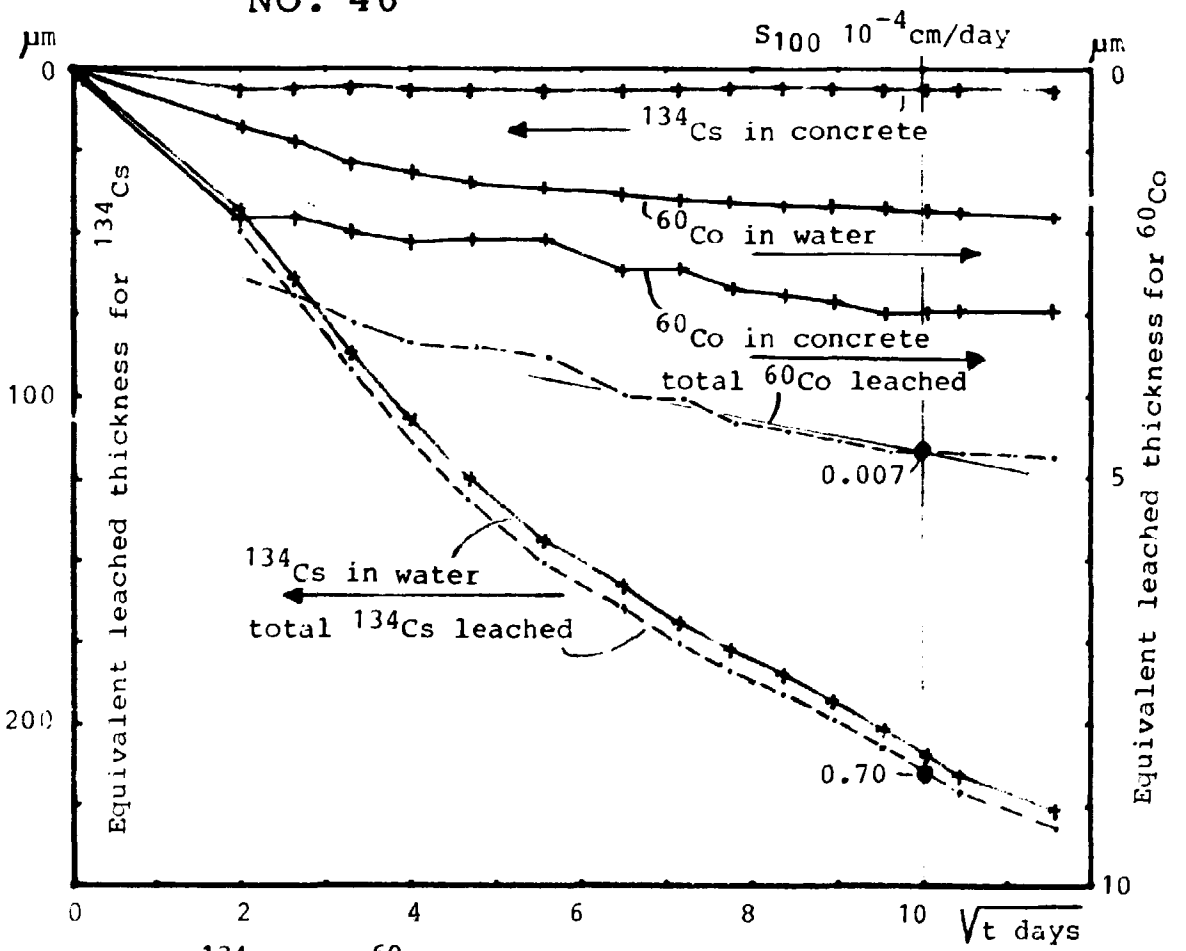

Fig. 31. ^{134}Cs and ^{60}Co removed with leach water or transferred to a concrete block placed on top of a sample of bituminized cation-exchange resin
60% Mexphalte 40/50 + 40% granular IR 120 on sodium form.
Water changed in connection with sampling.

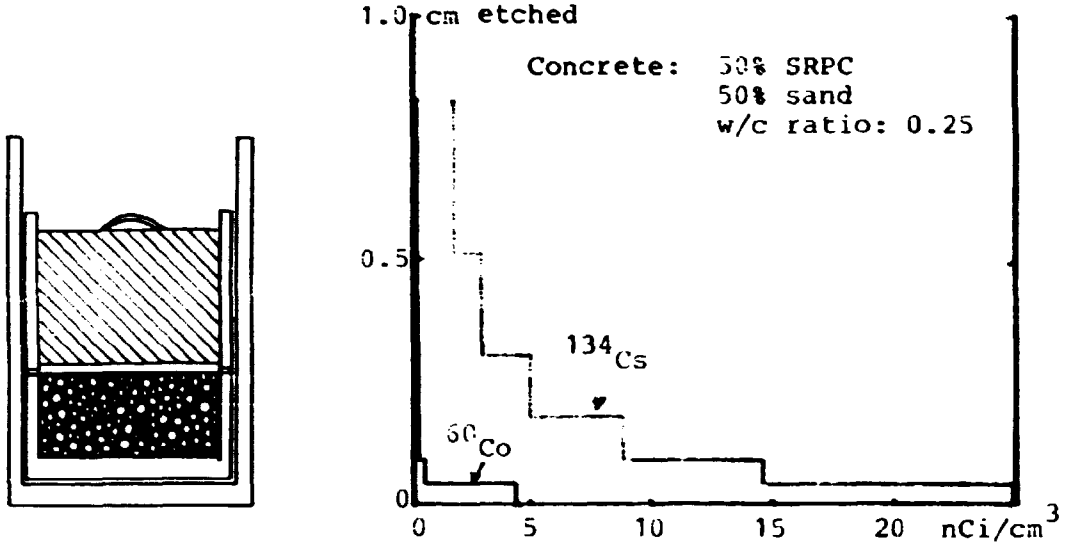

Concentration profile in concrete cylinder at the end of the experiment.

No. 45

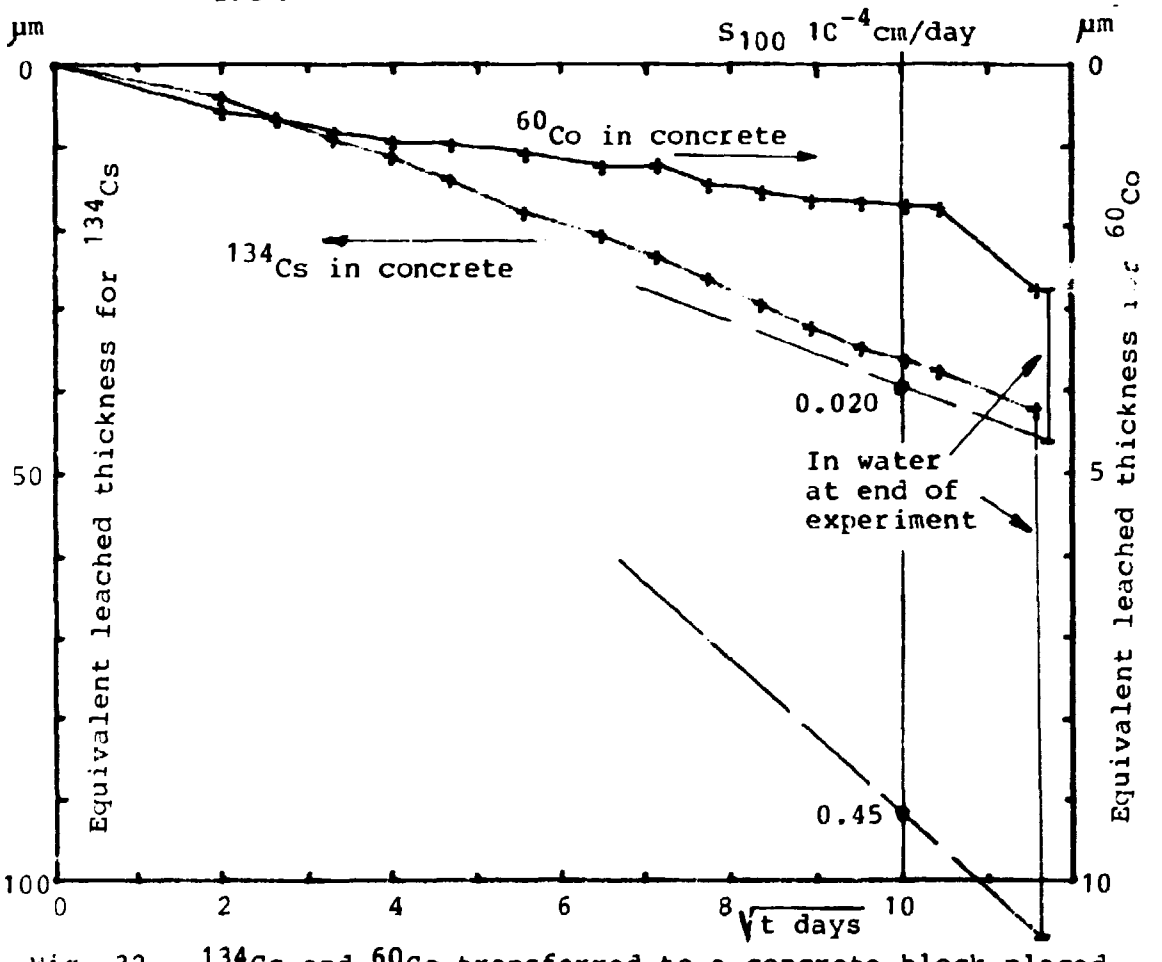

Fig. 32. ^{134}Cs and ^{60}Co transferred to a concrete block placed on top of a sample of bituminized cation-exchange resin.
60% Mexphalte 40/50 + 40% granular IR 120 on sodium form.
Stagnant water system.

granulated concrete. However, this could partly be due to experimental errors since the amount of activity found by etching the concrete samples was only about half of that found by direct measurements on the samples. The problem can be associated with the assumed counting geometry for the concrete samples, but it could also be due to only partial extraction of the activity by the etching procedure. Unfortunately, this was not investigated in time.

It is seen from these four experiments that Cs is released relatively rapidly when bituminized cation-exchange resin is leached by cement-conditioned water. In a "flow" system the leach rate seems typically to be about $7 \cdot 10^{-5}$ cm/day. This can be compared, for example, with the Cs leach rates for a similar material given in Fig. 25a. Here values about $4 \cdot 10^{-5}$ cm/day were found for leaching in 0.01 M NaCl and about $3 \cdot 10^{-5}$ cm/day for leaching in ~ 5 M NaCl.

The Co leach rates at 100 days are about 10^{-6} cm/day. This can be compared, for example, with the Co leach rate about 10^{-5} cm/day obtained for the sterile samples in Figs. 34 and 36. This indicates that the high pH values in cement-conditioned water prevents the diffusion of Co^{++} out of the bituminized materials to some extent. However, other differences in water chemistry, such as concentrations of cations, may also influence the leaching. A summary of the leach rates at 100 days (representing total material removed with water + absorbed on the concrete) as estimated from Figs. 29 to 32, is given in Table 12. The relative amounts of activities absorbed on the concrete are also indicated in the table.

It is seen that the leached cobalt tends to be absorbed on the surface of the concrete cylinders while cesium either is carried away with the leach water or has penetrated to a considerable depth into the concrete in the case of the stagnant water system.

The leach rates are not very dependent on the type of interaction system between the bituminized ion exchange resin and the

Table 12. Leach rates after 100 days of contact between concrete, water and 60 % Mexphalte 40/50 + 40 % IR 120 on sodium form.

10^{-4} cm/day % on concrete	No. 43 Granulated cement. Contact	No. 44 Granulated cement conditioned water	No. 46 Concrete cylinder. Water replaced	No. 45 Concrete cylinder. Stagnant water
^{134}Cs	0.70 40 %	0.65 ~0 %	0.70 3 %	0.45 40 %
^{60}Co	0.008 74 %	0.012 ~0 %	0.007 40 %	0.20 60 %

concrete. However, if water flow is absent (or very slow) there seems to be a slight effect. In such a system a solution with relatively high concentrations of soluble salts will be formed in the gap between the waste and the concrete sample. The concentration of, for example, Cs in this water will be determined by the relative rates of diffusion of Cs out of the waste and into the concrete. These rates are themselves functions of the Cs concentration in the water. It would be interesting with a more detailed investigation of the water chemistry in such a system. The influence of the presence or absence of CO_2 on the behaviour of the system should also be investigated.

The conditioning of water by contact with concrete may have an influence on the tendency to water uptake in the waste material. This has not been investigated in these experiments.

Other types of waste materials than the bituminized cation-exchange resin used here will probably behave quite differently in contact with concrete.

A practical problem regarding laboratory technique is whether the etching technique used to determine the penetration depth into the concrete results in artificially high penetrations due to back-contamination from isotopes which have gone into solution.

It is felt that the type of experiments described here gives some information which cannot be obtained from normal leach-rate measurements. It should be possible to develop the methods so that they can be used to study more complete simulated versions of the barrier systems which may be used in repositories.

2.10. Degradation of bituminized waste by micro-organisms

Bacteria and fungi, which are able to decompose hydrocarbons and utilize them as a carbon- and energy source, are common everywhere in the upper soil layers. It is known from various practical applications of bitumen and some laboratory investigations (15) that at least some of these micro-organisms are able to attack components of the bitumen. For the safety evaluation of disposal of such materials it is therefore of some importance to investigate whether the growth of micro-organisms could result in rapid deterioration of bituminized waste, and under which circumstances this is possible.

The primary purpose of the experiment presented below has been to establish methods which makes it possible to determine whether a degradation process is proceeding at a rate which is significant for the overall behaviour of the system. This means that the investigated system must have some properties which can be measured and which are linked more or less directly with the growth of the micro-organisms and the degradation of the bitumen. This rather obvious requirement is not so easy to establish with certainty in slowly growing biological systems.

2.10.1. Leaching of bituminized ion-exchange resin with and without presence of micro-organisms

One possible experimental approach is to investigate the influence of growth of micro-organisms on the leach rate of bituminized waste.

Results from an experiment performed at Risø some years ago (11) seem to indicate that the presence of micro-organisms en-

hance the leaching of ^{134}Cs from bituminized cation-exchange resin. This experiment has been repeated twice since that time, but it has not been possible to reproduce the previous results.

The experimental set-up is shown in Fig. 33. It is identical to the one used in the original experiment. The samples (60% Mexphalte 40/50 + 40% dry IR 120 cation exchange resin on sodium form contaminated with ^{134}Cs and ^{60}Co) were cast at the bottom of a perspex tube and covered with a layer of coarse quartz sand. The sand just above the sample surface in two of the units was inocculated with a bacteria culture, which had been prepared about a month before, in the form of a moist mixture of ordinary soil and sand coated with a thin layer of bitumen (see Section 2.10.2 for further details).

The possible influence of the microbes on leaching from two samples was measured directly by measuring the amounts of ^{134}Cs and ^{60}Co leached from the sample out into the nutrient solution which also served as leach water. The composition of the solution is given in Fig. 33. The sampling frequency was once every week at the beginning. 50 ml solution was removed for analysis by γ-spectroscopy from the outlet just above the sample surface. The water was replaced by fresh solution from above.

A third sample was used as a control. To secure that this system remained sterile a small amount of Hg^{++} (0.05 g $HgCl_2$/l) was added to the nutrient solution which was used as leach water also in this case. The experimental results for the three samples used in the first set of repeated experiments are shown in Figs. 33 and 34.

A significant difference from the original experiment was the unexpected development of anaerobic conditions in the two systems with micro-organisms. A pronounced smell of H_2S could be noticed when sampling the water. The hydrogen sulphide was probably produced from components in the nutrient solution, i.e. SO_4^{--} reduced by NH_4^+ by the micro-organisms. This indicates the development of a wrong population of micro-organisms. The systems were therefore drained after about 120 days of

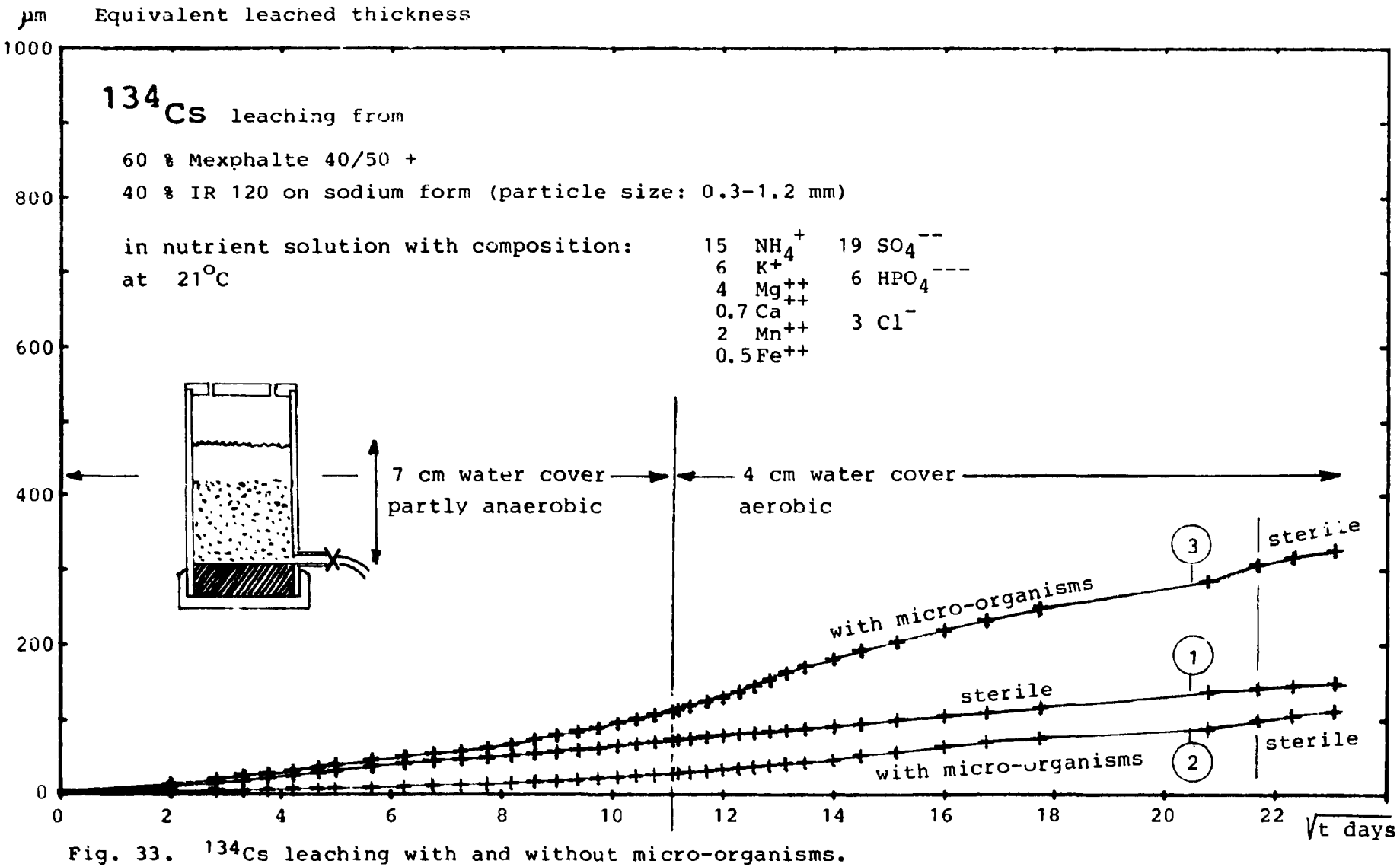

Fig. 33. ^{134}Cs leaching with and without micro-organisms.

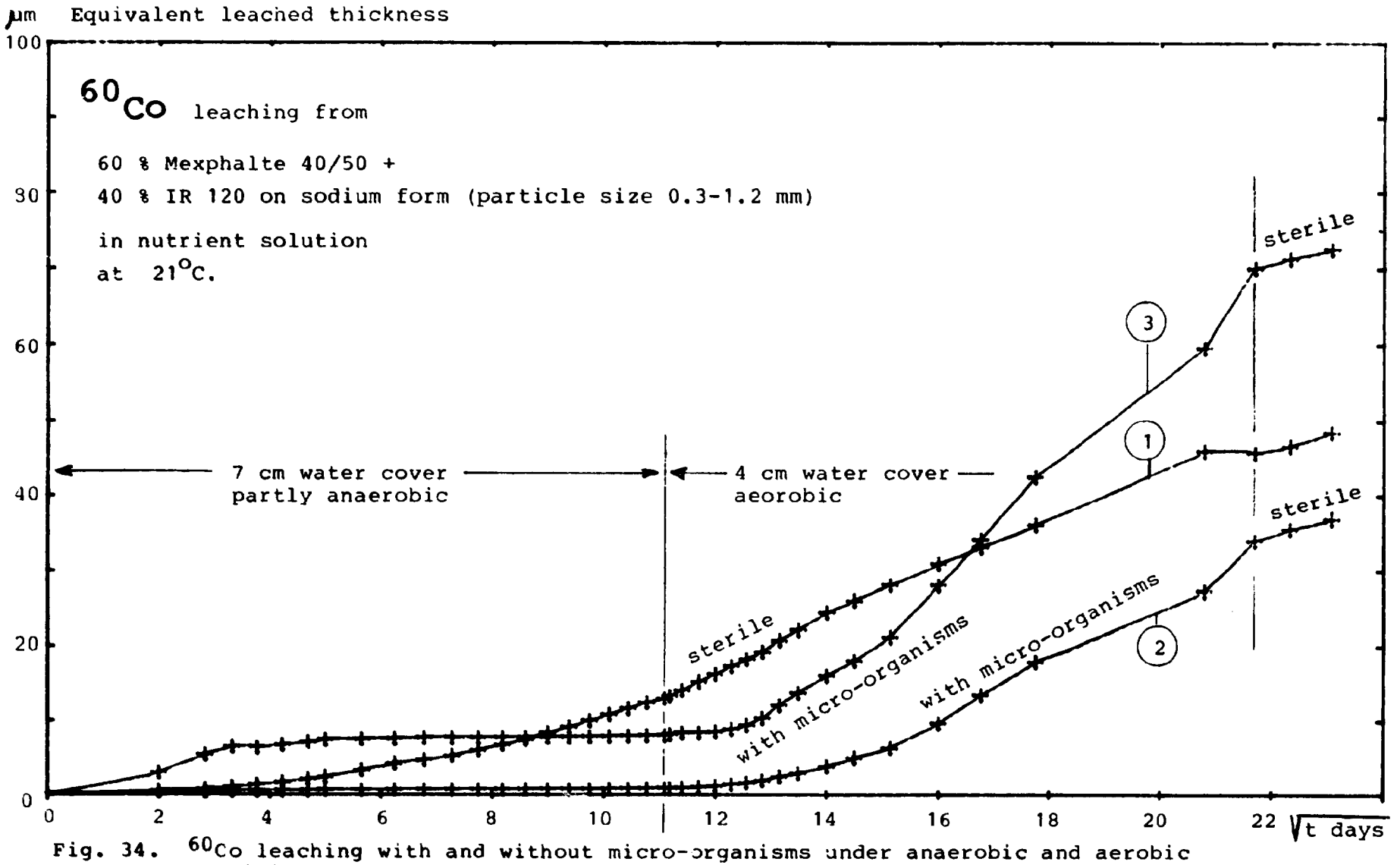

Fig. 34. ^{60}Co leaching with and without micro-organisms under anaerobic and aerobic conditions. (Same system as in Fig. 34.)

leaching and inocculated with a new portion of the enrichment culture before the leaching was resumed. In the first period the samples were covered by a 7-cm thick layer of water-saturated quartz sand. In the following period, the thickness of this layer was reduced to about 4 cm by changing the procedure so that at each sampling 50 ml nutrient solution was added to the system and permitted to drain through the quartz sand layer by keeping the bottom outlet open for about a quarter of an hour. No problems with non-oxidizing conditions were encountered after this change in procedure.

It is seen from Fig. 33 that there is a considerable difference in the slope of the cesium leach curves for the three supposedly identical samples. This is in agreement with the poor reproducibility of leach rates from bituminized granular resin which has been observed for other samples as well. Control sample No. 1, which was leached under sterile but otherwise identical conditions as the two samples with micro-organisms, was leached with a rate intermediate between the leach rates for the two samples with micro-organisms. The possible effect of the presence of micro-organisms on leaching is therefore not so large that it can be distinguished from the random variation in leach rate, at least not for bituminized granular ion-exchange resin.

It is seen from the curves in Fig. 33 that the new sampling procedure introduced after 120 days results in a slight increase in the slope of the Cs leach curves for the two samples with micro-organisms, especially sample No. 3, and no change at all in Cs leaching from the sterile sample.

The curves in Fig. 34 showing Co leaching from the same samples are quite different. It is interesting that the anaerobic condition in the systems with micro-organisms during the initial period results in extremely low cobalt leach rates. Various explanations are possible, such as precipitation of cobalt sulfide or, less probable, the use of a major part of the leached cobalt as a micro-nutrient. After the change in procedure the Co leach rates, with some delay, were increased to values approaching Cs leaching. A slight but immediate increase

in Co leaching from the sterile sample was also observed after the change in procedure.

At the end of the experiment the ordinary nutrient solution was substituted with the sterilizing one containing a small amount of Hg^{++} to see whether this would result in a decrease in slope of the leach curves for samples 1 and 2. A decrease would probably be conclusive evidence for a contribution of the micro-organisms to the leach rates measured before sterilization, since the leaching properties of a single sample seem to be rather well defined and stable. The problem with bad reproducibility from sample to sample can at least partially be circumvented in this manner. No significant change in Cs leaching was observed after the sterilization, but a decrease in Co leach rate of about a factor 4 can be obtained from Fig. 35. The material is too slight to draw any conclusions.

A second set of three samples of bituminized granular IR 120 cation-exchange resin has been leached under drained conditions from the beginning of the experiment. Otherwise, it was an exact reproduction of the previous experiment. The same leaching and nutrient solution and the same culture of micro-organisms were used. Two of the samples were inocculated with the culture while the third was kept sterile by Hg^{++} addition to the leach water. The leach curves obtained for ^{134}Cs and ^{60}Co are shown in Figs. 35 and 36 in the same scale as in Figs. 33 and 34.

It is seen that the leach rates in the new set of experiments are somewhat higher than in the previous one. This is probably due to variability of the sample properties as discussed previously.

It is not possible to see any difference in Cs leaching for the systems with or without micro-organisms. The Co leaching was more variable. Sample 41 may have had a period with anaerobic conditions between 50 and 140 days. No systematic trend can be seen due to sterilization at the end of the experiment.

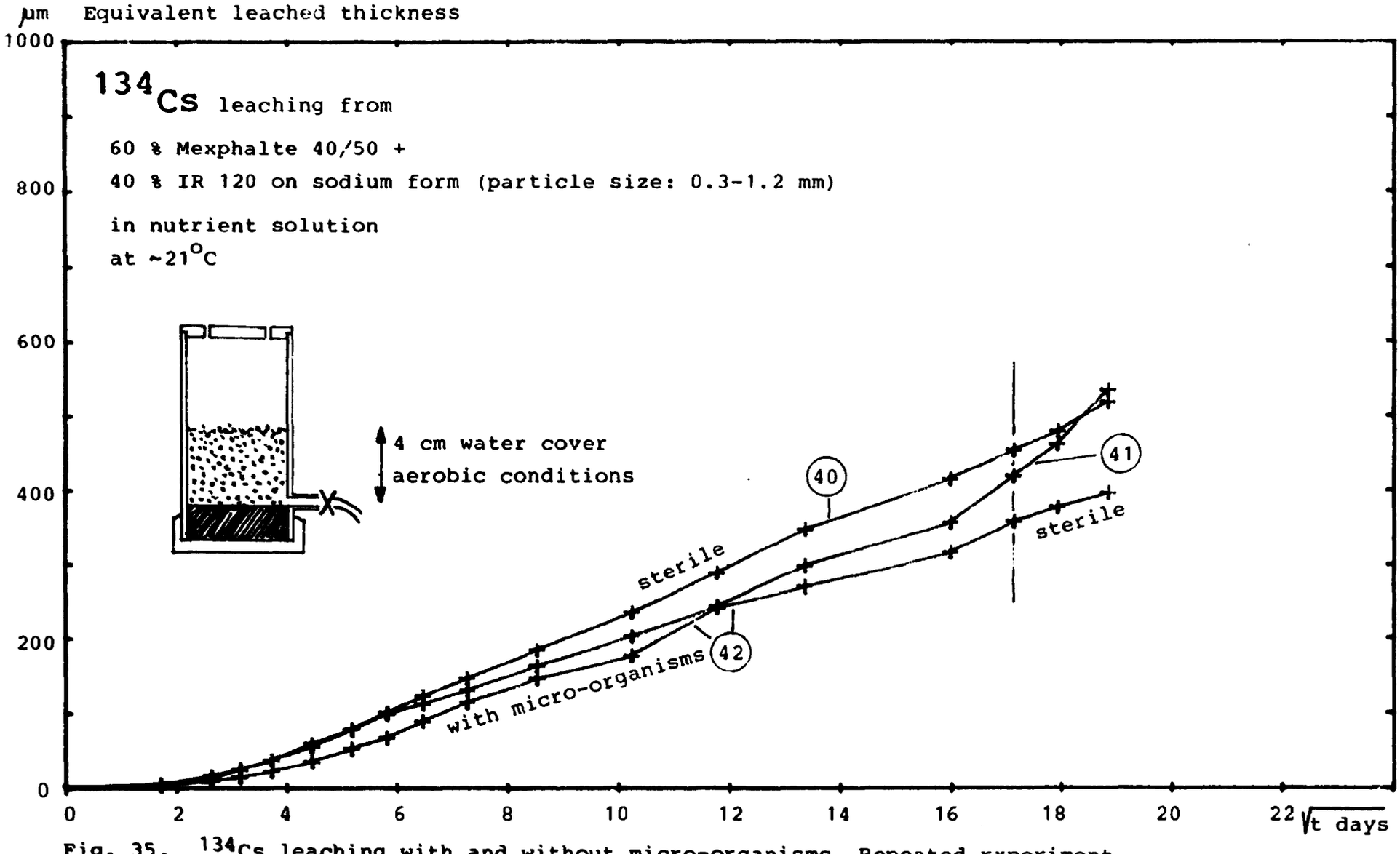

Fig. 35. ^{134}Cs leaching with and without micro-organisms. Repeated rxperiment.

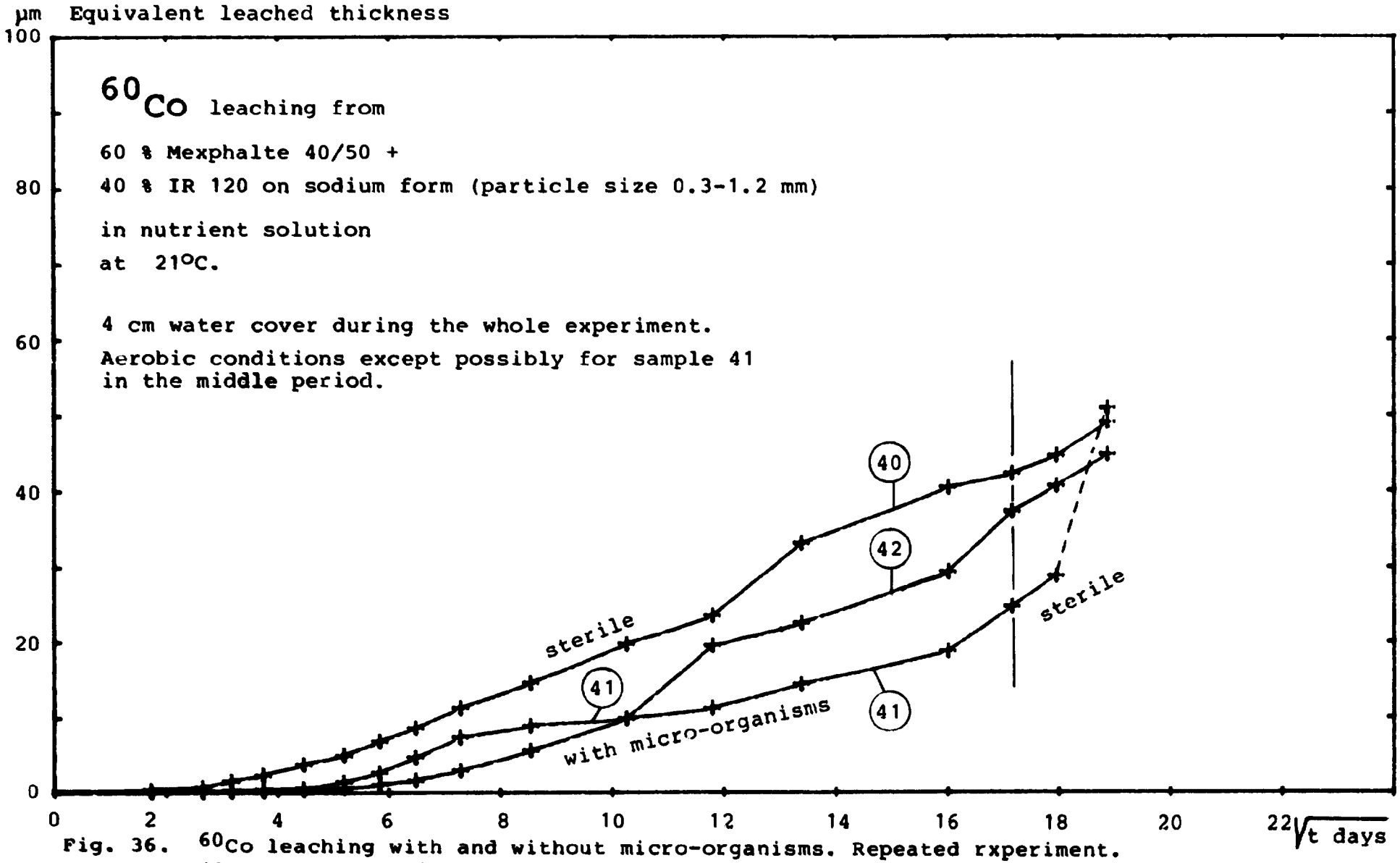

Fig. 36. ^{60}Co leaching with and without micro-organisms. Repeated rxperiment. (Same system as in Fig. 36.)

It is the intention to make further leaching experiments with and without the presence of micro-organisms since such experiments give information of direct relevance to safety analysis. However, it would be preferable to investigate bituminized waste materials with leach rates which are more reproducible from sample to sample than is the case for bituminized ion-exchange resin.

2.10.2. Degradation of pure bitumen as a coating on sand particles mixed with soil

One reason for the absence of a significant effect of micro-organisms on the leach rate measurements could be that the mixture of micro-organisms used to inocculate the leaching systems did not contain species which were able to utilize bitumen as carbon source. This is not very probable since hydrocarbons consuming micro-organisms are quite common in ordinary soil, and an enrichment culture grown on a mixture of 50% ordinary surface soil + 50% sand coated with a thin layer of bitumen was used for the inocculation. The mixture had been kept moist for about one month before start-up of the first leaching experiments and much longer before reinocculation of the systems in connection with the change from water-saturated to drained conditions. The large surface area of the bitumen-coated sand - about 30 cm^2/g dry mixture, estimated from the particle-size distribution of the sand - should enhance the growth of micro-organisms which are able to utilize the bitumen and should probably at the same time - due to competition about other nutrients - result in a decrease in the number of micro-organisms which do not have this ability. As a further means of ensuring the presence of bitumen-destroying micro-organisms small amounts of material scraped from bitumen-coated surfaces of old asphalt drums which had been exposed to the weather for a long period and material collected from the surface and the rim of old asphalt-paved roads were added to the mixture.

No attempt has been made to make monocultures of pure strains of the bacteria and fungi in the mixture, but an analysis of the types of bacteria present in the mixture has been made at

Cadarach, France (16).

The content of bitumen in the mixture has been analysed by extraction with Xylene at various times after the preparation. The results are shown in Fig. 37. A slow but steady decrease in content of extractable bitumen is noticed. Using the estimated specific surface area of 30 cm^2 bitumen/g dry mixture and a bitumen density of about 1 g/cm^3, this can be translated into a bitumen degradation rate of about $3 \cdot 10^{-7}$ cm/day. This indicates that degradation of bitumen is a relatively slow process, but it should also be noticed that about 10% of the original amount

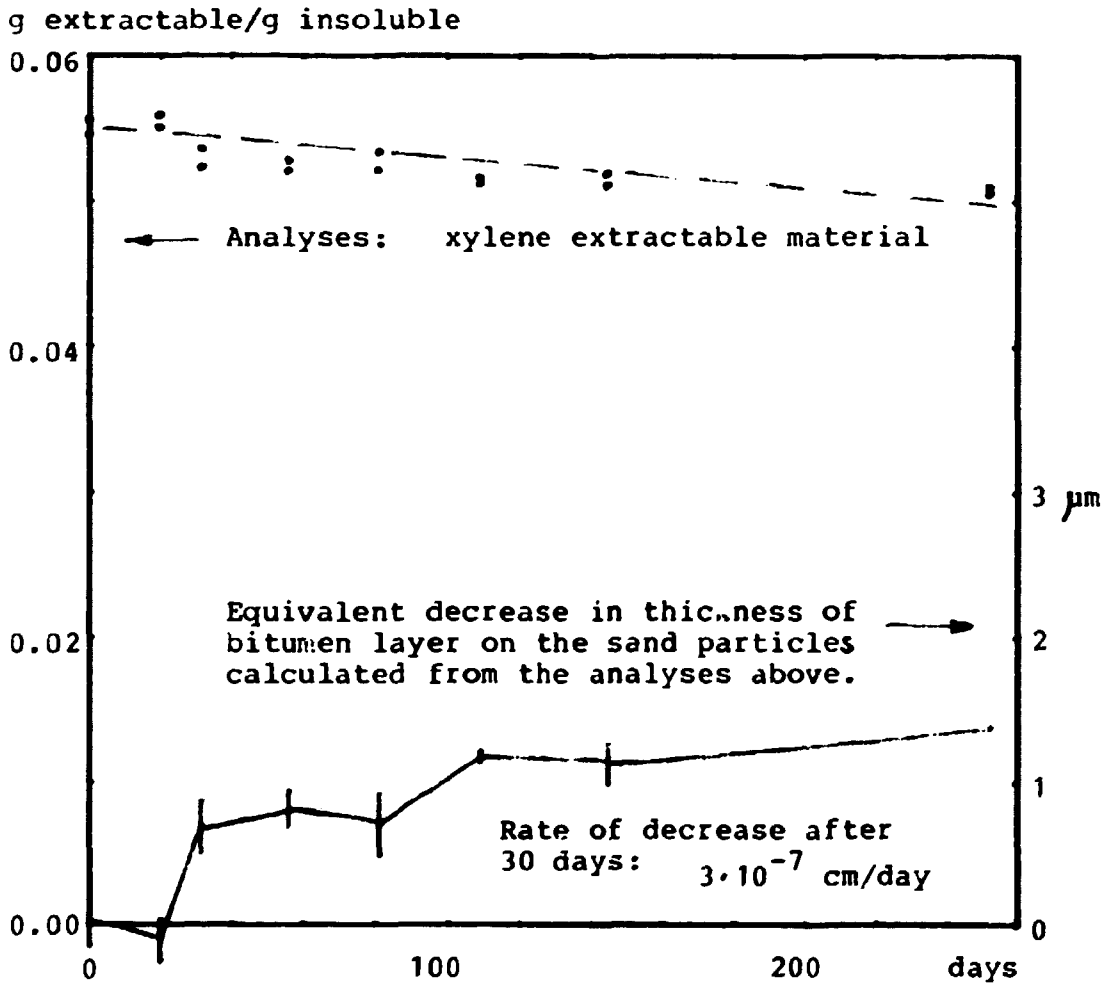

Fig. 37. Decrease in xylene-extractable material and the equivalent calculated decrease in thickness of the bitumen layer on the sand particles in a moist mixture of bitumen-coated sand + soil as a function of time after initiation of growth of micro-organisms in the mixture.
Thickness of the original bitumen layer: ~ 16 µm.

of bitumen in the mixture has disappeared after 230 days. It is probably only a relatively minor part of the bitumen - primarily the aliphatic hydrocarbons - which is consumed by the micro-organisms, but this will change the properties of the remaining material such as asphaltenes to something which is probably not very valuable as a barrier against leaching.

2.10.3. Respiration of micro-organisms growing on bitumen

As a supplement to the above investigations a method has been developed for measuring the oxygen consumption in systems consisting of bitumen + water + micro-organisms. A measurement of the so-called respiration of the culture is a usual feature in the study of the metabolism of micro-organisms, but the experiments turned out to be somewhat complicated due to the low reaction rates in these systems. Variations of the classic Warburg principle were used but not in the usual micro-scale equipment.

The first experiment was made by measuring the decrease in pressure in a primitive apparatus built from QVF glass equipment (shown in Fig. 38a). The pressure decrease is due to the metabolism of the micro-organisms which results in oxidation of the bitumen:

$$\overset{|}{\underset{|}{CH_2}} + 1^1/_2\ O_2 = CO_2 + H_2O$$

and to the subsequent absorption of the CO_2 produced in NaOH solution contained in the bottom of the apparatus.

30 g of bitumen-coated sand with grain size 1-2 mm and a specific surface area after mixing with 10% bitumen of about 10.4 cm^2/g were used as substrate for the culture. This gives a relatively large bitumen area exposed to the micro-organisms. However, the pressure decrease due to the oxidation of the bitumen turned out to be much smaller than the variations caused by changes in temperature and atmospheric pressure. Although corrections for these external influences could be made by employing a suitable calculation program, considerable uncertainties

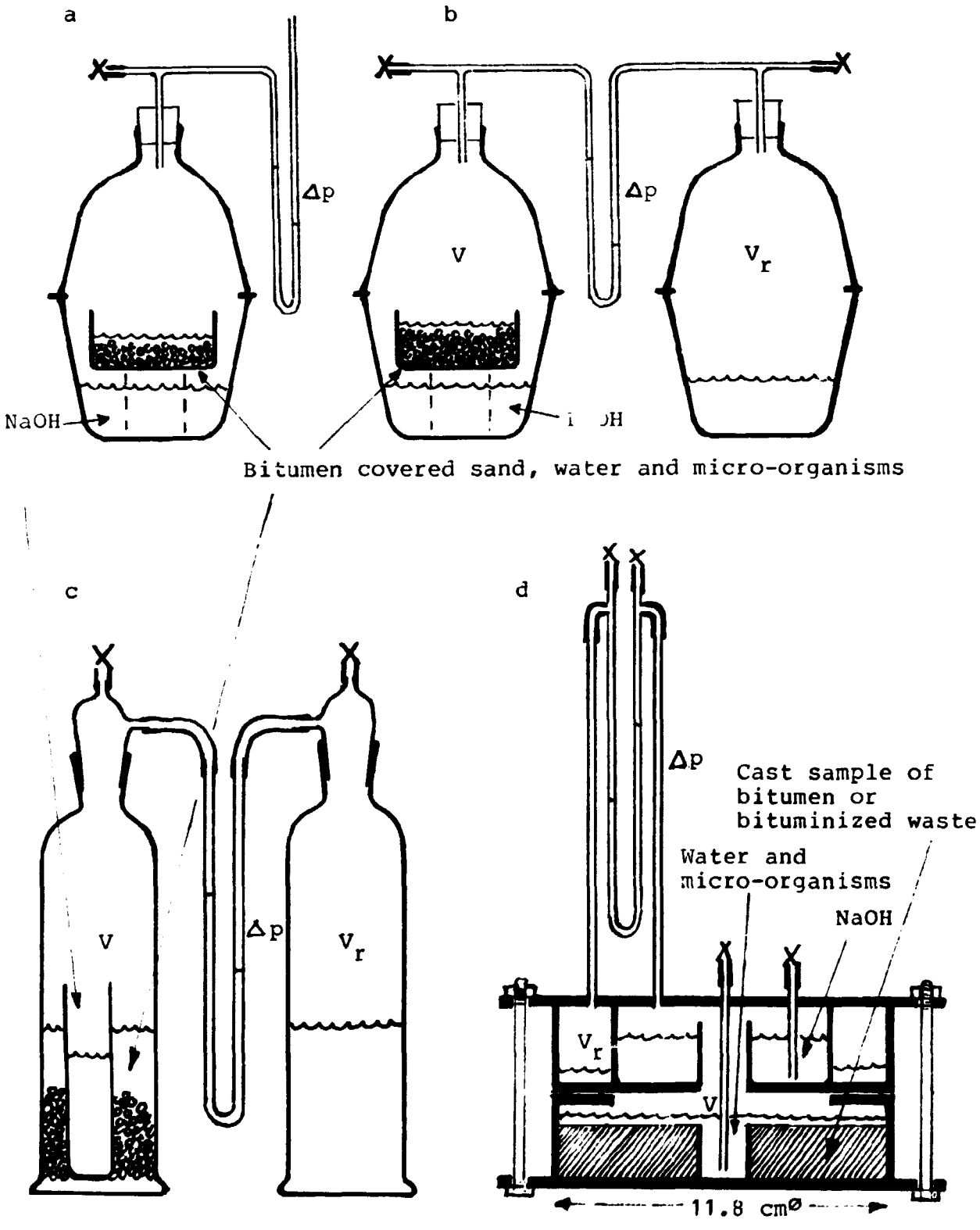

Fig. 38a,b,c, and d. Experimental equipment used in determination of respiration of micro-organisms growing on bitumen.

were introduced. The results shown as the upper curve in Fig. 39 were obtained. In this figure the pressure variations are converted to equivalent thickness of a totally consumed bitumen layer distributed evenly over the surface of all the bitumen-coated sand particles. The right-hand scale gives the accumulative oxygen consumption in the system. The first part of the curve with the relative rapid increase is probably an artifact caused by oxydation of NH_4^+ in a small amount of nutrient solution added to the system at the beginning of the experiment. The last part of the curve is curious due to the large variations corresponding to occasional pressure increases. The reason for such increases is not obvious and they are probably not real. The mean slope of the later part of the curve corresponds to a bitumen-consumption-rate of $2 \cdot 10^{-8}$ cm/day, but this value must be regarded with much reservation. The experiment was re-

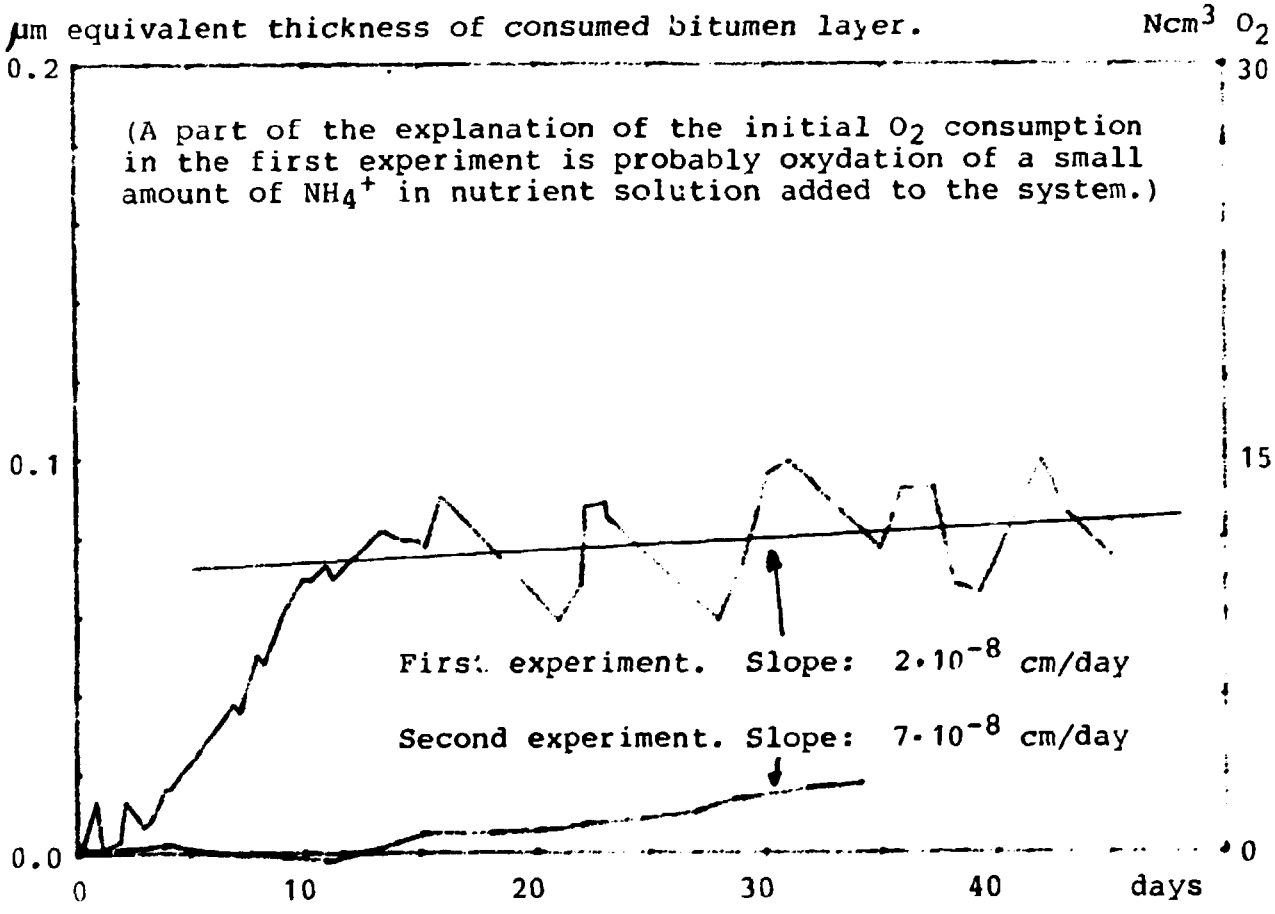

Fig. 39. Estimate of rate of bitumen degradation based on measurement of respiration, i.e. consumption of O_2 by a system consisting of bitumen-covered sand particles, water and hydro-carbon-consuming micro-organisms.

peated using a larger amount of bitumen-coated sand: 90 g equal to a surface of about 1800 cm^2. This should improve the signal-to-noise ratio by a factor 3. More important was that a reference container with approximately the same volume as the culture chamber was included in the system as shown in Fig. 39b. This isolates the system completely from the outside and eliminates the need for correcting variations in atmospheric pressure. Corrections for temperature variations are also unnecessary, provided the two chambers are at the same temperature and both contain some water. It is, of course, a requirement that the system is completely air-tight.

By application of the gas law on such a system it can be shown that the relationship between the gas consumption in the culture chamber, ΔN mol O_2 and the measured pressure difference Δp cm H_2O, the gas volume in the culture chamber (which should be approximately the same as the gas-filled volume of the reference chamber) $V = V_r$ cm^3, and the cross-section of the water-filled U-tube used as manometer A_u cm^2, is given with good approximation by:

$$\Delta N = \Delta p \cdot \left(A_u \frac{p_o}{R \cdot T_o} + \frac{V}{R \cdot T_n} \right) \text{ mol } O_2 \ .$$

where p_o can be approximated with normal atmospheric pressure: 1030 cm H_2O.

$$T_o \cong T_n \sim \text{room temperature} \sim 298^oK$$

and

$$R = 84770 \ cm^3 \cdot cm \ H_2O/mol \cdot {}^oK$$

which gives:

$$\Delta N = \Delta p \cdot (0.91 \cdot A_u + 0.00089 \cdot V) \ N \ cm^3 \ O_2 \ .$$

The contribution from the volume variations caused by the change in manometer level can be quite important or even essential for

the calculation of ΔN becausse of the relatively small values of V typical for the equipment.

ΔN is converted to g bitumen consumed simply by assuming that $1^1/2$ mol O_2 is used for oxidation of each CH_2 group, i.e. 0.42 mg bitumen/ml O_2 consumed. This, of course, is not strictly correct since bitumen also contains other components and the oxidation does not always proceed completely to CO_2 and water.

The result of the experiment with the equipment in Fig. 38b is shown as the lower curve in Fig. 39. In this case no nutrient solution was added, i.e. the culture contained only bitumen-coated sand and water inocculated with a very small amount of the mixture of micro-organisms described in Section 2.10.2. This illustrates a dilemma associated with this type of experiment depending on measurement of gas consumption: All materials which contribute to the oxygen consumption - or supply oxygen, or produce other gases - will give a false signal. An example is the NH_4^+ nitrification mentioned in connection with the first experiment. On the other hand, if necessary nutrients are omitted, the result wil be a system which is starving, i.e. limited in growth, not due to resistance of the bitumen against attack, but due to the lack of other nutrients. The rate of bitumen consumption was found to be about $7 \cdot 10^{-8}$ cm/day in this second experiment. The measurements are not in doubt in this case, but the system is almost certainly starving due to lack of nitrogen and phosphates, i.e. the rate of attack could be considerably higher under more favourable conditions. A control analysis of the composition of the gas in the culture chamber after the experiment did show the expected slight decrease in O_2 relative to N_2 content. No CH_4 or H_2 could be detected.

2.10.4. Experimental difficulties with anaerobic systems

In Fig. 38c an experimental set-up is shown, in principle identical with the system in Fig. 38b, but built from standard Quickfit glassware. Rubber packings are necessary between the glass parts of type b equipment. They are avoided in type c. This is an advantage since they may serve as an undesirable

additional substrate for micro-organisms.

An attempt to make a first experiment with bitumen degradation under anaerobic conditions using type c equipment and argon as cover-gas has resulted in identification of some principal difficulties which must be taken into account when making anaerobic experiments with these types of equipment. Argon seems to be diffusing out of the flexible PVC tubes used to connect the containers with the glass U-tube serving as manometer. Some indiffusion of air into the argon atmosphere inside the tube connecting the culture chamber with the U-tube is probably also taking place - and may destroy the anaerobic conditions - but the rate of out-diffusion of argon is faster, resulting in the development of a negative pressure in the culture chamber. The difference in the rates of diffusion gives a change in Δp with time which corresponds to an approximate outflow of 0.01 N cm^3 gas/day/cm^2 tube surface at room temperature and a partial pressure difference of 1 atmosphere over a tube wall with thickness 0.08 cm.

However, this is not the only interfering phenomenon. In a system with argon on one side and air on the other side of the water in the U-tube used as manometer there seems to be an interchange of gases through the water. This can also give a false signal for gas consumption. With pure argon in the culture chamber both phenomena are so important for the long-term development of Δp that they cannot be tolerated. The interconnecting flexible tubes between the glass parts must therefore be avoided or they should at least be as short as possible ($<$ 1 cm). Diffusion through the U-tube is avoided if the reference chamber as well as the culture chamber are filled with argon.

When the equipment is used under aerobic conditions with air inside both chambers the possibility of interference from these phenomena is much smaller, since only slight differences in partial pressure will occur between the two chambers and between the air outside and inside the tubes. However, also in this case the length of the flexible tube should be kept at a minimum.

It is the intention to continue the work on bitumen degradation under anaerobic conditions, for example whether a reaction of the type:

$$5\ \overset{|}{\underset{|}{CH_2}} + 6\ NO_3^- \rightarrow 5\ CO_2 + 2\ H_2O + 3\ N_2 + 6\ OH^-$$

may serve as an energy source for anaerobic degradation of bituminized sodium nitrate. Micro-organisms in anaerobic digested sewage sludge will be used as inocculant. This is reasonable since such sludges often contain some hydrocarbons so that hydrocarbon-consuming organisms can be expected to be present, if they exist at all under anaerobic conditions.

The rate of degradation of bitumen under anaerobic conditions is expected to be (much ?) lower than under aerobic. In connection with the experimental difficulties this will make it difficult to show with certainty that degradation takes place and that it is due to micro-organisms growing under truly anaerobic conditions. However, the information is important for safety analyses since such conditions must be expected in below-surface repositories some time after closure.

2.10.5. Respiration of micro-organisms growing on thick samples of bitumen or bituminized waste

In Fig. 38d a unit is shown which differs from the previous ones by the use of the upper surface of a thick, cast sample of bitumen or bituminized waste as substrate for the growth of the micro-organisms. This will reduce the rate of oxygen consumption by a factor 10 to 20 compared with systems with bitumen-coated sand, since this is the approximate ratio between the exposed bitumen areas in the two types of systems. To retain some of the sensitivity of the system the unit has been designed with air volumes as small as possible. That this is an advantage can be seen by reference to the formula for ΔN in Section 2.10.3. A ring-shaped reference chamber and the container for NaOH solution is part of the lid. This ensures identical temperatures of the culture and the reference chambers. Large temperature

variations of the unit as a whole may give false Δp-signals due to the relatively large thermal expansion of the bitumen, but this does not result in a systematic bias. The unit is made of stainless steel. The lid and the bottom sections are bolted together and sealed with soft teflon cord. Both the NaOH solution and water covering the bitumen can be sampled during the experiment. This makes it possible to measure correlated oxygen consumptions, absorbed CO_2 and leached material for a sample undergoing microbial degradation.

Two units were made. One of them has given trouble with airtightness, but the other has produced interesting results for micro-organisms growing on a sample of bituminized sodium nitrate.

The sample was cast from a mixture of 40% $NaNO_3$ and 60% Mexphalte 40/50 in the bottom part of the unit as indicated in Fig. 38d. It was covered by deionized water inocculated with a small amount of the same culture of micro-organisms as used in the previous experiments. 0.1 N NaOH was used for CO_2 absorption. Calculations based on the Δp-measurements during a period of 270 days gave the result shown in Fig. 40. The calculation principle is the same as in Fig. 39.

A pressure decrease in the culture chamber of up to 12 to 18 cm H_2O was reached 13 times in the period. The pressure difference was equalized at the end of each of these periods. At the first and the third ones the valves were simply opened and closed again immediately. There was therefore only a very limited replacement of air from inside the apparatus with fresh air. On the second occasion at about 20 days the valves were left open for about 3 hours while the NaOH solution and the water covering the bituminized sodium nitrate were sampled and replenished.

This has probably resulted in a complete renewal of the air in the culture chamber. Good venting of the air in the culture chamber was also ensured in connection with later equalizing of the pressure difference. A decrease in oxygen concentration during a period between ventings may explain why the curve in

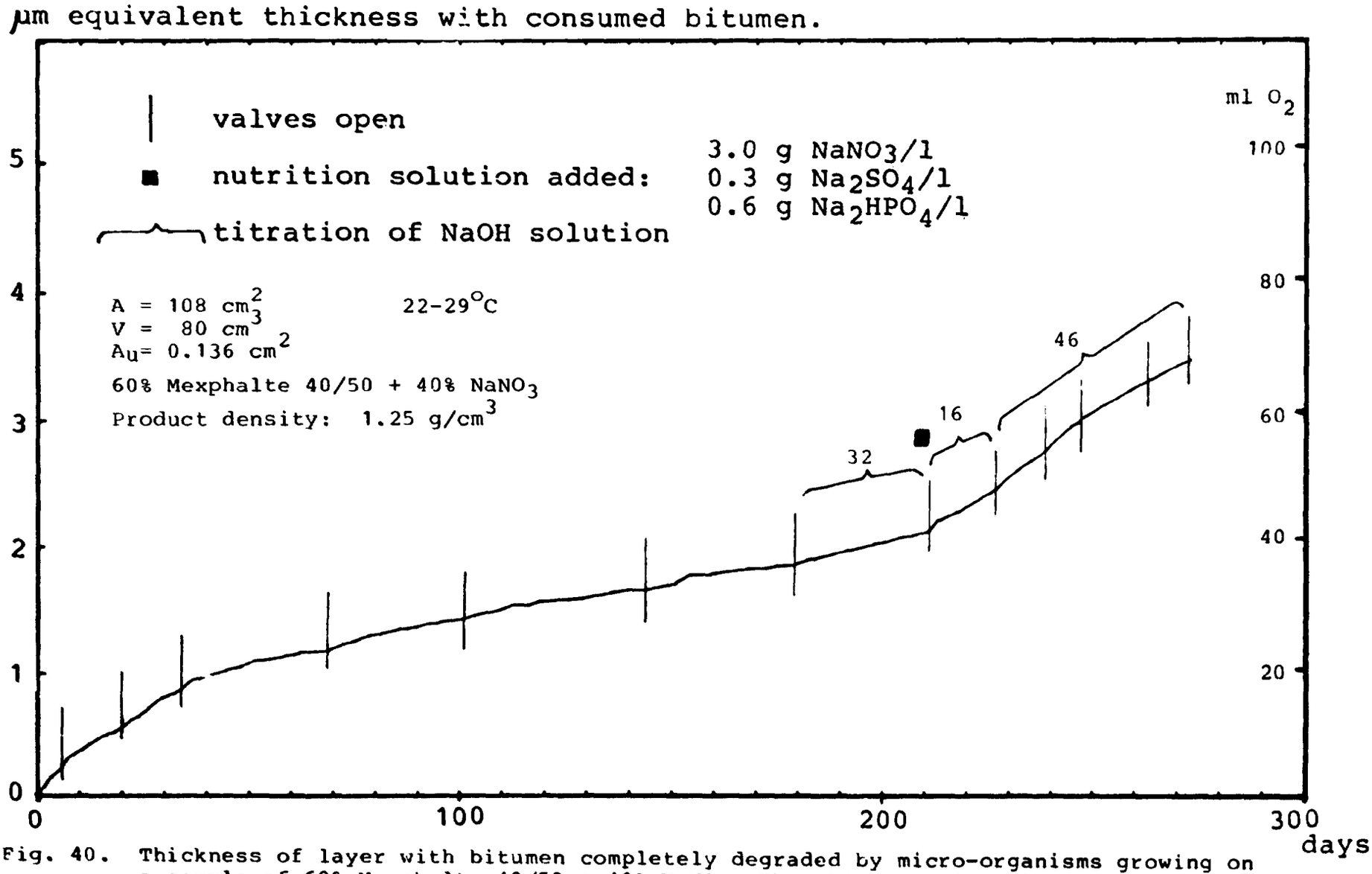

Fig. 40. Thickness of layer with bitumen completely degraded by micro-organisms growing on a sample of 60% Mexphalte 40/50 + 40% $NaNO_3$. The thickness is calculated from the respiration of the system and includes the bitumen as well as the sodium nitrate.

Fig. 40 tends to show some decrease in rate of oxygen consumption at the end of each period. From the oxygen consumption shown by the right-hand scale on the figure and from an air volume of the culture chamber of about 80 cm^3, it is seen that the oxygen concentration is decreased from the original 20% to about 10% at the end of the periods. This is likely to result in some decrease in the vitality of the micro-organisms.

Lack of essential nutrients seems also to result in a decrease in the rate of oxygen consumption:

Two slopes of the curve in Fig. 40 are apparent: the larger one, about $1.5 \cdot 10^{-6}$ cm/day is typical for the situation at the beginning and after addition of the nutrient solution with composition as given in the figure. The smaller one, about $0.4 \cdot 10^{-6}$ cm/day seems therefore to be the result of lack of essential nutrients, probably phosphate, since nitrate is present from leaching of the crystals embedded in the bitumen.

The rate of oxygen consumption and bitumen degradation calculated from the Δp measurements and from titration analyses of the CO_2 absorbed in the NaOH solution were compared for three periods at the end of the experiment. The values are shown in Table 13. The two methods give results in reasonable agreement with each other. This means that the formula:

$$CH_2 + 1^1/_2\ O_2 = CO_2 + H_2O$$

represents a valid approximation to the overall process in the system. It is a minor fraction of the oxygen which seems to be used in producing only partly oxidized organic materials. However, the information is insufficient since it cannot be excluded that some reduction of NO_3^- takes place under N_2 production. This will tend to decrease the Δp values and increase the amount of CO_2 found in the NaOH solution. Further studies are necessary to see whether or not this is the case.

Inspection of the surface of the sample after the experiment showed a pronounced growth of micro-organisms together with the

Table 13. Oxygen consumption and bitumen degradation obtained from Δp measurements and by titration analyses.

From:	Period length	O_2 consumed in period	Rate of oxygen consumption	Equivalent rate of increase in thickness of layer with consumed bitumen
	days	10^{-4} mol	10^{-4} mol/day	10^{-6} cm/day
Δp	32	1.6	0.05	0.5
titration		2.0	0.06	0.7
Δp	16	2.0	0.13	1.4
titration		1.1	0.11	0.8
Δp	46	5.8	0.13	1.5
titration		6.1	0.13	1.5

(This table is presented also in (16) unfortunately with some minor calculation errors.)

crater-like structures typical of leaching of coarse sodium nitrate crystals embedded in bitumen.

With sufficient nutrients present the rate of increase in thickness of the layer with degraded bitumen is about $1.5 \cdot 10^{-6}$ cm/day. This is about a factor 20 higher than the value given for the starved system in Fig. 39. However, the rate is still considerably lower than the leach rates for bituminized sodium nitrate, which typically have values about $2 \cdot 10^{-5}$ cm/day. (Compare, for example, with Fig. 11 in this report.)

Although the thickness of the layer, which actually is influenced by the presence of the micro-organisms, is expected to be considerably larger than the calculated equivalent thickness of a layer with completely consumed bitumen, the low rate of attack seems to indicate that the micro-organisms investigated here would be of relatively minor importance for the long-term behaviour of bituminized sodium nitrate.

3. POLYMER SOLIDIFIED MATERIALS

3.1. Preliminary experiments with production of samples of polystyrene-solidified ion-exchange resin

(Ref. Waste No. 4)

A major difference between bituminized and polymer-solidified ion-exchange resin is that it is posible to incorporate moist ion-exchange resin (~ 50% water) in suitable polymers while the bituminization processes result in more or less dehydrated products.

It would be interesting to investigate the volume stability of ion-exchange resin with from 0 to 50% water solidified in polymer material and compare them to the swelling and leaching behaviour of bituminized resin using methods described in Sections 2.2, 2.8, 2.9 and maybe 2.10. To do this it is necessary to be able to produce (or obtain) the relevant samples.

Some preliminary experiments with the solidification of moist IR-120 cation exchange resin on sodium form in polystyrene have been made. The starting point has been the recipe given for the German STEAG process (p. 1032 in Ref. 17). Unfortunately, the information given in the article is insufficient as a basis for producing material which is exactly similar to the STEAG product. A series of mixtures containing various catalysts, accelerators and dispersion agents was therefore made to see how they influence the gel- and hardening-time of the styrene/divinylbenzene monomer mixture used in the solidification process.

Without moist ion-exchange resin present it is easy to obtain products with reasonable hardening-times at room temperature. With moist resin present, this is much more difficult. It was necessary to heat to 45°-60°C for some days to obtain a hardened product. However, this apparent deviation from the STEAG process could be due to the small sample size used in the ex-

periments. In a full-scale solidification operation temperatures in the range mentioned above could easily be reached in the drums without external heating after the exothermic polymerization process has begun. Too high temperatures which result in boiling of the mixture may even be a problem.

After heating 2 days at 45° and 1 day at 60°C a mixture with th composition shown in Table 14 gave a product with reasonable mechanical properties. However, products containing a small amount of polyester styrene were generally of better appearance and were more easily polymerized.

Later experiments have shown that the maximum content of moist ion-exchange resin probably should be reduced to '50 g per 100 g matrix material.

It is not possible to cast samples with a well-defined upper surface. Either the top layer is not impregnated sufficiently or it is covered by a layer of pure matrix material. This means that the samples must be cut or mounted in some way before they can be used for characterization experiments.

Table 14.

Example of a styrene-based mixture which can be used as solidification matrix for moist ion exchange resin.

Monomer:	Styrene	93.6 g
Crosslinking agent:	Divinylbenzene 50%	1.0 g
Emulgator:	ATLAS Tween 80*	2.7 g
Catalyst:	NORPOL**	1.5 g
Accelerator:	(Cobolt naphtenate)	1.2 g
		100 g
+ IR 120 with 50 % water:	maximum	180 g
	Total:	280 g

* necessary to disperse water droplets from the ion exchange resin; seems to have a softening effect on the polymerized material.

** from the Jotun group, probably solution of azodiisobutanoic acid nitril.

4. CEMENTED WASTE MATERIALS

4.1. The effect of silica-fume additive and of cracked containers on leaching from cemented sodium nitrate (Ref. Waste No. 8)

The primary purpose of the experiments with cemented waste has been to try to develop an experimental methodology which combines the advantage of simple geometry, i.e. leaching from a single plane surface of a sample of semi-infinite thickness inherent in the old IAEA standard method (Hespe) with a reasonable certainty that the leaching takes place only through this surface. The problem is that samples of cemented waste cast in ordinary cylindrical containers may develop fine cracks between the sample and the container wall as the material contracts slightly during the hardening period. The area exposed to water will therefore be somewhat undefined.

In a first attempt to solve the problem, samples were cast in slightly conical cylindrical containers of styrene material. Two samples were cast in clean untreated containers. Two others were cast in the same way but, after the hardening period, were transferred to a new container which had been coated on the inside with hydrophobic material (vaseline). The last two samples were cast on top of approximately 1/2-cm thick layer of foam plastic placed at the bottom of a container coated with vaseline on the walls. After hardening, the samples were simply pressed slightly lower down in the containers. The three types of samples are shown in Fig. 41.

A second purpose of the experiments was to investigate the effect on leach rate of the use of silica fume as an additive to cemented waste.

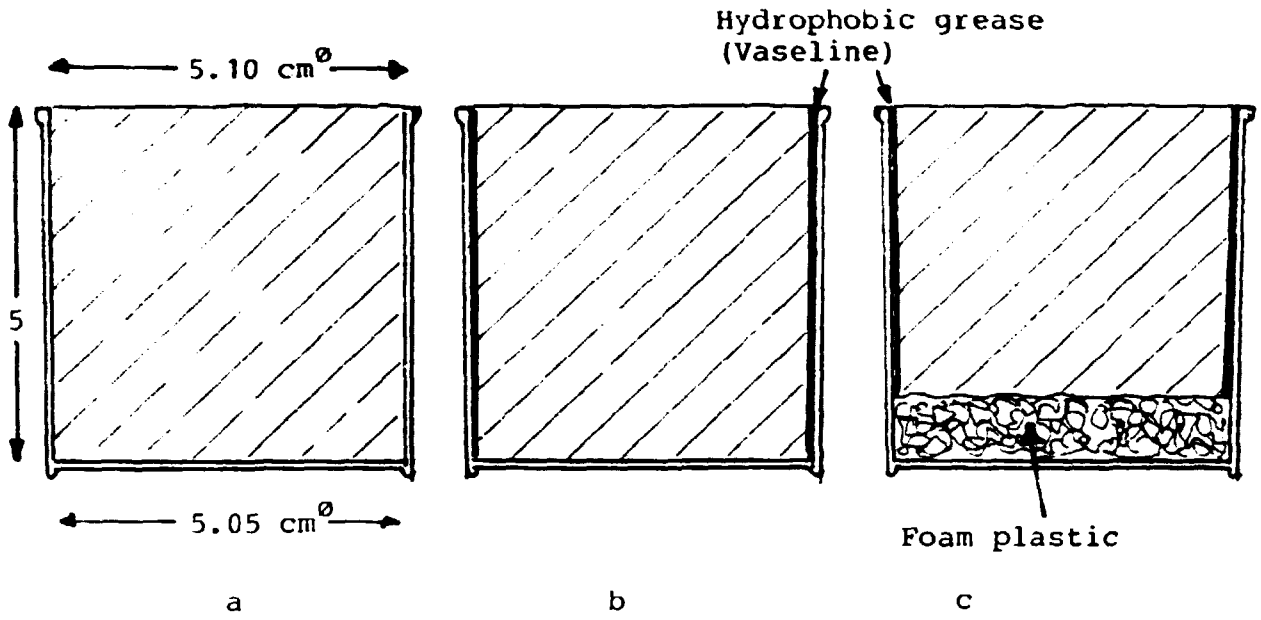

Fig. 41. Three variations of casting of cemented waste in slightly conical containers.

Silica-fume is a waste product from ferro-silicium production. It consists of nearly pure SiO_2 in the form of small spherical particles of diameter about 0.1 µm. Silica-fume is known to give very dense and strong products when added to concrete used for construction purposes. The material is called Densit and is also under investigation as a possible construction material for waste containers (16). The silica-fume particles are much smaller than typical cement particles and will therefore tend to fill the voids between them. This results in decreased porosity and especially in much more narrow channels for migration of dissolved materials in the product. A decrease in leach rate from cemented waste is therefore expected when silica-fume is used as additive.

The compositions of the materials used to cast samples for the experiments have somewhat arbitrarily been selected as given in Table 15. The type of cement used was in both cases low-alkali sulphate-resistant Portland cement (SRPC) supplied by Ålborg Portland Cement Factories. Mighty is a commercially available

Table 15 Composition of two types of cemented waste.

	Cement/waste mixture with silica fume	Cement/waste mixture with sand.
	g per 100 g cement	
SRPC	100	100
Sand: 0-0.25 mm	-	20
Silica fume: ~0.1 μm	20	-
Mighty	1.7	0.2
$NaNO_3$ as simulated waste dissolved in	12	12
Water	25	25
CsCl carrier	0.02	0.02
	uCi/ ml mixture	
^{134}Cs tracer	0.45	0.77

organic superplasticizer. The use of such a material is necessary when making silica-fume-containing cement paste with low water/cement ratio. A water content corresponding to w/c = 0.25 was used in both types of mixture. The content of $NaNO_3$ in the product is approximately as specified but the waste composition is simplified and the matrix material different from the specifications for ref. waste No. 8 (3).

Samples were prepared by casting the mixtures in containers as shown in Fig. 41. The samples were cured in a moist atmosphere for ~ 40 days before the leaching was initiated. Leaching took place in an ordinary plastic beaker covered by a loose-fitting lid. Some absorption of CO_2 must therefore have taken place. The exposed upper area of the samples were A = 20.4 cm^2. The samples were leached by immersion in M = 150 cm^3 deionized water corresponding to a volume-to-surface ratio: M/A = 7.5 cm. Once a week m = 50 cm^3 leach solution was removed from each system for analysis by γ-spectroscopy and replaced by flesh deionized water. This is equal to a mean replacement rate of m/(A•7) = 0.35 cm/day normalized to a sample area of 1 cm^2.

Typical leach curves are shown in Figs. 42 and 43 for two sets of identical samples of cemented sodium nitrate without additives and the silica-fume containing material, respectively.

The equivalent leached thickness of material is shown as a function of the square root of leaching time t days. Effective diffusion coefficients D_e as well as leach rates S_{100} at t = 100 days calculated from linear approximations to the measurements are also indicated in the figure. ($D_e = \pi \cdot \alpha^2/(4 \cdot 24 \cdot 3600)$ cm^2/sec and $S_{100} = \sqrt{\frac{D_e \cdot 24 \cdot 3600}{\pi \cdot 100}} = 16.6\sqrt{D_e}$ cm/day where α is the slope of the linear approximation in $cm \cdot day^{-1/2}$). The reproducibility of the leach rate for undamaged sample containers is seen to be good (the initial part of the curves in Figs. 42 and 43).

A total of six samples of each type of material were measured. As mentioned above, the purpose was to study possible methods of preventing cracks, that may develop between the container and the sample due to contraction of the material during hardening, from influencing the measured leach rates. The D_e and S_{100} values for all the samples are shown in Table 16.

Table 16 Comparison between ^{134}Cs diffusion coefficients and extrapolated leach rates at t=100 days for undamaged samples of cemented sodium nitrate with and without silica-fume additive.

	Cement/$NaNO_3$ mixture with silica-fume			Cement/$NaNO_3$ mixture with sand.		
	No	D_e $10^{-10}\ \frac{cm^2}{sec}$	S_{100} $10^{-4}\ \frac{cm}{day}$	No	D_e $10^{-10}\ \frac{cm^2}{sec}$	S_{100} $10^{-4}\ \frac{cm}{day}$
Slightly conical untreated container.	4A	0.7	1.4	1A	17	6.3
	4B	1.0	1.7	1B	25	8.3
Container with hydrophobic grease on inside.	5A	1.4	2.0	2A	28	8.7
	5B	1.4	2.0	2B	45	11
Container with grease. Sample pressed downward after curing.	6A	1.6	2.1	3A	29	8.9
	6B	3.1	2.9	3B	15	6.3
Mean values:		1.5	2.0		27	8.3

It is seen from the table that use of the silica-fume additive diminishes the leach rate for cesium about a factor 4.

No significant differences between the three types of container treatment can be noted. This may indicate that cracks between the container wall and sample are not very important with these types of systems, but a firm conclusion cannot be drawn.

The slightly conical thin-walled polystyrene containers used for casting the samples turned out to be not strong enough. Some of them cracked spontaneously after some time in water. A curious phenomenon in the form of unexpectedly high leach rates from samples in such cracked containers was first noticed in connection with the experiments with cemented sodium nitrate without additives (see Fig. 42).

A similar phenomenon, although somewhat less pronounced, was demonstrated later also in connection with the silica-fume-containing samples (Fig. 43). In the experiments with this material the containers cracked spontaneously only in two out of six cases. With two other samples the container was cracked intentionally and in the two last cases the container was removed completely. This was also done after some time with one of the samples which had a spontaneously cracked container.

After these operations the leaching was continued using the same sampling schedule and calculating the equivalent leached thickness as if the leaching still took place only through the originally exposed upper surface area of the sample: A = 20.4 cm^2. Some of the leach curves obtained are shown as examples in the right part of Figs. 42 and 43. A large increase in leaching can be observed, but is of course partly due to the increase in exposed sample surface. In all cases the accumulative leaching was highest when the container was removed completely, but the results are not so very different from the results obtained for similar samples with cracked containers. At least in some cases, the difference is due mainly to high leaching in the first sampling period after removing the container.

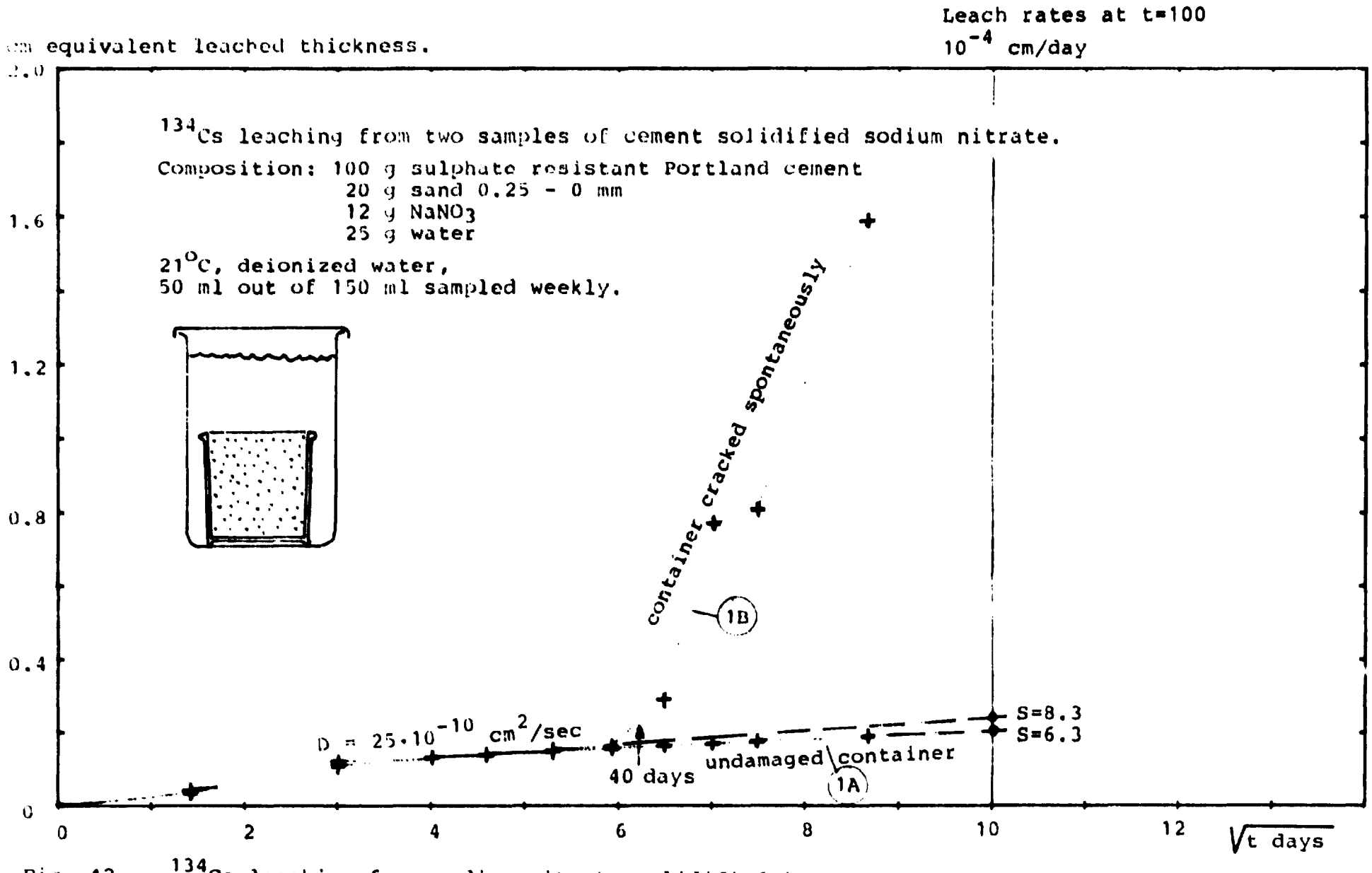

Fig. 42. ^{134}Cs leaching from sodium nitrate solidified in sulphate-resistant Portland cement. One sample container cracked spontaneously after about 40 days.

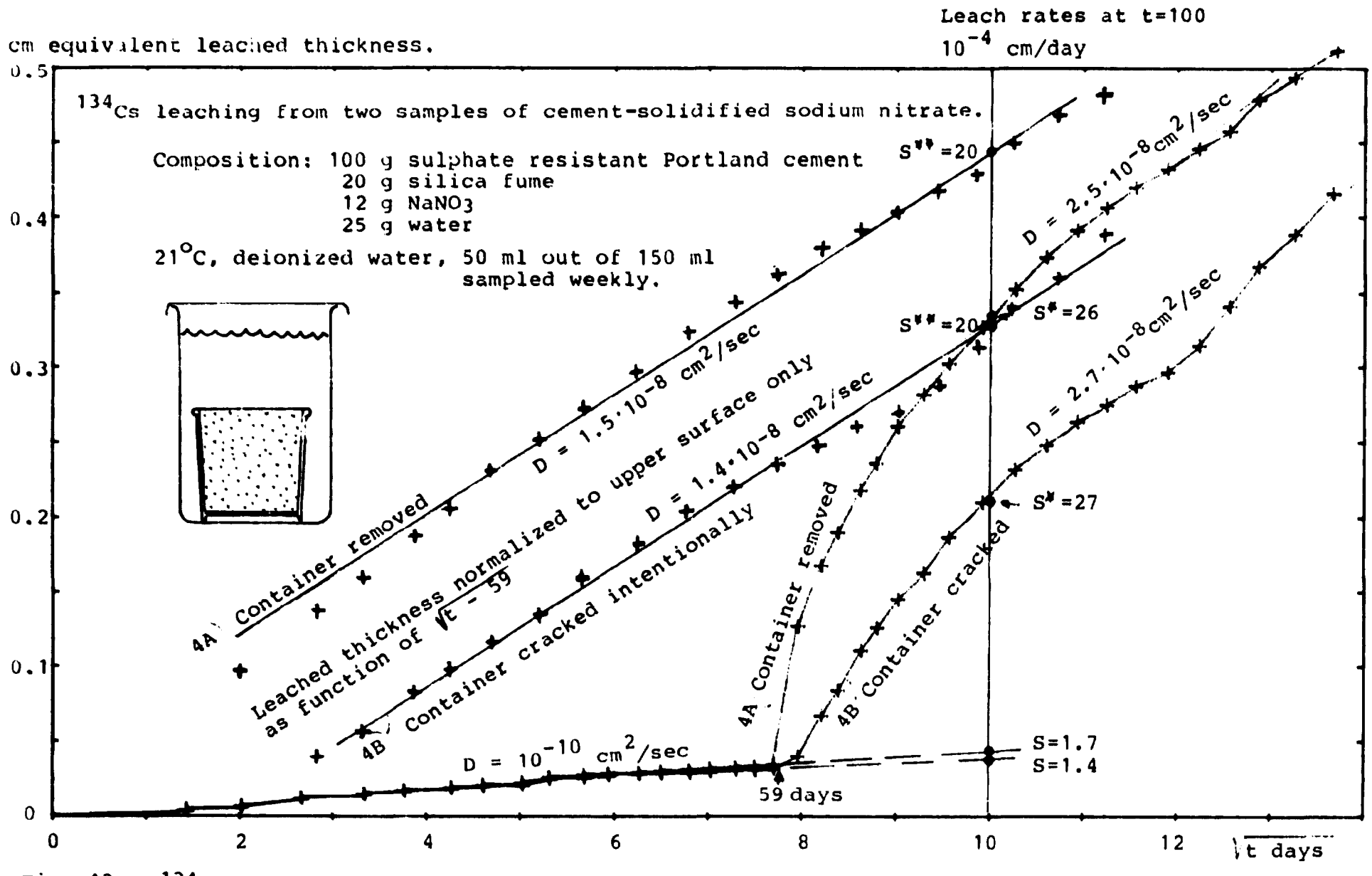

Fig. 43. ^{134}Cs leaching from sodium nitrate solidified in sulphate-resistant Portland cement using silica-fume as additive. The sample containers are cracked or removed after 59 days.

Leach rates S^{*}_{100} at t = 100 days were calculated from the slope of the later parts of the leach curves, but since the $\sqrt{t}$ law is strictly applicable only if diffusion-governed leaching starts from a fresh surface at t = 0, a second leach rate S^{**}_{100} was also calculated from linear approximations to the accumulative leaching as a function of $\sqrt{t-t^{*}}$ where t* is the time at which cracking or removal of the container took place. This transformation results in curves which are quite good approximations to straight lines as illustrated by the not-interconnected crosses in Fig. 42. However, this procedure is not quite correct theoretically either. The real value is probably somewhere between S^{*}_{100} and S^{**}_{100}.

The values of S^{*}_{100} and S^{**}_{100} for all the experiments are given in Table 17 together with the ratios S^{*}_{100}/S_{100} and S^{**}_{100}/S_{100} where S_{100} is the leach rates given in Table 16 for the same samples in undamaged containers.

The exposed surface of a cylindrical sample with height h ≅ diameter d is increased a factor $2 + 4 \cdot \frac{h}{d} = 6$ when a container covering the sides and one end is removed completely. If the leach rates normalized to the same time (for example t = 100 days) is the same for the newly exposed surface as for the originally exposed upper end of the cylinder, then 6 is the value one would expect for the ratio S^{**}_{100}/S_{100}. If only a part of the surface is uncovered the value of S^{**}_{100}/S_{100} should be less than 6. The crack made in the containers was simply a vertical fissure in the wall extending from the rim to the centre of the bottom. Such a cracked container should still provide a good protection of the surface and prevent easy mixing with the main bulk of leach water. This is illustrated by the ability of such a cracked container to keep water for a considerable time.

It is seen from Table 17 that values of S**/S from about 10 to 20 are typical for the SRPC/$NaNO_3$ mixture with sand. When silica-fume was used as additive, values from 4 to 12 were attained when the container was removed, while 3 to 14 seem typical for cracked containers. The conclusion is that leach rates from the side and bottom of cylindrical samples are about 3 times higher

Table 17.

Relative effects of cracking of the container wall or complete removal of the container on ^{134}Cs leach rates calculated as if only the upper surface was exposed.

No	Undamaged container S_{100} 10^{-4}cm/day	Damaged containers: Container condition	after t days	S^{*}_{100} 10^{-4}cm/day	S^{**}_{100} 10^{-4}cm/day	S^{*}/S	S^{**}/S
SRPC/$NaNO_3$ mixture with silica-fume additive							
4A	1.4	cracked intentionally	59	27	20	19	14
4B	1.7	removed	59	26	20	15	12
5A	2.0	cracked intentionally	59	17	7.3	9	3.6
5B	2.0	removed	59	50	21	25	11
6A	2.1	cracked spontaneously	29	18	13	9	6
6B	2.9	cracked spontaneously	21	15	9.5	5	3.2
		container removed	59	31	12.4	11	4
SRPC/$NaNO_3$ mixture with sand.							
1A	6.3	undamaged					
1B	8.3	cracked spontaneously	38	260	180	31	22
2A	8.7	cracked spontaneously	36	190	106	22	12
2B	11	cracked spontaneously	23	250	155	23	14
3A	8.9	cracked spontaneously	49	240	100	27	11
3B	6.3	undamaged					

Note: A value of the ratio $S^{**}/S > 6$ indicates increased leach rate from the vertical surface of the sample compared with the leach rate from the originally exposed upper horizontal surface.

than from the upper end in the case of the unmodified cemented waste product, and about a factor 2 higher in the case of a similar silica-fume-containing material. The cracked containers seem to provide some protection in some cases, but the effect is slight and may be non-existent when the containers are not greased on the inside.

It is surprising that the thin cracks permit such large increases in leaching. A posible explanation could be a density-driven circulation due to the formation of a thin layer with high sodium nitrate concentration and therefore increased density between the container and the sample. It seems reasonable that such a mechanism should be less pronounced in the case of the silica-fume-containing material due to its generally lower leachability.

4.2. Influence of sample geometry on diffusion-controlled leaching

Leaching from a sample of solidified waste material is a function of the material properties and of the geometry of the system. The simplest case of one-dimensional geometry is represented by a sample with constant cross-section which is exposed only through one flat (or two plane-parallel) end-surfaces to well-mixed water or to water contained in saturated columns of porous solid material of the same cross-section as the sample.

Such systems are relatively easy to model mathematically especially if the thickness of the sample is large compared with the equivalent leached thickness L cm, i.e. a semi-infinitely thick sample.

From diffusion theory (Ref. 6, p. 48) it follows that diffusion-governed leaching from a plane sheet with half-thickness a and exposed to water from both sides is given by:

$$\frac{L}{a} = \frac{F_t}{F_\infty} = 2\sqrt{\frac{Dt}{a^2}} \cdot \left(\frac{1}{\sqrt{\pi}} + 2\sum_{n=1}^{\infty} (-1)^n \text{ierfc}\left(n\sqrt{\frac{a^2}{Dt}}\right)\right)$$

and since $\text{ierfc}\left(n \cdot \sqrt{\frac{a^2}{Dt}}\right) \cong 0$ when $4a^2 > Dt$ it follows that

$$L \cong 2\sqrt{\frac{Dt}{\pi}} \text{ when the leached fraction } \frac{F_t}{F_\infty} < \frac{1}{\sqrt{\pi}} = 0.56.$$

A sample can therefore be regarded as infinitely thick when $L <$ ca. $0.6 \cdot a$.

(See also Fig. 44 where the lower curve represents the theoretically leached fraction from a flat sheet exposed to water from both sides.)

The fractional leaching from an infinitely long cylinder with radius a can for the initial part of the leaching be approximated by (Ref. 6, p. 74):

$$\frac{a^2-(a-L)^2}{a^2} = \frac{F_t}{F_\infty} = \frac{4}{\sqrt{\pi}}\sqrt{\frac{Dt}{a^2}} - \frac{Dt}{a^2} - \frac{1}{3\sqrt{\pi}}\frac{Dt}{a^2}\sqrt{\frac{Dt}{a^2}} + \ldots$$

As illustrated by the upper curve in Fig. 44, this relatively complex relationship can be approximated with:

$$\frac{F_t}{F_\infty} \cong 2\sqrt{\frac{Dt}{a^2}} \quad \text{when} \quad \frac{F_t}{F_\infty} < 0.6.$$

This permits the evaluation of D from an ordinary $\sqrt{t}$ plot of the leached fraction of material from a sample of cylindrical geometry.

The correlation between L and $\frac{F_t}{F_\infty}$ is nonlinear:

$$L = a\left(1 - \sqrt{1 - \frac{F_t}{F_\infty}}\right)$$

but if L << a is

$$L \cong \frac{F_t}{F_\infty} \cdot \frac{a}{2} \cong 2 \cdot \sqrt{\frac{Dt}{\pi}}$$

i.e. if the thickness of the leached layer L is small compared with the sample radius a, the usual formula for equivalent leached thickness of a plane sample is applicable also on cylinders (or samples of other shapes).

Unfortunately, this is not the case in leaching experiments with laboratory samples of cemented waste where the thickness of the leached layer often is quite large compared with the dimensions of the sample. This introduces complicated geometrical considerations when leaching takes place from samples exposed to water from all sides.

In the case of cylinders, a practical problem which must be solved to ensure well-defined simple geometry is the elimination of the contribution of leached materials from the end surfaces of the samples. This can be done, at least partially, by selecting a large height-to-diameter ratio for the samples.

With plane samples having one-dimensional geometry the problem is the same as the one well known from column experiments: to prevent the tendency to leakage between the wall of the container and the fill material, or expressed in another way, to secure that the ease of transport of dissolved materials is not significantly higher in possible cracks between container and sample than in the bulk of the sample material. The importance of this possible source of error decreases with increasing exposed area of the sample.

The investigation described in Section 4.1 of the use of slightly conical sample containers as a mean to prevent or suppress the tendency to crack formation between sample and container due to contraction during the hardening period, do not indicate that the problem is serious, but have, on the other hand, not re-

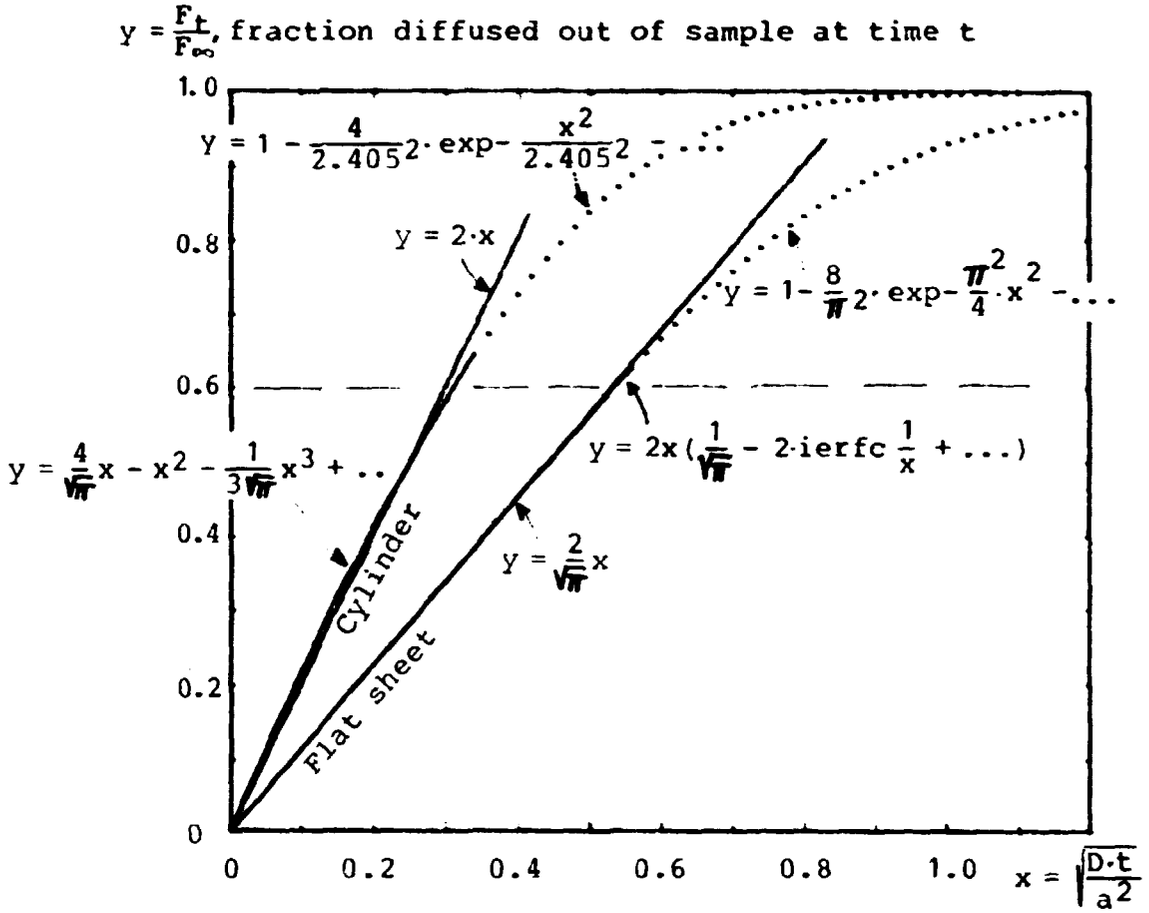

Fig. 44. Theoretical evaluation of leached fractions from a flat sheet or a cylinder compared with approximative formulas for the leached fractions.
The parameter a is the radius of the cylinder or the half thickness of the sheet which is supposed to be exposed to water from both sides.

sulted in a usable experimental method. Another approach to the same problem has therefore been tried:

4.3. An improved leach configuration and leaching from cemented sodium nitrate under various conditions

(Ref. Waste No. 8)

A matrix of experiments was designed and is shown schematically in Fig. 45. In all cases the containers used were ordinary 500 ml wide-necked laboratory bottles of low-density polyethylene (from Kautex, West Germany). Identical sample of cemented waste

were cast in the bottom of most of the containers and cured for one month with the bottles closed by the lid. The composition of the material is the same as given in Table 16 for the cemented waste with sand. Pure sodium nitrate was used as simulated waste.

At the end of the hardening period a rubber ring was placed around the bottle on the outside, just below the surface of the sample, and a tightening ring was placed around the rubber ring so that the relatively soft bottle wall was pressed steadily against the sample sides. This is supposed to eliminate any cracks which may have developed between the sample cylinder and bottle wall.

Deionized water was then introduced as leach water. The containers were sampled on a weekly schedule for the first 84 days. Thereafter, the frequency was decreased to once every fortnight. Various combinations of the water column to surface area: M/A cm and the water replacement ratio m/7A cm/day were tried (see Fig. 45).

Two parallel investigations were run: one with the lids on, that is without or nearly without CO_2-access from the atmosphere, and the other without the lids and therefore with a considerable CO_2 absorption in the alkaline leach water. The two units to the left in the bottom row of the matrix in Fig. 45 are designed to investigate the phenomena associated with the cracked containers described in Section 4.1, and the two units to the right are some first examples of leaching from cemented waste out in water-saturated granulated material, in this case granulated cement paste of the same type as used in the experiments described in Section 2.9.

^{134}Cs in the leach water was analysed by γ-spectroscopy, inactive Na^+ and Ca^{++} was measured by flame photometry and pH and alkalinity was determined by titration. This gives a relatively complete characterization of the chemical system in the leach water. Unfortunately, there are some uncertainties associated with the Na^+ and Ca^{++} analyses which sometimes gave rather er-

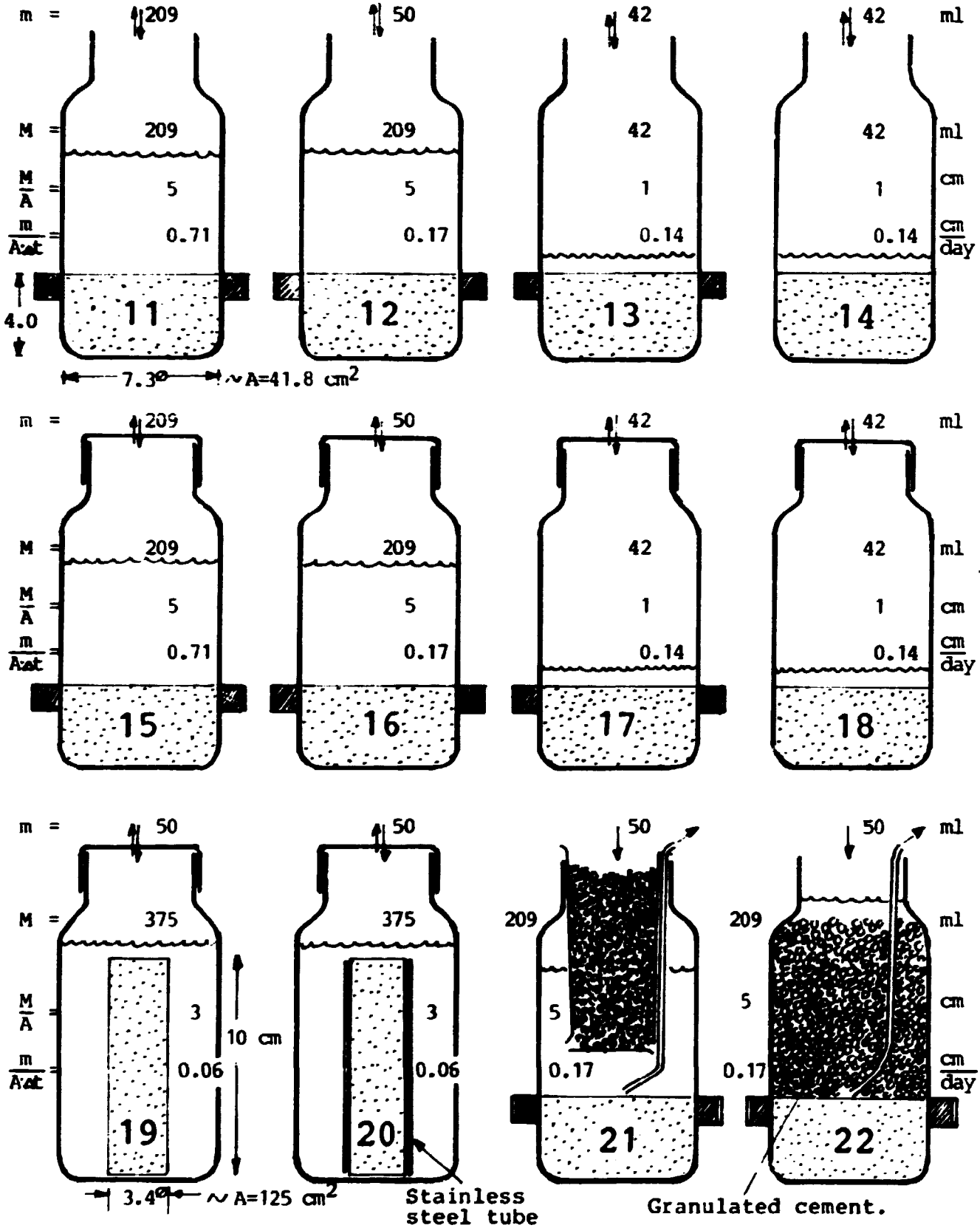

Fig. 45. Leaching from cemented sodium nitrate.
12 different system configurations, sampling procedures and more or less "cement-saturated" water.
With and without access of carbon dioxide from the atmosphere, etc.
Sampling frequency Δt = 7 days in the first period.

ratic results. At least the sodium values are probably systematically too high, maybe up by a factor $1^1/_2$.

Some typical results for the 8 systems in the two upper rows in Fig. 45 are shown in Figs. 46, 47, 48 and 49. Each figure is divided into two parts. The lower part shows the development in the water chemistry based on the above-mentioned analyses. The logarithm to the concentration (mol/l) of Na^+, Ca^{++}, OH^- and, where present, HCO_3^- and CO_3^{--} are given. The NO_3^- concentration was calculated from the concentrations of the other ions and the principle of electro-neutrality, i.e. no other major ions are presumed to be present in the solution. (Small amounts of SO_4^{--} and SiO_4^{----} will be supplied by the cement but are disregarded here.)

The upper part of the figures shows the equivalent leached thickness as a function of $\sqrt{t}$ for Ca^{++} and Na^+ based on the chemical water analyses. $^{134}Cs^+$ leaching based on γ-analyses of the leach water is also shown. The step curve illustrates the schedule used for sampling and water replacement in the various systems. The height of the initial step is M/A, the volume-to-surface ratio, while the height of the successive steps are m/A, the volume-to-surface ratio for the water replacements at each sampling. In most of the experiments the replacements were less than M/A, i.e. only a fraction of the water was replenished at each sampling. $(M + \Sigma m)/A$ cm is a measure for the volume of water which has been available per cm^2 sample surface during the experiment. This value is important in the case of solubility-limited leaching. It varies, in the about half-year long experiments reported here, between ~ 100 cm (Nos. 11 and 15) and 15 cm. This corresponds to a water flow between 200 and 30 cm^3/cm^2 exposed surface per year, which is rather large compared with reasonable repository conditions.

The results for all the experiments are summarized in Table 18 in the form of diffusion coefficients calculated from the slopes of linear approximations to the leach curves using the theory given in Section 4.2. The values in the table are discussed in the following on the background of examples of the experimental

results shown in more detail in Figs. 46-51.

Figure 46 shows the results for system No. 11 which together with No. 15 had the highest degree of water change. Sample No. 11 is from the series with CO_2 access, but from the plot of the water composition it is seen that it took about a month before appreciable CO_3^{--} and HCO_3^- could be measured by titration of the leach water. The explanation is probably that the high Ca^{++} and OH^- concentrations in the beginning of the experiment only permit a low CO_3^{--} concentration due to $CaCO_3$ precipitation. The solubility product of $CaCO_3$ is: $[Ca^{++}][CO_3^{--}] = 0.93 \cdot 10^{-8}$ at 20°C, which means that a Ca^{++} concentration of 10^{-3} corresponds to a CO_3^{--} concentration of about 10^{-5} Mol/l. This is below the sensitivity of the titration.

The accumulative leached thickness at the end of the experiment was about 0.9 cm for Na^+, 0.4 cm for $^{134}Cs^+$ and (the bottom, right scale of the upper figure) only 0.002 cm for Ca^{++} due to Ca solubility limitations caused by the presence of CO_2.

Figure 47 shows the results for system No. 12 which is similar to No. 11 except that only part of the water is removed and replaced at each sampling, i.e. the "water-flow rate" is about a factor 4 lower. This seems to diminish the leaching of Na^+ and $^{134}Cs^+$ with about a factor 1.5 to 2, while Ca leaching is diminished even further. The sodium nitrate concentration in the water is, as expected, higher than in the case of sample No. 11 while the OH^- concentration decreases more rapidly. This could be caused by the relatively thick layer of pure water through which the CO_2 has to diffuse after each sampling of system No. 11.

Figure 48 shows the results for system No. 13 which also is from the series with CO_2 access, but where the thickness of the water layer present in the system is reduced to only 1/5 of the value in systems Nos. 11 and 12. The total amount of water which has passed through the system is slightly less than with No. 12 (the step curve). This results in a further decrease in Na^+ and $^{134}Cs^+$ leaching and in a very low leaching of Ca^{++} corresponding

Table 18. Diffusion coefficents and leach rates at t=100 days for Na and Cs leaching from cemented sodium nitrate calculated from the slope of liniar approximations to the accumulative leached materials plotted against $\sqrt{t}$.

The leach rates given for Ca are mean values corresponding to the leached material in the period from about 10 to 100 days.

No.	D 10^{-9} cm^2/sec	S_{100} 10^{-4} cm/day	D 10^{-9} cm^2/sec	S_{100} 10^{-4} cm/day	D 10^{-9} cm^2/sec	S_{100} 10^{-4} cm/day	D 10^{-9} cm^2/sec	S_{100} 10^{-4} cm/day
	11		12		13		14	
Na	14	20	7.4	14	2.9	9.0	6.0	13
Cs	1.7	6.8	0.38	3.2	1.0	5.4	3.0	9.1
Ca		0.04		0.01		0.01		0.01
	15		16		17		18	
Na	14	20	15	20	5.7	13	7.8	15
Cs	1.7	6.8	1.5	6.4	1.9	7.1	5.0	12
Ca		2.0		1.3		1.1		1.2
	19 cylinder		20 cylinder		21		22	
Na	10	-	14	-	7.4	14	7.1	14
Cs	4.7	-	4.4	-	0.56	3.9	0.78	4.7
Ca	-	0.4	-	0.4	-	-	-	-

to an accumulative equivalent leached thickness of only about 0.0001 cm. In this case CO_3^{--} and HCO_3^- were present already at the first sampling. In continuation of the argument given above the reason could be that the smaller thickness of the water layer promote the contact between CO_2 from the atmosphere and OH^- from the cement sample.

Similar results were obtained with system No. 14 which is identical to No. 13 except that the tightening ring was omitted. The water chemistry was almost exactly the same, however, there was a slight but systematic increase in Na^+ as well as $^{134}Cs^+$ leaching. This indicates that the use of the rubber- and tightening rings is not superfluous: Cracks between the wall of the polyethylene bottle and the sample can give a contribution to the leached material corresponding to a false increase in leach rate of a factor 1.5 to 2 for the systems investigated here. (Compare the diffusion coefficients and leach rates for samples Nos. 13 and 14 in Table 18.)

Figure 49 shows the measurements for system No. 17 which is identical to system No. 13, but from the series which were leached in bottles with the lid on. A comparison with Fig. 48 shows the differences in water chemistry which could be expected from the absence of CO_2: Ca^{++} and OH^- concentrations about 10^{-2} Mol/l in reasonable agreement with the solubility product for $Ca(OH)_2$: $[Ca^{++}][OH^-]^2 = 6 \cdot 10^{-6}$. The slight decrease in Ca^{++} and OH^- concentrations during the experiment could be caused by dilution and decreasing leach rates for $Ca(OH)_2$, but another possible explanation is slow diffusion of CO_2 through the bottle wall in amounts sufficient to influence the Ca leaching. Assuming that the permeability for CO_2 in low-density polyethylene is $280 \cdot 10^{-10}$ N $cm^3/(sec \cdot cm^2 \cdot cm\ Hg/mm)$ an amount of about 10^{-4} mol CO_2 will diffuse into the systems in a half-year if the bottles were kept in pure atmospheric air with 0.033% CO_2. The amount of CO_2 introduced during sampling could be of the same magnitude. This is rather insignificant, but begins to be of importance if increased a factor 10 which easily could happen in impure indoor air.

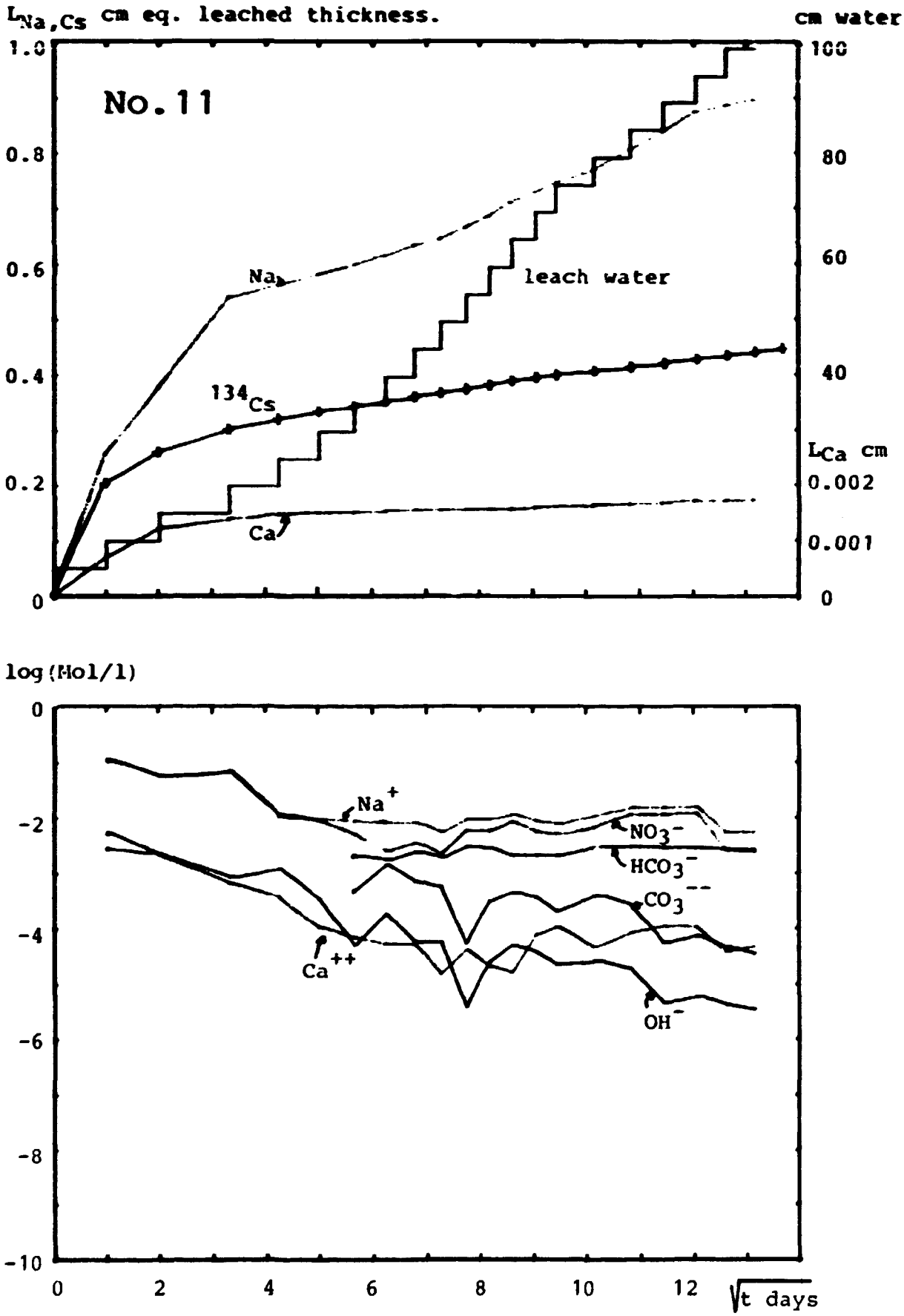

Fig. 46. Leaching and water chemistry for sample No. 11. With access of CO_2. Thick water-layer changed completely at each sampling.

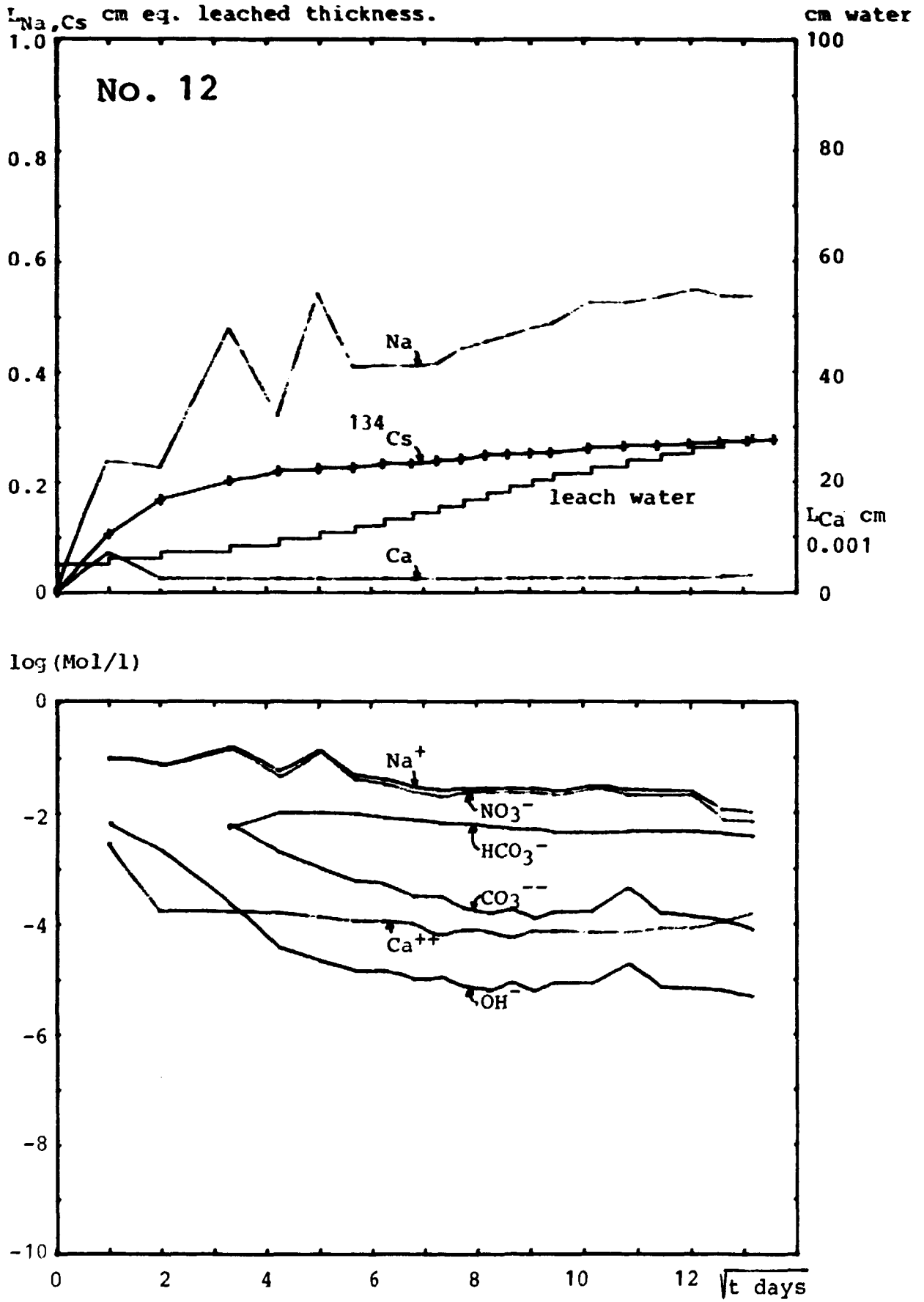

Fig. 47. Leaching and water chemistry for system No. 12. With access of CO_2. Thick water-layer, 1/8 changed at each sampling.

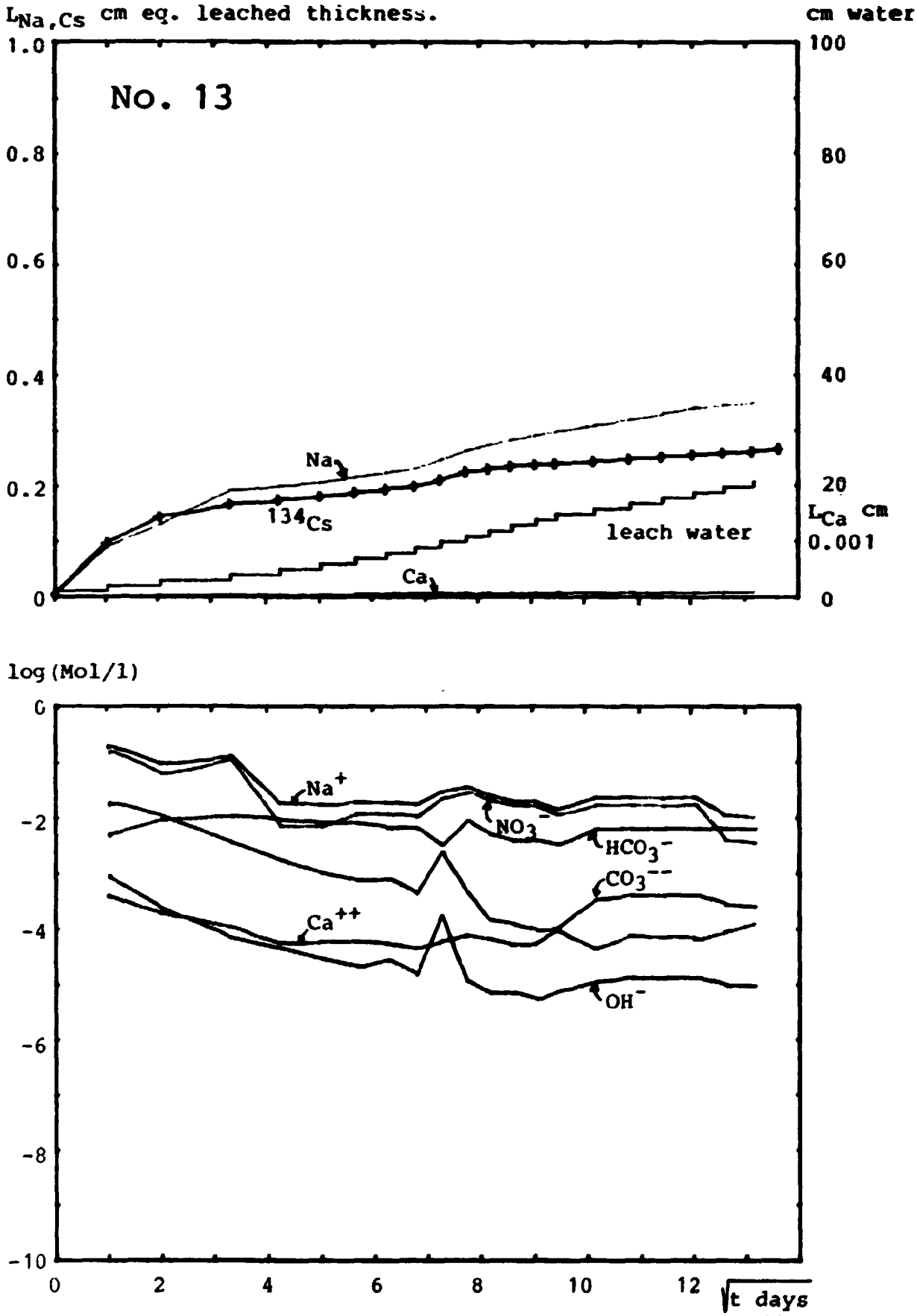

Fig. 48. Leaching and water chemistry for system No. 13. With access of CO_2. Thick water-layer changed completely at each sampling.

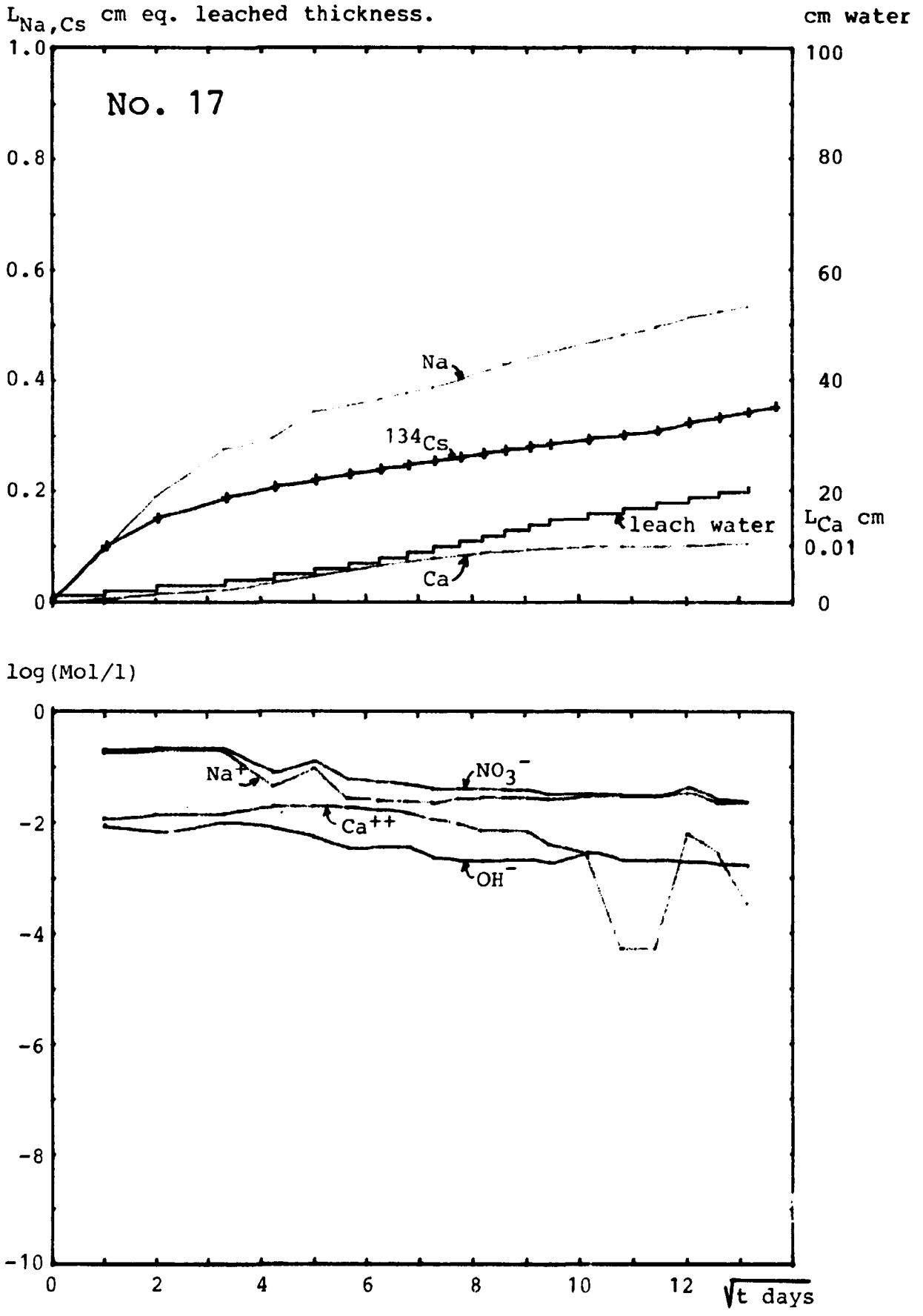

Fig. 49. Leaching and water chemistry for system No. 17. No access of CO_2, otherwise identical to No. 13.

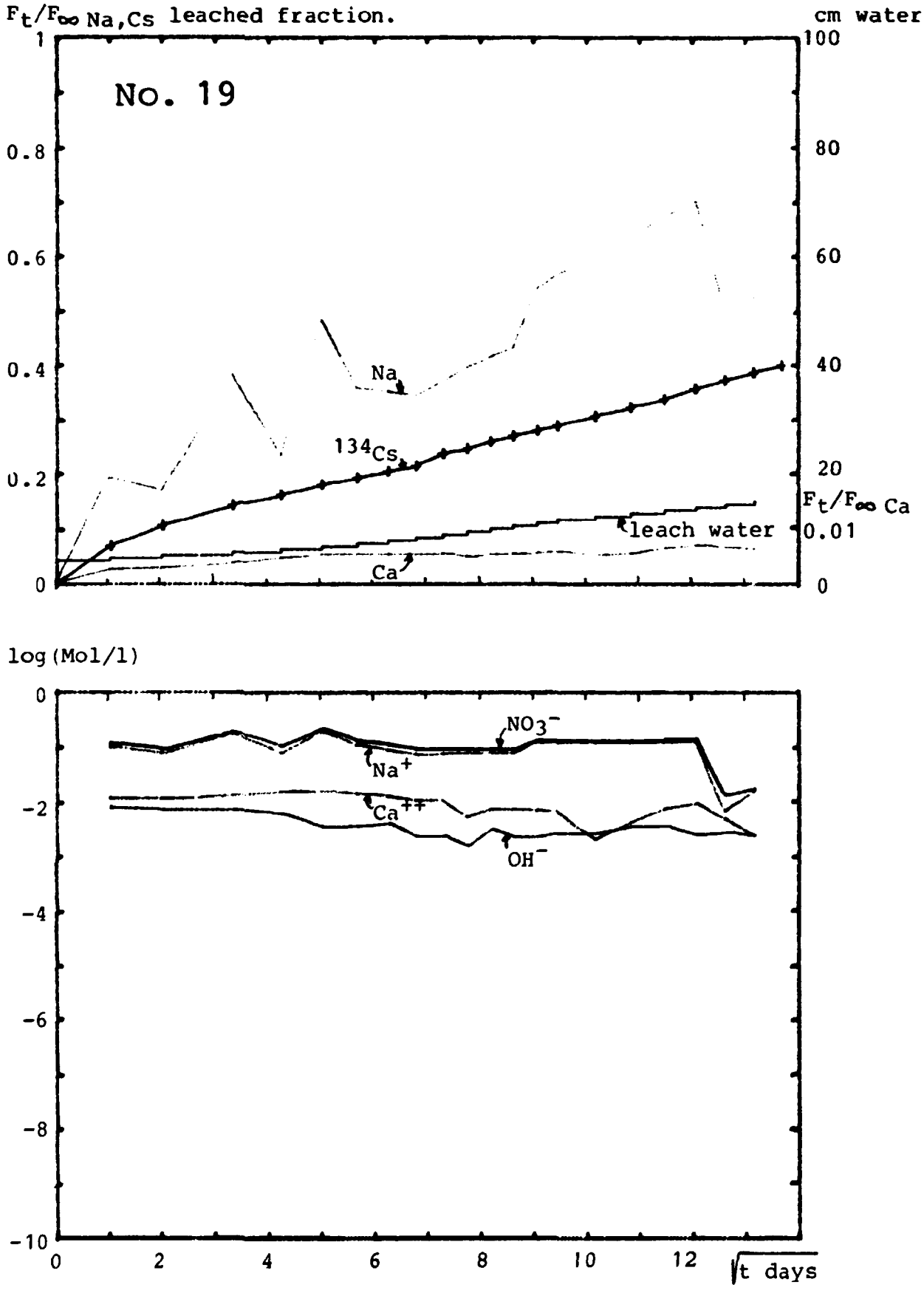

Fig. 50. Fractional leaching and water chemistry for system No. 19. Cylindrical geometry. No access of CO_2.

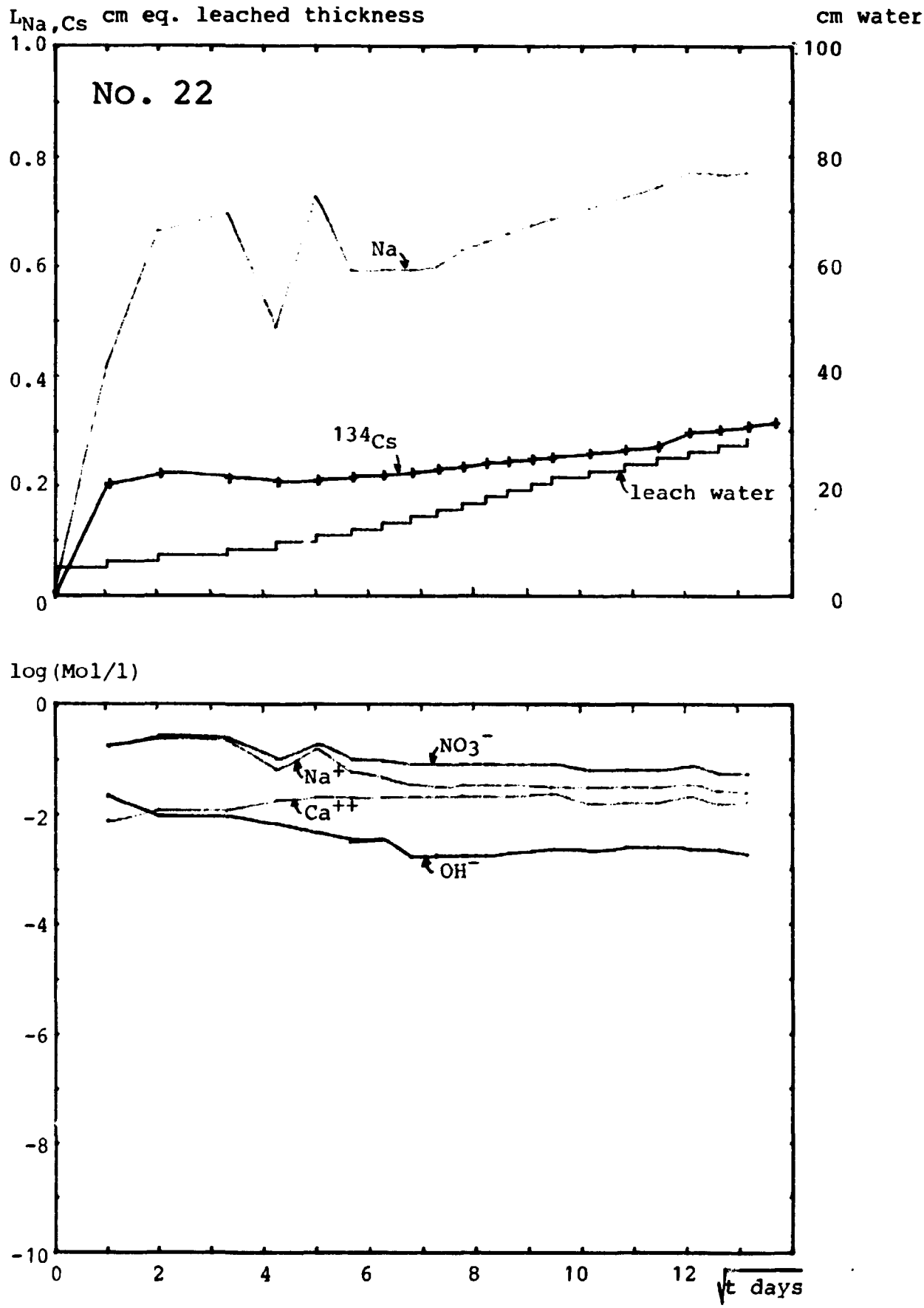

Fig. 51. Leaching and water chemistry for system No. 22. Leaching in contact with granulated cement paste. No access of CO_2.

The sodium concentration in system No. 17 is somewhat higher than for system No. 13 corresponding to a slightly higher leach rate in the system with no CO_2.

The same tendencies are observed for system No. 18 which also shows the slight false increase in leach rate caused by the absence of the rubber- and tightening ring. (Compare the values for samples Nos. 13, 14, 17 and 18 in Table 18.)

The decreases in leach rates of Na^+ and Cs^+ caused by the presence of CO_2 are relatively small, up to a factor 2. It tends to be absent in the systems with large water volumes. (Compare the values for samples Nos. 11, 12, 15 and 16 in Table 18.)

The influence of CO_2 on Ca leaching is, as expected, much larger. The leach rate is governed by solubility limitations and therefore also much dependent on the water flow through the system. Values of the leach rates for Ca at 100 days corresponding to sampling frequency once a week have been estimated and are given in Table 18. Diffusion coefficients cannot be calculated in these solubility-limited cases.

When CO_2 is absent the Ca leach rates are not more than a factor 3 to 10 lower than the Cs leach rates for the same systems. Furthermore, if it is taken into account that only about 30% of the calcium in hardened cement is present as easily soluble $Ca(OH)_2$, even this difference tends to disappear. This is of course important for understanding leaching behaviour in cemented waste, as it indicates that the layer through which the diffusion of Cs^+ and other radioactive species are taking place may consist of hydrated calcium silicates nearly depleted in $Ca(OH)_2$ or in other ways is likely to undergo considerable change due to Ca leaching. The condition for simple diffusion-governed behaviour of the radioactive species, that the properties of the already leached layer are unchanging with time, is therefore not fulfilled. This makes extrapolation of the otherwise quite nice linear dependence of Cs leaching on $\sqrt{t}$ a somewhat dubious procedure.

Due to the similarities in chemistry between Ca and Sr and the quite considerable content of inactive Sr present in the cement (about 0.1% in SRPC), it is probable that the presence of CO_2 also will have a large influence on Sr leaching. This was not investigated in connection with the experiments reported here but has been confirmed by later experiments (12).

Figure 50 shows the measurements for system No. 19 with a cylindrical sample. Almost exactly identical results were obtained for system No. 20 with a similar cylindrical sample placed inside a stainless steel tube with a gap of approximately 0.2 mm between the tube and the cylinder surface. The water chemistry is similar to the other systems without CO_2 access. In this case the fraction of leached material is shown in the upper figure since the concept of an equivalent leached layer is not useable with these relatively thin cylinders. Diffusion coefficients were calculated from these plots according to the theory given in Section 4.2. The values obtained for sodium are approximately the same as for the flat sample No. 16 which was leached under approximately the same conditions. The values for Cs is about a factor 3 higher for the cylinders.

The similarity between the results for systems Nos. 19 and 20 indicates that there indeed is a density-driven mechanism which ensures the circulation of leach water through narrow gaps between sample and container (when the gap is open in both ends). This was used as explanation of the phenomena described in Section 4.1. The increase in diffusion rate for Cs compared with the value for sample 16 is also in agreement with the postulated increased leach rates from vertical compared with horizontal surfaces. However, this is contradicted by the similarity of the diffusion coefficients for sodium. This discrepancy of the behaviour of Cs and Na cannot be explained on the basis of the present experiments.

Figure 51 shows the results for sample No. 22 leached in contact with water-saturated granulated concrete. Similar results were obtained for system No. 21 with no direct contact between sample and the granulated material. There was access of CO_2 to the top

of the granulated cement, but carbon dioxide is not expected to have penetrated to the bottom influencing the chemistry of the leach water near the sample. The concentration of OH^- does also in this case show a decreasing tendency but now associated with an increase in Ca^{++} concentration corresponding to the $Ca(OH)_2$ solubility product. The behaviour is probably mainly due to leaching and dilution of the calcium hydroxide originally present in the granulated cement. The Cs as well as the Na leach curves show a large initial pulse. This is probably due to dissolution of a Cs- and $NaNO_3$-rich surface layer which can be expected to be present on the upper surface of a flat sample cast in the manner used here. The pulse is similar in size to the initial leaching in system No. 11. It is nearly absent in the case of the cylindrical samples which were cast with only a very small free horizontal surface. Later in experiments with Nos. 21 and 22 the Cs leaching decreased to the lowest values obtained in this series of experiments. However, this may be due to absorption on the granulated cement. This was not investigated. Ca leaching cannot be measured in combined systems of this type.

In general, the following can be concluded for the series of experiments with leaching from cemented sodium nitrate:

- The diffusion coefficient for Cs leaching from this material lies in the range from 10^{-9} to $5 \cdot 10^{-9}$ cm^2/sec corresponding to leach rates at 100 days from $0.5 \cdot 10^{-4}$ to 10^{-4} cm/day.

- The sodium leach rates are somewhat higher (even if the possible systematic error in sodium analyses is taken into account).

- The calcium leach rate is lower and determined by solubility limitations. It is therefore dependent on the flow rate through the system.

- When the system is in contact with CO_2 (and the pH remains high) the Ca leach rates are sharply reduced due to precipitation of calcium carbonate.

- Cs and Na leach rates are decreased slightly by the presence of CO_2 and by decreasing flow rates, but the effects are of no practical importance at least with the flow rates investigated here.

- There is some, but no conclusive, evidence for a slightly increased leach rate from vertical compared with horizontal surfaces. Again the phenomenon is probably without any practical importance for safety analyses. The possible creation of circulation systems driven by density differences in solutions in gaps between concrete and container could, however, be of considerable importance.

- The leaching system using L.D. polyethylene bottles and a rubber ring surrounded by a steel tightening ring seems to diminish the influence of cracks between container wall and sample.

4.4. Leaching from cemented sodium sulphate

(Ref. Waste No. 1)

Samples of a material made from Italian Portland cement supplied by Nucleco, Casaccia, Italy, and sodium sulphate according to recommendations for reference waste No. 1 (3) were cast in the bottom of polyethylene bottles. After hardening a rubber ring and a tightening ring were placed around each bottle. The system is the same as used for the studies of leaching from cemented sodium nitrate. Experiments using various schedules for water change have been made. Some of the systems were with CO_2 access, some without. A set of additional samples was prepared and placed for half a year under various storage conditions: dry, in water, in various salt solutions, at 20 or 40°C. Experiments to investigate whether such treatments result in changes in the leaching behaviour are in progress. Details of

the total experiment are reported in (12), but an example of the results is shown in Fig. 52.

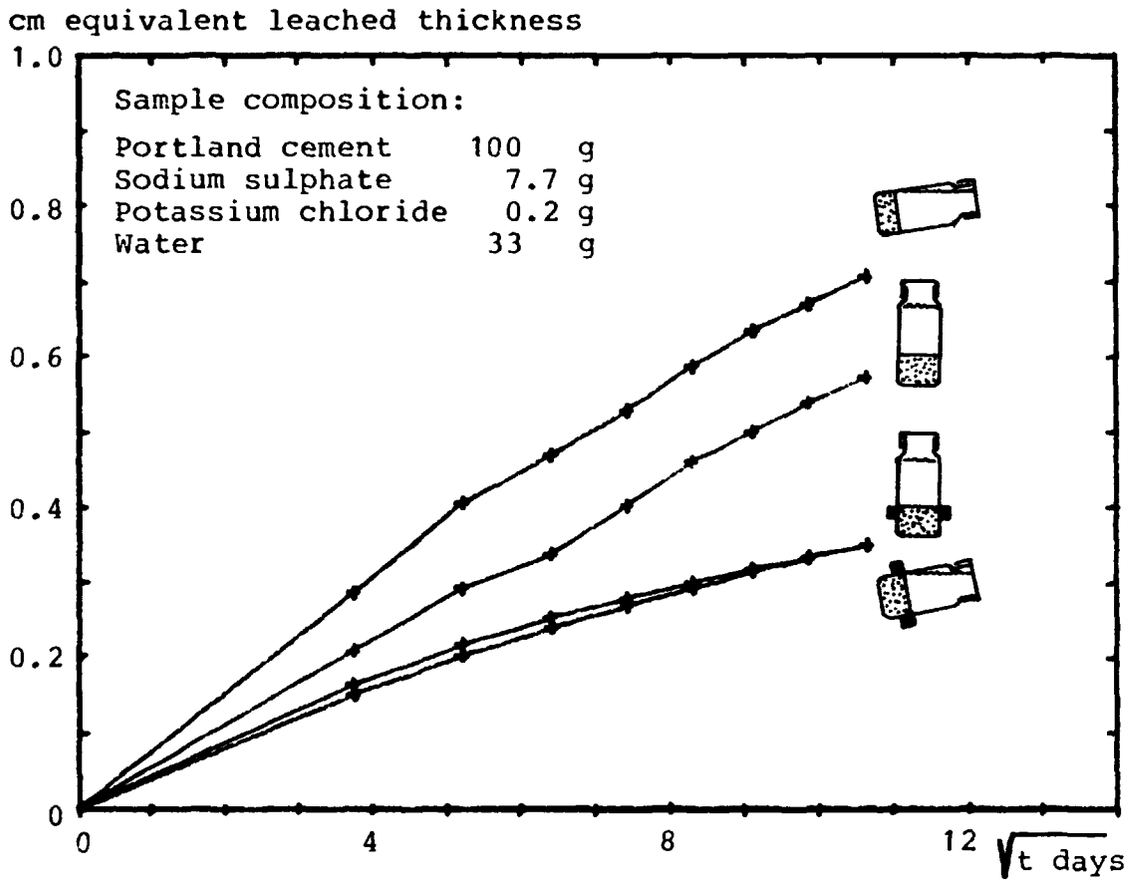

Fig. 52. Accumulative ^{134}Cs leaching from cemented sodium sulphate for two systems with tightening rings and two without. The exposed surfaces are either in a horizontal or a nearly vertical position. The equivalent leached thicknesses are plotted as if the leaching took place only through the freely exposed end-surfaces of the samples.

The curves illustrate the effect of the rubber- and tightening rings on leaching of ^{134}Cs from 4 identical samples in systems without CO_2 access. Two of the samples were placed with the exposed surface in a horizontal position and two with the surface in a nearly vertical position. It is seen that the two systems with rings show approximately the same leaching behaviour. The effective diffusion coefficient is about $6 \cdot 10^{-9}$ cm^2/sec and the corresponding leach rate at 100 days is ~ 10^{-4} cm/day. The leaching from the systems without rings seems to be higher due to some leaching of ^{134}Cs also from the sides of the samples.

As expected, the contribution is greatest in the case where the free surface is placed in a nearly vertical position. In this case it is possible to get circulation driven by density differences in the gap between the bottle wall and the sample. This is in general agreement with the conclusions made for the cemented sodium nitrate systems in Section 4.3. In the case of the sodium sulphate samples no increased Cs leaching from vertical surfaces could be observed for the samples with rings.

5. REFERENCES

1. Comparative Study of Test Method for Bituminized and Other Low- and Medium-Level Solidified Waste Materials. Contract WAS 235 DK (G). Progress report covering the period 1/1-30/6 1981.
2. Ibid. Progress report covering the period 1/7-1981 to 1/7-1982.
3. SAMBEL, R.A.J., ed. Characterization of Low- and Medium-Level Radioactive Waste Forms. CEC Joint Annual Report for 1981. EUR 8663 EN.
4. VEJMELKA, P., ed. Characterization of Low- and Medium-Level Radioactive Waste Forms. CEC Joint Annual Report for 1982. In preparation.
5. BRODERSEN, K., A general survey over aging and other phenomena influencing long-term behaviour of bituminized radioactive waste. Safety Research in Energy Production. Nordic Projects. NKA-AVF(82)208. Risø July 1982. (Draft)
6. J. CRANK. The Mathematics of Diffusion. Second edition. Clarendon Press, Oxford. 1975.
7. H. KRAUSE, ed. Jahresbericht 1976, Abteilung Behandlung radioaktiver Abfälle. Kernforschungszentrum Karlsruhe. KfK 2519, Dec. 1977.
8. W. KLUGER, R. KÖSTER, H. KRAUSE. Übersicht über Producteigenschaften von mit Bitumen verfestigter Abfallkonzentraten aus Wideraufarbeitung, Kernforschungseinrichtungen und Kernkraftwerken. KfK 2796, März 1979.
9. De BATIST, R. et al. Characterization of bituminized intermediate level Eurochemic waste. Contribution to: CEC Seminar on Testing, Evaluation and Shallow Land Burial of Low and Medium Radioactive Waste Forms. Geel, Sept. 1983.
10. LARSEN, I., Incorporation in Bitumen of Low-Level Radioactive Waste-Water Evaporator Concentrate at the Danish Atomic Energy Commission Research Establishment Risø. Risø Report No. 276. October 1972.

11. BRODERSEN, K., VINTHER, A. Leaching of Bituminized Radioactive Cation-Exchange Resin. Enlarged Nordic Cooperative Program on Nuclear Safety. AO-A:1 System and risk analysis of reactor waste. NKA/AO(80)46. Risø, Jan. 1981.
12. BRODERSEN, K. et al. Comparative Study of Test Methods for Conditioned Low- and Medium-Level Radioactive Waste. Contract WAS-303-83-13-DK (G). Progress report covering the period 1/1-31/12 1983. In preparation.
13. AITTOLA, J.P. et al. Swelling of Bituminized Ion-Exchange Resins. A summary report based on data from Nordic research for the period 1978-1982. KBS/NKA, Studsvik arbetsrapport NW-82/269. Draft. Dec. 1982.
14. BRODERSEN, K. et al. Contraction, Density and Viscosity Changes of Bitumen and Bituminized Waste Products during Dry Storage. Safety Research in Energy Production, Nordic Projects. Risø contribution to AVF2: Long-Term Behaviour of Waste Products. In preparation.
15. BRODERSEN, K. Mikroorganismers betydning for udludning af aktivitet fra bitumenindstøbt radioaktivt affald. En litteratur-gennemgang og nogle generelle betragtninger. Udvidet Nordisk samarbejde på Kernesikkerhedsområdet. NKA-AO(79) 19 A. Risø Maj 1979.
16. MOSE PEDERSEN, B., ABDELLAH, A. Microbial Degradation of Bitumen Used for Conditioning of Low- and Medium-Level Radioactive Waste. Contribution to: CEC Seminar on Testing, Evaluation and Shallow Land Burial of Low and Medium Radioactive Waste Forms. Geel, Sept. 1983.
17. Einbettung von Reaktorbetriebsabfällen in Kunstoff. STEAG Kernenergie GmbH. (EUR 6418 DE). Eur. App. Res. Rep. Vol. 1 Number 4, 1974, p. 993.
18. BRODERSEN, K., LARSEN, V.V. et al. Development of Waste Unit for Use in Shallow Land Burial. Contract 195-71-6 WASDK. Final Report for period 1/1-1981 to 30/6-1983. In preparation.

APPENDIX 1.

Calculation model for the presentation of experimental results concerning water uptake, water penetration, leaching of soluble salts and swelling of bituminized waste materials.

The water uptake and swelling curves presented in various figures in the report have been calculated from weight increases and other measurements on the samples and the solutions they were immersed in. Relatively simple models suitable for the various systems were used. In the following a more general model is developed and discussed.

The system is shown schematically in Fig. A1.

It consists of a sample of bituminized (or polymer solidified) waste material cast in a container, so that only one plane surface with area A cm^2 is exposed, when the sample is placed in water. The thickness of the sample before exposure is u_o cm.

(The model is also valid for samples with two exposed plane-parallel surfaces with a combined area A cm^2 and a thickness u_o = the half-thickness of the sample.)

The material is supposed to consist of a bituminized mixture of an insoluble material: i (for example ion-exchange resin) and a soluble salt: a (for example sodium sulphate or nitrate.) The insoluble material as well as the salt is supposed to be able to form solid hydrates with well-defined water contents. Cases where one of the materials do not form hydrate or is absent from the bituminized product can also be calculated by the model. Examples are pure bituminized ion-exchange resin, pure bituminized sodium nitrate etc.

On the macroscopic scale bituminized (or polymer solidified) waste materials are homogeneous mixtures of salt crystals and particles of insoluble material in bitumen, but to visualize the system the three solid phases are shown as separate layers of dry material in Fig. A1. A fourth layer representing the

total water content in the sample before and after exposure to water is also shown in the figure. Some or the whole amount will, in practice, be present in form of hydrated solid materials.

The water uptake is supposed to give rise to swelling of the sample from thickness u_o to u_o+S_n cm. The swelling S_n may be reduced or can even be negative due to dissolution of the soluble salt or contraction of the insoluble material or the bitumen.

Practical preparation of samples is described in section 2.2. of the main report. The mathematical treatment developed in the following can of course also be used on other types of samples with suitable geometry, provided the necessary measurements are made: Weight in air, weight immersed in the solution and compositional (and density) changes of the solution.

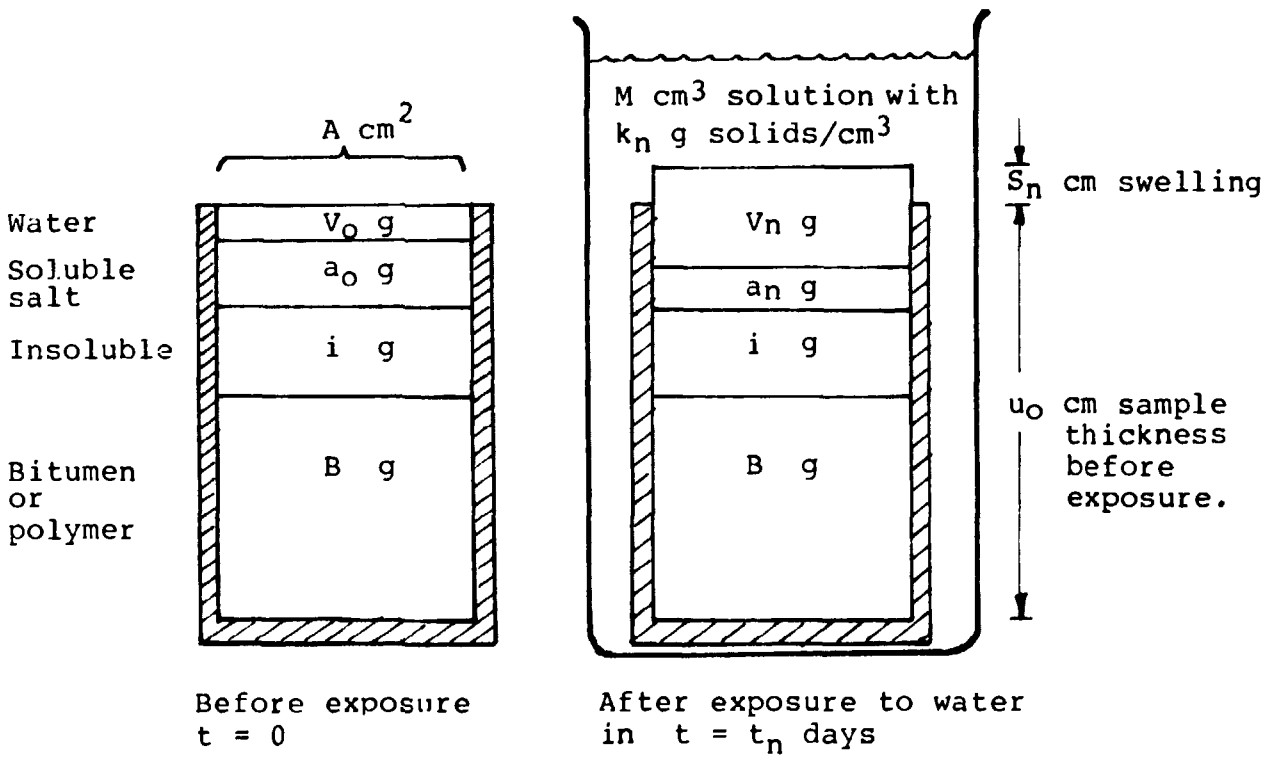

Fig. A1. Schematic presentation of a sample of bituminized material before and after water uptake.

Initial situation: $t = 0$

Weight of sample: W_o g inclusive weight of container: W_r g.

Weight immersed in solution with density ρ_{Vo} g/cm^3: W_{Vo} g.

Volume inclusive container: $(W_o - W_{Vo})/\rho_{Vo}$ cm^3

Mass-balance:

$$B + i + a_o + V_o = W_o - W_r \qquad \text{(I)}$$

The values in this equation represents the weight fractions of the various components in the sample at the beginning of the experiment. They are all supposed to be known.

Water system:

The sample is placed in a beaker in M_n cm^3 in water or in a solution with known composition containing k_n g dissolved material/cm^3.

At each sampling of the system at $t = t_n$ days a constant volume of solution, m cm^3 is supposed to be removed for analysis and replaced by water or fresh solution.

The total volume of solution, M_n cm^3 will be somewhat variable due to swelling of the sample and due to variations in the density ρ_{Vn} of the solution.

M_n is determined by adding pure water to the system as substitute for evaporated water until constant weight of the total system: W_{total} g. This gives:

$$M_n = (W_{total} - W_{\substack{beaker\\empty}} - W_n)/\rho_{Vn} \quad \text{cm}^3 \qquad \text{(II)}$$

The density of the solution ρ_{Vn} must be determined experimentally (this is most easily done by weighing a known piece of stainless steel or other stable material immersed in the solution), or it can be calculated if the variation of density with concentration k_n g/cm^3 of solute in the water is known. In precision work it is important to maintain constant temperature of sample as well as solution during the weight measurements.

Water uptake and leaching.

At sampling No. n after $t = t_n$ days in water is:

The weight of sample + container: W_n g

The weight of sample + container immersed in the solution: W_{Vn} g

The concentration of the solution: k_n g/cm^3

From the relations:

$$W_n - W_r = B + i + a_n + V_n$$

$$W_o - W_r = B + i + a_n + M_n \cdot k_n - M_o \cdot k_o + \sum_{n}^{n-1} m(k_n - k_o)$$

which follow from the mass-balances over the system one gets an expression for the amount of water taken up in the sample:

$$V_n = W_n - W_o + M_n \cdot k_n - M_o \cdot k_o + \sum_{n}^{n-1} m(k_n - k_o) \qquad \text{(III)}$$

where the summation represents the amount of salt removed (or added) during previous samplings of the system.

In combination with (I) the expression gives the obvious relationsship for the leached amount of salt:

$$a_o - a_n = M_n \cdot k_n - M_o \cdot k_o + \sum_{n}^{n-1} m(k_n - k_o) \qquad \text{(IV)}$$

The values for M_n is obtained from (II).

It has been assumed here, that the soluble embedded salt, a, and the solute in the solution is the same material. This simplification facilitates the mathematical interpretation, which rapidly gets rather complex with more than one type of salt present. However, it may in some cases be an impermissible oversimplification.

Swelling measurements.

The swelling of the sample, S_n cm, can be obtained directly from the weights of the sample+container measured in air: W_n g and immersed in the solution: W_{Vn} g if it is assumed that the swelling takes place uniformly distributed over the exposed area A cm^2. The increase in volume of the sample is then $S_n \cdot A$ cm^3 and it follows from a simple application of Archimede's principle that:

$$S_n = \frac{(W_n - W_{Vn})}{A \cdot \rho_{Vn}} - \frac{(W_o - W_{Vo})}{A \cdot \rho_{Vo}} \qquad \text{(V)}$$

Water penetration and layer structure.

The amount of water initially present in the sample, V_o g, or absorbed into the sample, $V_n - V_o$ g, can be present as crystal water bound to the soluble material a, as hydrate water bound to the insoluble material i (for example ion-exchange resin), and/or in some more or less concentrated solution in pores in the material.

The absorption of water starts at the surface of the sample at time t=0 whereafter the water penetrates slowly into the interior of the sample. During the process four different layers can be postulated to be present as indicated schematically on Fig. A2.

The u-layer:

Initially the entire sample thickness, u_o cm, consits of the original material. A bottom or central layer of this material may remain unchanged for a long time, but it will have a steadily decreasing thickness: u_n cm.

If water was originally present in the amount V_o g, then it is assumed that the water concentration in the remaining layer is maintained at the original value, i.e. the amount of water in the u-layer is:

$$V_u = V_o \cdot \frac{u_n}{u_o} \qquad \text{(VI)}$$

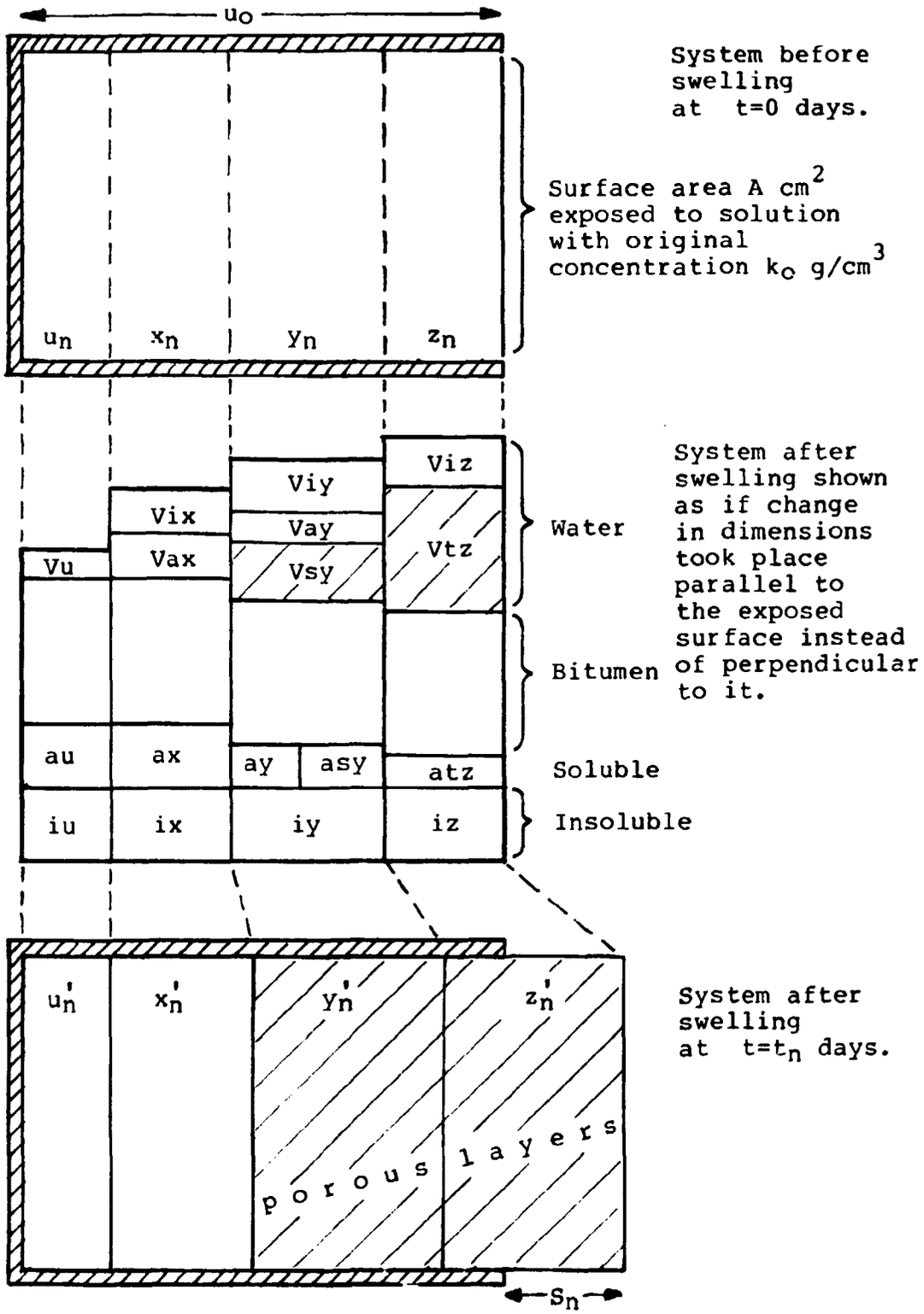

Fig. A2. Schematic presentation of postulated layer structure due to water uptake in sample of bituminized material.

It has recently been demonstrated that some types of bituminized materials contract when stored without any external influences on the material. The phenomenon is a bulk property, and the contraction must therefore be proportional to the sample thickness. If needed and if the time dependence of the contraction is known it can be introduced in the model by multiplication with a time-dependent correction factor:

$$u_n' = f_{(t)} \cdot u_n \qquad 0 \ll f_{(t)} \leq 1 \qquad \text{(VII)}$$

It is assumed arbitrarily that the contraction disappears when the material is penetrated by water. Whether this is correct or not is of minor importance as long as the thickness of the water-containing layer is small compared with the sample thickness u_o.

The x-layer.

In contact with the layer of unchanged material it is reasonable to postulate a layer where the water, which has penetrated into the sample, is taken up in hydrated materials of either type a or i.

Only in case of materials forming well-defined hydrates of fixed composition there will be a sharp division plane between the u-layer with original material and the x-layer with completely hydrated materials. Otherwise the ratio between x_n and u_n can be regarded as a measure of the mean degree of hydration of the materials in x_n and u_n together. For example, in an ion-exchange resin-containing sample the degree of hydration of the resin must be assumed to decrease steadily from saturation at the outer surface of the x-layer to a low value in the interior of the sample. This value may originally be zero or defined by the homogeneously distributed water content V_o g in the sample before immersion in water. The separation into two layers u and x is in this case simply a convenient way to present the state of the system.

The amounts of water in the x-layer associated with the contents of dry materials ax and ix, are Vax and Vix g, respectively. The water uptake results in some swelling so that the thickness of the layer: x_n' is somewhat greater than the thickness x_n of original sample material contained in the swelled x-layer.

Introducing the densities of the water-free materials: ρ_i and ρ_a g/cm^3, the densities of completely hydrated materials: ρ_{hi} and ρ_{ha} g/cm^3 and the contents of water in the completely hydrated materials: q_{hi} and q_{ha} g water/g hydrate, gives the following expression for the volume increase due to water uptake in the x-layer:

$$x_n' \cdot A - x_n \cdot A = \frac{ix+Vix}{\rho_{hi}} + \frac{ax+Vax}{\rho_{ha}} - \frac{x_n}{u_o}\left(\frac{i}{\rho_i} - \frac{a_o}{\rho_a}\right)$$

Inserting $\frac{ax}{ax+Vax} = 1-q_{ha}$ and $\frac{ix}{ix+Vix} = 1-q_{hi}$

together with the constant:

$$K = A \cdot u_o + i\left(\frac{1}{(1-q_{hi})\rho_{hi}} - \frac{1}{\rho_i}\right) - \frac{a_o}{\rho_a} \qquad \text{(VIII)}$$

gives:

$$x_n' = \frac{1}{A}\left(\frac{x_n}{u_o} \cdot K + \frac{ax}{(1-q_{ha})\rho_{ha}}\right) \qquad \text{(IX)}$$

The amount of material a in the x-layer is ax g. It may in some cases be less than the original amount calculated from the formula: $ax_o = \frac{x_n}{u_o} \cdot a_o$, if some leaching of the soluble material has taken place. The amount ax must be determined from a mass-balance over the whole system.

The amount of water in the x-layer is:

$$Vx = Vix + Vax = ix \cdot \frac{q_{hi}}{1-q_{hi}} + ax \cdot \frac{q_{ha}}{1-q_{ha}}$$

or:

$$Vx = \frac{x_n}{u_o} i \cdot \frac{q_{hi}}{1-q_{hi}} + ax \cdot \frac{q_{ha}}{1-q_{ha}} \qquad \text{(X)}$$

The y-layer.

The next layer with the original thickness y_n is somewhat more complicated in structure. As in the x-layer, completely hydrated insoluble material iy with an associated amount of water Viy is supposed to be present. The same is the case for an amount of solid soluble material ay which is supposed to be present as completely hydrated material which contains the amount of water Vay.

Besides the solid materials a saturated solution of the soluble salt is also assumed to be present in pores in the material. The volume of solution corresponds to a porosity ε . The saturated solution contains asy g salt in Vsy g water. The density of the saturated solution is ρ_s g/cm^3 and the water content is q_s g water/g solution.

The expression for the volume increase of the y-layer is then:

$$y_n'\cdot A - y_n\cdot A = \frac{iy+Viy}{\rho_{hi}} + \frac{ay+Vay}{\rho_{ha}} + y_n'\cdot\varepsilon\cdot A - \frac{y_n}{u_o}\left(\frac{i}{\rho_i} + \frac{a_o}{\rho_a}\right)$$

which, using relationships corresponding to the ones introduced in the case of the x-layer, can be reduced to:

$$y_n' = \frac{1}{(1-\varepsilon)A}\left(\frac{y_n}{u_o}\cdot K + \frac{ay}{(1-q_{ha})\rho_{ha}}\right) \qquad \text{(XI)}$$

The amount of water in the y-layer is: Vy = Viy+Vay+Vsy

$$Vy = iy\cdot\frac{q_{hi}}{1-q_{hi}} + ay\cdot\frac{q_{ha}}{1-q_{ha}} + y_n'\cdot A\cdot\rho_s\cdot q_s\cdot\varepsilon \qquad \text{(XII)}$$

or:

$$Vy = \frac{y_n\cdot i}{u_o}\cdot\frac{q_{hi}}{1-q_{hi}} + ay\cdot\frac{q_{ha}}{1-q_{ha}} + \frac{\varepsilon}{1-\varepsilon}\rho_s\cdot q_s\cdot\left(\frac{y_n}{u_o}\cdot K + \frac{ay}{(1-q_{ha})\rho_{ha}}\right)$$

The amount of the soluble salt in the y-layer is the sum of the undissolved and dissolved material: ay + asy and since

the content of salt in the saturated solution in the pores is:

$$asy = y_n' \cdot A \cdot \varepsilon \cdot \rho_s (1-q_s)$$

it follows that:

$$ay+asy = ay + \frac{\varepsilon}{1-\varepsilon} \cdot \rho_s \cdot (1-q_s) \left(\frac{y_n}{u_o} \cdot K + \frac{ay}{(1-q_{ha})\rho_{ha}}\right) \qquad \text{(XIII)}$$

where ay must be determined from an over-all mass-balance.

The z-layer.

The last layer with the original thickness z_n is in direct contact with the water covering the sample surface. In this layer the amount of soluble salt which originally was present, is assumed to be completely dissolved and partly leached out in the surrounding water. Some of the material remains, however, in solution in the pore water contained in the porosity ε^*. The pososity is postulated to be distributed evenly over the layer thickness.

The concentration of the salt in the pore solution is supposed to decrease liniarily over the thickness of the z-layer, from the saturated solution in the y-layer to the concentration k_n measured in the surrounding water. When k_n is measured in g/cm^3 solution and the density of the solution is $_{Vn}$ g/cm^3 then the water content in the surrounding solution is:

$$q_{Vn} = 1 - \frac{k_n}{\rho_{Vn}} \qquad \text{g water/g solution.}$$

In the z-layer it is assumed that the mean water content of the solution in the pores is:

$$q_t = \tfrac{1}{2}(q_s + q_{Vn}) = \tfrac{1}{2}\left(q_s + 1 - \frac{k_n}{\rho_{Vn}}\right)$$

and that the mean density of the solution is, approximately:

$$\rho_t = \tfrac{1}{2}(\rho_s + \rho_{Vn})$$

Completely hydrated insoluble material will also be present in the z-layer. The degree of swelling of for example ion-exchange resin will be dependent on the concentration of the solute in the water in contact with the resin. Such a relationship can be introduced if necessary, but is disregarded here.

The expression for the volume increase of the z-layer is then:

$$z_n' A - z_n A = \frac{iz+Viz}{\rho_{hi}} + \varepsilon^* \cdot z_n' \cdot A - \frac{z_n}{u_o} \cdot \left(\frac{i}{\rho_i} + \frac{a_o}{\rho_a} \right)$$

which, using relationships corresponding to the ones introduced in the case of the x- and y-layers, can be reduced to:

$$z_n' = \frac{1}{(1-\varepsilon^*) \cdot A} \cdot \frac{z_n}{u_o} \cdot K \qquad \text{(XIV)}$$

The amount of water in the z-layer is: $Vz = Viz+Vtz$

$$Vz = iz \cdot \frac{q_{hi}}{1-q_{hi}} + z_n' \cdot A \cdot \varepsilon^* \cdot \rho_t \cdot q_t$$

$$Vz = \frac{z_n \cdot i}{u_o} \cdot \frac{q_{hi}}{1-q_{hi}} + \frac{\varepsilon^*}{1-\varepsilon^*} \cdot \frac{z_n}{u_o} \cdot \frac{K}{4} \left(q_s + 1 - \frac{k_n}{\rho_{Vn}}\right) (\rho_s + \rho_{Vn}) \qquad \text{(XV)}$$

The content of salt in the unsaturated solution in the pores is:

$$atz = z_n' \cdot A \cdot \varepsilon^* \cdot \rho_t (1-q_t)$$

It follows that:

$$atz = \frac{\varepsilon^*}{(1-\varepsilon^*)} \cdot \frac{z_n}{u_o} \cdot \frac{K}{4} \cdot \left(1-q_s + \frac{k_n}{\rho_{Vn}}\right) (\rho_s + \rho_{Vn}) \qquad \text{(XVI)}$$

This complete the description of the four-layer structure shown in Fig. A2.

The total sample.

Combining the expression for total sample thickness obtained from Fig. A2:

$$u_o + S_n = u_n' + x_n' + y_n' + z_n'$$

with equation VII, IX, XI, and XIV gives:

(XVII)

$$S_n = f \cdot u_n - u_o + \frac{K}{A \cdot u_o}\left(x_n + \frac{y_n}{1-\varepsilon} + \frac{z_n}{1-\varepsilon^*}\right) + \frac{ax + ay/(1-\varepsilon)}{A \cdot (1-q_{ha}) \cdot \varrho_{ha}}$$

The total water content in the sample is:

$$V_n = Vu + Vx + Vy + Vz$$

which together with equations VI, X, XII and XV gives:

(XVIII)

$$V_n = V_o \frac{u_n}{u_o} + \frac{i \cdot q_{hi}}{u_o(1-q_{hi})}(x_n+y_n+z_n) + (ax+ay)\frac{q_{ha}}{1-q_{ha}}$$

$$+ \frac{\varepsilon}{1-\varepsilon} \cdot \varrho_s \cdot q_s \cdot \left(\frac{y_n}{u_o} K + \frac{ay}{(1-q_{ha})\varrho_{ha}}\right) + \frac{\varepsilon^*}{1-\varepsilon^*} \frac{z_n}{u_o} \frac{K}{4} \left(q_s + 1 - \frac{k_n}{\varrho_{Vn}}\right)(\varrho_s + \varrho_{Vn})$$

The total salt content remaining in the sample is:

$$a_n = au + ax + ay + asy + atz$$

which together with equations XIII and XVI gives:

(XIX)

$$a_n = a_o \frac{u_n}{u_o} + ax + ay + \frac{\varepsilon}{1-\varepsilon} \cdot \varrho_s \cdot (1-q_s)\left(\frac{y_n}{u_o} K + \frac{ay}{(1-q_{ha})\varrho_{ha}}\right)$$

$$+ \frac{\varepsilon^*}{1-\varepsilon^*} \cdot \frac{z_n}{u_o} \cdot \frac{K}{4} \cdot \left(1 - q_s + \frac{k_n}{\varrho_{Vn}}\right)(\varrho_s + \varrho_{Vn})$$

Introducing the experimentally determined values for S_n, V_n and a_n (equations V, III and IV) into XVII, XVIII and XIX

gives together with the definition (Fig. A2):

$$u_o = u_n + x_n + y_n + z_n \qquad \text{(XX)}$$

four independent equations from which a selection of four out of the 8 independent parameters: u_n, x_n, y_n, z_n, ay, ax, ε and ε^* can be determined.

To obtain a complete description of the system more independent measurements of properties of the water containing layers are necessary, or some arbitrary assumptions must be made about interconnections between the parameters. A reasonable assumption could, for example, in many cases be, that $ax = a_o \frac{x_n}{u_o}$, i.e. that no leaching takes place from the layer in which there are only hydrates but no free liquid present.

The limitation that u_n, x_n, y_n and $z_n \geqq 0$ will, in some cases, define some of the parameters.

If the composition of the system is simpler than assumed in this general example, simplifications of the equation system follows directly. For example:

<u>Bituminized ion-exchange resin.</u>

In the case of bituminized ion-exchange resin without any salt present in the sample or in the leach water, the y-layer is irrelevant: $ax=ay=y_n=\varepsilon=k_n=0$ and $q_s=\varrho_s=\varrho_{Vn}=1$ which introduced into the four general equations gives:

$$S_n = f \cdot u_n - u_o + \frac{K}{A \cdot u_o}\left(x_n + \frac{z_n}{1-\varepsilon^*}\right)$$

$$V_n = V_o \frac{u_n}{u_o} + \frac{i \cdot q_{hi}}{u_o \cdot (1-q_{hi})}(x_n+z_n) + \frac{\varepsilon^*}{1-\varepsilon^*}\frac{z_n}{u_o} \cdot K$$

$$a_n = 0$$

$$u_o = u_n + x_n + z_n$$

i.e., 3 equations to determine the 4 unknown: u_n, x_n, z_n and ε^*.

If it further more is assumed that the porosity is distributed evenly over the entire layer with hydrated resin, i.e. $x_n = 0$, a further simplification is achieved:

$$S_n = f \cdot u_n - u_o + \frac{K \cdot z_n}{A \cdot u_o \, (1-\varepsilon^*)}$$

$$V_n = V_o \frac{u_n}{u_o} + \frac{i \cdot q_{hi} \cdot z_n}{u_o \cdot (1-q_{hi})} + \frac{\varepsilon^*}{1-\varepsilon^*} \frac{z_n}{u_o} \cdot K$$

which, assuming $V_o = 0$ and $f = 1$, and introducing $u_n = u_o - z_n$ gives:

$$\varepsilon^* = \frac{V_n \cdot K - A \cdot u_o \cdot V_n - S_n \cdot A \cdot i \cdot \frac{q_{hi}}{1-q_{hi}}}{A \, (K \cdot S_n - S_n \cdot i \cdot \frac{q_{hi}}{1-q_{hi}} - u_o V_n)}$$

and

$$z_n = S_n / (\frac{K}{A \cdot u_o \cdot (1-\varepsilon^*)} - 1)$$

$$z_n' = S_n \cdot K / (K - A \cdot u_o \cdot (1-\varepsilon^*))$$

where

$$K = A \cdot u_o + i \, (\frac{1}{(1-q_{hi}) \rho_{hi}} - \frac{1}{\rho_i})$$

These type of formulas was used to calculate Figs. 16, 17 and 18 in the main report.

Similar simplified relationships can be derived for bituminized pure salts such as $NaNO_3$ or Na_2SO_4, but also in these cases it is not possible to destinguish between the y- and the z-layer without additional measurements.

The relationships derived in this appendix are used as a tool for presentation of experimental results. They are mainly descriptive but can also indirectly say something about the physical and chemical phenomena determining the water uptake and leaching of bituminized materials. An important point in this connection is the presence or absence of free water inside the samples, i.e. whether ε or $\varepsilon^* > 0$.

Risø National Laboratory

Risø - M - 2415

Title and author(s)

COMPARATIVE STUDY OF TEST METHODS FOR BITUMINIZED AND OTHER LOW- AND MEDIUM-LEVEL SOLIDIFIED WASTE MATERIALS

Knud Brodersen, Bodil Mose Pedersen and Arne Vinther

Date December 1983

Department or group

Chemistry

Group's own registration number(s)

159 pages + tables + illustrations

Abstract

Various aspects of the behaviour of bituminized or cemented simulated low- or medium-level radioactive waste in contact with water have been investigated.

The solubility (~ 0.5%) and the diffusion coefficient (~ $5 \cdot 10^{-9}$ cm^2/sec) determining transport of water in pure bitumen have been measured for Mexphalte 40/50 at room temperature.

A weighing method has been and used to study the behaviour of bituminized sodium nitrate, sodium sulphate or cation-exchange resin in contact with water or various salt solutions. This method permits the simultaneous measurement of water uptake; swelling and leaching. The particle size of the embedded waste material was found to be an important parameter. Development of solution-filled porosity in the samples was demonstrated in many cases. The swelling of samples in contact with water or weak salt solutions was in some cases very pronounced. In strong salt solutions the tendency to swell is much less.

Available on request from Risø Library, Risø National Laboratory (Risø Bibliotek), Forsøgsanlæg Risø), DK-4000 Roskilde, Denmark
Telephone: (03) 37 12 12, ext. 2262. Telex: 43116

Copies to

Thermal pre-treatment of cation-exchange resin before bituminization was investigated; it does not seem to improve the quality of the final product.

The interaction between bituminized ion-exchange resin and concrete barrier materials has been studied.

Microbial degradation of bitumen and bituminized sodium nitrate under aerobic conditions has been investigated. The phenomenon seems to be of minor importance as far as leaching from the materials is concerned.

A method for measuring the leaching from a plane surface of cemented waste has been developed. The method avoids the problem of cracks between the sample and the container. It was demonstrated that such cracks can introduce considerable errors in the measured leach rates.

Leaching of cemented sodium nitrate or sodium sulphate was investigated. The absorption of CO_2 from the atmosphere was found to influence the chemistry of the leach solution. This had only a minor effect on Cs- and Na-leaching but gave a very pronounced decrease in Ca-leaching.

The use of silica fume as an additive to cemented sodium nitrate decreased the leach rates by about a factor 4.

The leaching behaviour for bituminized as well as cemented waste materials was found in most cases to be diffusion controlled, i.e. the leach rate decreases with $\sqrt{t}$. However, exceptions were encountered which makes extrapolation uncertain.